

**Influence of Climate and Vegetation
on Root Zone Storage Capacity**
A case study in Australia

Mengya Wei

Influence of Climate and Vegetation on Root Zone Storage Capacity

A case study in Australia

By

M. Wei

in partial fulfilment of the requirements for the degree of

Master of Science
in Civil Engineering

to be defended publicly on Monday May 11th, 2020, at 9:00 am.

Supervisor:	Dr. Markus Hrachowitz	
Thesis committee:	Dr. Markus Hrachowitz,	TU Delft
	Dr.ir. Miriam Coenders,	TU Delft
	Dr.ir. Jeremy Bricker,	TU Delft

An electronic version of this thesis is available at <http://repository.tudelft.nl/>.

Acknowledgement

This is a special period in many ways. I often liken the upcoming final defense to "wedding in war", which is simple, unapplauded yet memorable. Hoping everyone can be safe and healthy, and get rid of the pandemic as soon as possible. It is the end of my rather difficult and somewhat regrettable master's career and the begging of an unpredictable and challenging future for me. I have received unconditional support and understanding from my parents countless times. They are extremely steadfast, warm, and powerful, supporting me continue to believe the life I choose. Whether it is academic or life, although there are hardships, but will eventually overcome.

My period in Delft was one of significant learning, which was accompanied by gains and challenges. Those excellent, inspiring, and warm-hearted peers at the Water Management faculty provide me many helps both in study and life, becoming one of the most important support of this process. Firstly, I would like to acknowledge my supervisor, Dr. Markus Harchowitz, for this effective guidance through each stage of the process. One of his words, "It's your life", inspired me to constantly explore myself both in study and life and be responsible for every choice I make. I am also grateful to all committee members, who have had key roles through this study. In particular, I thank Dr. Miriam Coenders for the detailed revised opinion on my thesis, Dr. Jeremy Bricker for noticing the error in the details of my thesis. I would like to thank them for providing invaluable advice during the elaboration of this study.

Then, my thanks would go to my beloved friends. Thanks to my old friends, Wangting Sun and Jingya Du, for witnessing the joy and hardship of my entire Master's life. There is a Chinese ancient poem, “何当共剪西窗烛，却话巴山夜雨时”，which is translated in English as "When, love/ Can we sit at the western window/ Together trimming the candle wick/ And let me tell you then/ About the mountain/ The night/ And the rain?", I am looking forward to that day. Thanks to my Bachelor's friends Yingnan Chen, Yunyue Chen, and Shuang Cui, who have never stopped share the excellent moments of their lives. Finally, I would like to appreciate my friends in Delft, Mengxin Yu, Yu Chen, Shiyu Feng, Chongchong Chen, and Jimmy Lee, thank them for their daily companionship, the time we together spent in the library, and the beautiful scenery and unforgettable moments we have seen.

Summary

Root zone storage capacity S_r is a significant variable for hydrology and climate studies, as it strongly influences the hydrological behaviour of a catchment. Recent studies have developed a climate data-based (water balance between precipitation and transpiration) method to estimate S_r , which is the water demand for vegetation survival and growth during the drought period. What the assumption is that vegetation adapts the root zone storage capacity to climatic and environmental changes, more specifically is to overcome the drought period. The climate-derived method has been implemented in several studies and the climate is identified importantly influence the development of S_r . Before this method, the studies much earlier estimated S_r from soil and vegetation data, which proved the significance of vegetation. It is expected to figure out what and how those various factors influence S_r . It is beneficial to future hydrology assessment by better understanding the correlation between S_r and various variables. For this, Australia was selected as the study area because of the vast land area which means different climatic conditions and vegetation cover types, and sufficient data resources can be obtained.

This study consists of two parts: the estimation of climate-derived root zone storage capacity and the correlation analysis between S_r and various catchment characteristics. 113 catchments were selected and the study period was identified 1981 – 2018 for all catchments. For the climate-derived method, the long-term discharge, precipitation, and potential evaporation time series data are needed. Based on the catchment locations, the long-term daily precipitation, maximum and minimum temperature are obtained and are converted to catchment areal data by Thiessen Polygon method. The potential evaporation is calculated using the Hamon Evapotranspiration method. For each catchment, a series of S_r values can be obtained after removing a long-drought period. Then the S_r with a drought return period of 20 years was estimated using the Gumbel distribution, which was regarded as the root zone storage capacity in this study. For correlation analysis, the catchment characteristics which are used to analyse the relation with S_r include three categories: climatic signatures (long-term mean annual discharge, precipitation, potential evaporation temperature, the seasonality index of these climate variables, and the similarity index which present the timing of precipitation), hydrological signatures (runoff coefficient, autocorrelation coefficient, declining limb density, and peak distribution) and vegetation signatures (NDVI and its seasonality index, vegetation types and irrigation condition). The Principal Component Analysis was used to analyse the correlation between S_r and catchment characteristics. The first three components taking up 70.8% of the total explained variance are taken into account, as S_r is higher correlated the first and the third component, compared with the second one. Eventually, transformed characteristics and S_r were clustered using the K-Means clustering method and seven clusters are summarized.

In general, S_r is important to understand the hydrological response, and it emphasizes the role of the co-evolution of climate and vegetation. When all study catchments are taken into account, the forest coverage rate is a key factor that determines which of the climate and vegetation signatures is more significant. The study found that climate plays a general role as a dominant factor affecting S_r , while when forest coverage of a catchment is higher than 80%, vegetation affects more than climate. Among the climate signatures, potential evaporation and seasonality of precipitation are slightly more important. The former is negatively correlated with S_r ; here the similarity index (reflecting precipitation seasonality and timing of precipitation) is introduced, according to whether the annual distribution of precipitation and evaporation is consistent, the catchments are divided into two categories: for catchments where larger evaporation and heavy rainfall occur in summer, S_r coincides with this, higher similarity index leads to higher S_r ; whereas for the catchments with larger evaporation in summer and more precipitation in winter, the relation is opposite. In terms of vegetation, the most important difference is the impact of eucalypt forests and other forests

(including rain forests, acacia, callitris, and casuarina) on S_r . A comparison between S_r and these two types of forests shows, in general a positive correlation between S_r and eucalypt forests and a negative correlation between S_r and other forests. When clustering results are considered in detail, for catchments with forest coverage of less than 80%, it is straightforward to distinguish whether a catchment is affected more by climate or vegetation; while for catchments in temperate zones, the combined effects of climate and vegetation become more complicated. Another important finding is that the influence of eucalypt forests may also be affected by the alpine topography. Located in the catchment with a higher elevation of the Great Dividing Range, the eucalypt forests have a negative impact on S_r , indicating that the topography or soil characteristics can also affect the distribution of the root system of the eucalypt forests, which needs further research.

Content

List of Acronyms	vi
List of Figures	vii
List of Tables	x
1 Introduction	1
1.1 Background	1
1.1.1 Previous investigation on root zone storage capacity	1
1.1.2 Climate-based approach on estimating root zone storage capacity	3
1.2 Problem statement	3
1.3 Research aim and objectives	3
2 Study catchments	5
2.1 Catchment selection criteria	6
2.1.1 Long-term discharge data	6
2.1.2 Catchment size	6
2.1.3 Long-term climate data	6
2.2 Catchment delineation	7
2.2.1 Digital Elevation Model (DEM)	7
2.2.2 Catchment delineation method	8
2.2.3 Catchment delineation results	8
2.3 Catchment characteristics	9
2.3.1 Climate	9
2.3.2 Land cover	10
3 Data sources	11
3.1 Discharge data	12
3.2 Precipitation data	13
3.2.1 Precipitation data correction	13
3.3.2 Convert point precipitation to areal precipitation	13
3.3 Temperature data	15
3.3.1 Temperature data correction	15
3.3.2 Convert point temperature to areal temperature	17
3.4 Vegetation indices (NDVI and EVI)	18
3.5 Vegetation types	18
3.6 Irrigated agriculture	19
4 Methodology	20
4.1 Potential evaporation	20
4.2 Climate-derived root zone storage capacity	22
4.2.1 Estimation of effective precipitation	22
4.2.2 Estimation of actual transpiration	22
4.2.3 Estimation of root zone storage capacity	23

4.2.4 Gumbel distribution	23
4.3 Climate signatures	26
4.3.1 Long-term mean annual precipitation and potential evaporation	26
4.3.2 Seasonality index of precipitation and potential evaporation	26
4.3.3 Aridity index	26
4.3.4 Similarity index	26
4.4 Hydrological signatures	28
4.4.1 Long-term mean annual discharge and the seasonality index.....	28
4.4.2 Seasonality index of discharge.....	28
4.4.3 Runoff Coefficient	28
4.4.4 Autocorrelation coefficient	28
4.4.5 Declining limb density	29
4.4.6 Peak distribution.....	30
4.5 Vegetation signatures	31
4.5.1 Catchment NDVI and EVI.....	31
4.5.2 Seasonality index of NDVI and EVI.....	31
4.5.3 Vegetation types.....	32
4.5.4 Irrigation condition.....	33
4.6 Principal component analysis (PCA)	34
4.6.1 PCA and processing	34
4.6.2 Interpretation of PCAs	35
4.7 K-Means clustering	37
5 Results	38
5.1 Root zone storage capacity and climate signatures.....	38
5.2 Root zone storage capacity and hydrological signatures	42
5.3 Root zone storage capacity and vegetation signatures	45
5.3.1 NDVI and EVI	45
5.3.2 Land cover and land use.....	47
5.4 Principal component analysis (PCA)	50
5.4.1 Input for PCA.....	50
5.4.2 PCA results.....	50
5.5 K-Means clustering	53
5.5.1 Catchments clustering results.....	53
5.5.2 Catchment clusters characteristics	54
6 Discussion.....	60
6.1 General characteristics of all study catchments	60
6.2 Specific characteristics of different clusters.....	61
7 Conclusion.....	64
Bibliography	66
A Station information	70
A.1 Discharge station summary	70
A.2 Precipitation and temperature station summary	76
B Climate condition (P, Ep, Q)	87
C Gumbel distribution results.....	90

List of Acronyms

ACLUMP	Australian Collaborative Land Use and Management Program
ALUM	Australia Land Use and Management
CDO	Climate Data Online
DEM	Digital Elevation Model
DEM-H	Hydrological Digital Elevation Model
EVI	Enhanced Vegetation Index
HRS	Hydrological Reference Stations
NDVI	Normalized Difference Vegetation Index
NSW	New South Wales
NT	North Territory
NVIS	National Vegetation Information System
QLD	Queensland
SA	South Australia
TAS	Tasmania
VIC	Victoria
WA	Western Australia
WDO	Water Online Data

List of Figures

1.1	Scope of main scientific studies on root zone storage capacity or root depth	2
1.2	Flowchart of solving the research aim.	4
2.1	Selected study catchments distribution across Australia	5
2.2	Flowchart of catchment delineation	7
2.3	The catchment [QLD_422334A] with the location of the discharge station.....	8
2.4	Diversity of the climate conditions throughout Australia represented by 19 catchments. Most of the catchments are not displayed can be considered an interpolation of the displayed one. Note that all y axes have the same scale.....	9
2.5	a) percentages of eucalyptus, other forests and total forests [%], b) percentages of dryland agriculture and irrigated agriculture [%].....	10
3.1	a) The unit-converted long-term discharge time series from a) Hydrological Reference Stations (HRS) and b) Water Data Online (WDO) with the unit [mm/day], b) the long-term discharge time series used for the catchment [QLD_422334A]	12
3.2	a) The original long-term precipitation time series of the selected raingauge stations [P_41018], [P_41256] and [P_41106] for the catchment [QLD_422334A]. After the dashed line only two time series data are available, b) The final long-term catchment mean precipitation time series used in following study.....	14
3.3	Thiessen Polygon for catchment [QLD_422334A], A_i represents a specific polygon area; P_i represents a raingauge.....	14
3.4	a) The original maximum temperature time series, b) the original minimum temperature time series, c) the corrected maximum, minimum and mean temperature time series for the catchment [QLD_422334A].....	16
3.5	The elevation sub-sections of the catchment [QLD_422334A]. The elevation range a) 436 – 501 m, b) 501 to 566 m, c) 566 – 631 m, d) 631 – 695 m, e) 695 – 811 m. The sub-section is highlighted in red.....	17
4.1	Schematization of implemented methodology	21
4.2	Derivation of root zone storage capacity (S_r) for a water year (1980 March to 1981 February) in the catchment [QLD_422334A] as difference between the cumulative precipitation (P_e) and the cumulative effective transpiration (E_t).....	23
4.3	The original S_r results for the catchment a) [TAS_302214], b) [QLD_422334], c) [NSW_401009]; S_r results removing long drought period for d) [QLD_422334] and e) [NSW_401009]. It is noted that if the water deficit returns back to zero within one year, shown in a), the S_r is the maximum value, if not, the S_r of the second year is calculated based on the value of last year, shown in c) and d).....	24
4.4	Root zone storgae capacities S_r related to different drought return periods as estimated using the Gumbel distribution for the catchment [TAS_302214] and [QLD_422334]. Blue dots indicate the annual S_r obtained by calimate-derived S_r , red dots indicate different return periods of S_r . The Gumbel distribution of all catchments are presented in Appendix B.	25
4.5	Conceptual description of monthly climate. a) example of a precipitation regime that the precipitation is out of phase with the temperature, [WA_606001], b) example of a precipitation regime that the precipitation is in phase with the temperature, [QLD_422334A]	27
4.6	Schematic example of autocorrelation (AC), derived from streamflow hydrograph of the catchment [QLD_108003], 1980 January.	29

4.7	Schematic example of declining limb density (DLD), derived from streamflow hydrograph of the catchment [QLD_108003], 1980 January.	29
4.8	Schematic example of peak flow distribution (PD), derived from streamflow hydrograph of the catchment [QLD_108003], 1980 January.	30
4.9	NDVI distribution of the catchment [QLD_422334A], (b) two types of cells with different weightage values. The cells in yellow are the edge with smaller weightages, the cells in pink are the inner with a weightage of one.	32
4.10	The distribution of the major vegetation species in catchment [QLD_422334A]. The eucalyptus of this catchment contains eucalypt open forests, eucalypt open woodlands and eucalypt woodlands.	33
4.11	The land use distribution of the catchment [QLD_422334A]. The irrigation area is colored with blue, which takes up 4.9% of the total catchment.	33
4.12	Examples showing the PCA processing. The three graphs a, b, c (in red) present the relation between S_r and T, and c, d, e (in green) present the relation between S_r and RC. a) and d) present variables (dots) with eigenvectors (dashed lines); b) and e) present PCA results; c) and f) present the loading values for PC_1	36
4.13	Illustration of possible relationships for PCA results: each vector represents a characteristic. The axes are formed by the first two components (PCs). a) highly dependent and positive correlated, b) highly dependent and negative correlated, c) highly uncorrelated. Note that the three diagrams just illustrate relatively ideal conditions.	36
5.1	Map with study catchment and a) mean annual precipitation, b) mean annual potential evaporation. Light colors mean lower values and dark colors mean higher values for all.	39
5.2	Map with study catchments and a) climate-derived root zone storage capacity S_r [mm], b) aridity index AI [-], c) similarity index δ [-], presenting the timing of precipitation, d) seasonality index of precipitation IS_P [-], e) seasonality index of potential evaporation IS_{Ep} [-]. The color changing from blue to white to red means the specific value ranges from lower to higher.	40
5.3	Root zone storage capacities and a) climate-derived root zone storage capacity S_r [mm], b) aridity index AI [-], c) similarity index δ [-], presenting the timing of precipitation, c) seasonality index of precipitation IS_P [-], d) seasonality index of potential evaporation IS_{Ep} [-], e) mean annual temperature T °C, and f) a region-based classification for the catchments. Note that this is a roughly climate-based and region-based classification in order to conveniently illustrate the relations between S_r and various signatures in the following sections. The titles of the sub-plots show the Spearman's correlation coefficients of the whole catchments (significant correlation for $p < 0.05$).	41
5.4	Root zone storage capacities and a) long-term mean discharge Q [mm], b) seasonality index of discharge IS_Q [-], c) autocorrelation coefficient AC [-], d) autocorrelation coefficient in low flow period AC_{low} [-], e) runoff coefficient RC[-], f) declining limb density DLD -, g) peak distribution PD [-], h) peak distribution in low flow period PD_{low} [-]. The titles of the sub-plots show the Spearman's correlation coefficients of the whole catchments (significant correlation for $p < 0.05$).	43
5.5	Map with study catchments and a) root zone storage capacity S_r [mm], b) mean annual discharge Q [mm], c) seasonality index of discharge IS_Q [-], d) runoff coefficient RC [-], e) peak distribution in low flow period PD_{low} , f) region classification. The color from blue to white to red represents an increase in value.	44
5.6	Root zone storage capacity S_r and a) mean annual NDVI, b) seasonality index of NDVI IS_{NDVI} , c) long-term mean annual EVI, d) seasonality index of EVI. The titles of the sub-plots show the Spearman's correlation coefficients of the whole catchments (significant	

	correlation for $p < 0.05$). The six classes with different colors are the same with the classification shown in Fig 5.3.....	45
5.7	Map with study catchments and a) root zone storage capacity S_r [mm], b) runoff coefficient R_C [-], c) peak distribution in low flow period PD_{low} , d) region classification. The color from blue to white to red represents an increase in value.	46
5.8	Root zone storage capacity S_r and a) total forests R_{TF} [%], b) eucalypt forests R_E [%], c) orther forests R_{OF} [%], and d) irrigated agriculture R_I [%]. Note that these values are the proportion of vegetation in the study catchments.	47
5.9	Total forests versus root zone storage capacity S_r . Larger circle means higher percentage of vegetation type or land use type for a) eucalypt forests [%], b) other forests proportion [%], c) total forests, the sum of eucalypt and other forests [%], d) irrigated agriculture [%]; and e) present the relationship between S_r and total forests. The titles of the sub-plots show the specific types with the Spearman's correlation coefficients of the whole catchments (significant correlation for $p < 0.05$).	48
5.10	Map with study catchments a) root zone storage capacity S_r [mm], b) total forests R_{TF} [%], c) eucalypt forests R_E [%], d) orther forests R_{OF} [%], and e) irrigated agriculture R_I [%], f) region classification	49
5.11	Principal component analysis with the catchment characteristics and S_r in this study. S_r and catchment characteristics with their loading on, a) PC_2 versus PC_1 , b) PC_3 versus PC_1 and d) PC_3 versus PC_2 . The signatures shown in different colors: S_r (black), climate signatures (red), hydrological signatures (blue) and vegetation signatures (green).	51
5.12	K-Means clustering results on S_r and catchments signatures (PCA-reduced data) for a) three-dimension plot including the first three principal components, b) PC_2 versus PC_1 , c) PC_3 versus PC_1 and d) PC_3 versus PC_2 . The catchments are divided into seven clusters, each cluster is specified with the same color in all four sub-figures.	53
5.13	Map with root zone storage capacity in seven clusters of the selected catchments throughout Australia.	54
5.14	The results of PCA and K-Means clustering for a) PC_2 versus PC_1 , b) PC_3 versus PC_1 and c) PC_3 versus PC_2 . It is a combination of Fig 5.10 and 5.11.	55
5.15.1	Root zone storage capacity S_r and long-term mean annual (1) temperature T , (2) precipitation P , (3) potential evaporation E_p , (4) discharge Q ; seasonality index of (5) precipitation IS_p , (6) potential evaporation IS_{E_p} , (7) discharge IS_Q ; (8) similarity index δ , reflecting the timing of precipitation.	58
5.15.2	Root zone storage capacity S_r and (9) runoff coefficient R_C , (10) peak distribution P_D , (11) peak distribution in low flow period PD_{low} , (12) Normalized difference vegetation index $NDVI$, (13) $NDVI$ seasonality index IS_{NDVI} , (14) Proportion of eucalypt forests R_E , (15) proportion of other forests (including rainforests and vine thickets, acacia, callitris, casuarina, melaleuca and others) R_{OF} , (16) proportion of total forests R_{TF}	59

List of Tables

3.1	Overview of consulted data sources during this study.....	11
3.2	Forest and woodland classifications with number and name considered in this study.	19
4.1	Correlation matrix of two cases	34
4.2	Eigenvectors and eigenvalues of two cases	34
5.1	Correlation matrix of the selected signatures.....	52
5.2	Eigenvectors and eigenvalues	52
5.3	The first three principal component loading matrix of the selected signatures.	52

1

Introduction

1.1 Background

Root zone storage capacity (S_r) The close linkage between water, climate, and vegetation (like the vegetation-atmosphere interactions, the carbon cycle, the eco-hydrological processes and so on) have long been acknowledged (Milly, 1994). The presence of vegetation increases the infiltration capacity in water-limited ecosystems (Scheffer et al., 2005) and the roots of plants affect the water retention (Ankenbauer and Loheide, 2017). Although many scientists have done a large number of investigations to figure out how water, climate, and vegetation relate and interact with each other, it is still unsatisfactory to explain it evidently in precise quantitative terms. Root zone storage capacity (S_r), which can be understood as a volume of water per unit area with the reach of plant root for transpiration, determines the available water in the root zone that can be used by vegetation and thus controls the extent and type of vegetation (Tang et al., 2015). In other words, S_r controls water partitioning between evaporation and drainage, and thus the long-term water balance of a catchment (Field et al., 1992). A good understanding of S_r is not only essential to understanding the hydrological processes of a catchment but also important for the climate and ecological processes (de Boer-Euser et al., 2019). Despite the significance of S_r is widely acknowledged, it is still relatively difficult to measure or estimate this value, especially at a large catchment scale as it remains problematic to integrate the point measurements to the catchment scale due to high spatial heterogeneity of soil and plant root properties (Crow et al., 2012). Even if the extremely ideal, the soil is assumed to be completely homogenous, there are still some difficulties in translating S_r from practical measure to application models.

1.1.1 Previous investigation on root zone storage capacity

Estimating S_r or relevant variables has been previously undertaken employing various approaches (which are summarized in Fig 1.1).

The field observation approach Zeng (2001) provided estimates of rooting depths based on rooting depth measurements. They showed a general illustration of vegetation type and root fraction, demonstrating that vegetation root distribution is one of the factors that determine the soil water holding capacity. However, Feddes *et al.*, 2001 indicated the possible applied spatial coverage of observation and available data are limited, and it suffers from risks of unlikely vegetation and soil combinations due to data uncertainty. On the other hand, it needs to make assumptions about water uptake from a certain part of the entire root profile. Observations indicate that many woody and herbaceous species can enter very deep layers under various soil conditions, however, very deep isolated roots do not necessarily mean that the entire landscape vegetation can

use the whole soil to reach that depth. Moreover, the maintenance of in situ field observation requires significant economic and human resources (even though lower than climatic stations) and, frequently, it is a non-trivial task to make a network operational for several (Dorigo, 2013).

The look-up table approach Wang-Erlandsson *et al.* (2014) used hydrological and land surface modeling to parameterize S_r based on literature values of mean biome rooting depth and soil texture data. Brocca *et al.*, 2017 indicated hydrological models are discretized at basin level and land surface model considers regular grids. The method assumes that S_r is merely related to land cover and soil type and plants of the same vegetation function type have the same rooting depth, with little consideration for climate adjustment. This is definitely a mistake since plants of the same vegetation type can exhibit different root-zone storage capacity in different climates and landscapes by adapting to environmental conditions (Collins and Bras, 2007). In addition, incompatibility may occur if the literature-based depth of root age is based on land cover classification different from that of the surface model.

The inverse modelling approach Kleidon (2004) used a specific model, using iterative methods to simulate a variable from satellite data (e.g., net or gross primary production, absorbed photosynthetically active radiation, or total terrestrial evaporation) to estimate the depth of the root and various rooting depth parameterizations. This method of indirect observation has large spatial coverage, depending on soil information and the performance of the surface model. More recently, Campos *et al.* (2016) applied this method approximates the storage capacity by using the minimum difference between simulated evaporation by water balance and remote sensing evaporation.

The calibration approach The calibration method is a very widely used method in hydrology (e.g. Werth and Güntner, 2009). S_r as a representative parameter in the model is estimated based on observed precipitation, discharge and evaporation data. However, due to the limitations of model structure and data uncertainty, the calculation parameters used in the model are often affected by other variables and cannot be completely equivalent to the measurable variables in nature. Also, parameter equifinality still remains a problem (Beven, 2006). Generally, the meteorological data limitation performs a huge influence on the accuracy of the calibration results, even though there is a well-performing model. It probably results from that the discharge data is often the only observed variable and it is difficult to obtain sufficient precipitation and evaporation data. For instance, high resolution modeled data (e.g. 500 m) could be obtained by using as inputs coarse scale meteorological forcings (e.g., precipitation data at 10-100 km resolution). Thus, the calibration approach is most suitable for catchment scale (Wang-Erlandsson *et al.*, 2016). For global hydrological models, parameters can be calibrated separately for a selection of gauged river basins and transferred to neighboring ungauged catchments (Widén-Nilsson *et al.*, 2007).

However, due to the limitations in data requirement, scale dependence, model uncertainty, these methods are less satisfactory. Generally, it is increasingly recognized that the accessible water amount is not necessarily related to root depth, but rather to root density. Growing scientific and experimental evidence indicates that vegetation dynamically adapts its root system to the climatic and environmental changes (Schymanski *et al.*, 2008). Water and vegetation interact in a co-evolutionary system toward establishing equilibrium conditions between vegetation and moisture availability in water-limited environments (Gao *et al.*, 2014). It emphasizes the interaction between climate and vegetation.

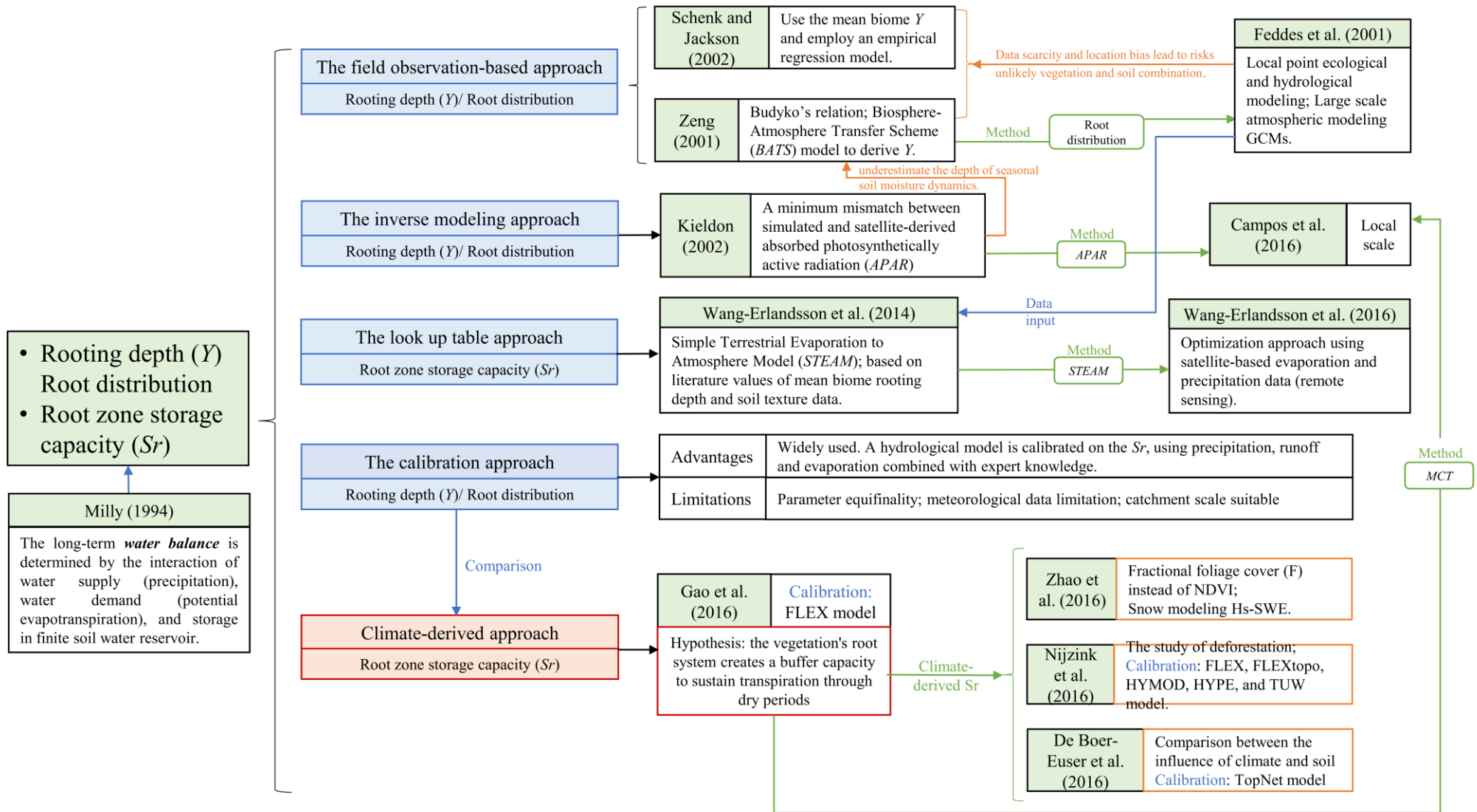


Figure 1.1 Scope of main scientific studies on root zone storage capacity or root depth and distribution.

1.1.2 Climate-based approach on estimating root zone storage capacity

Recently, Gao *et al.* (2014) used a climate-based (water-balance-derived) approach to estimate S_r of six catchments in Thailand and 323 catchments in the United States. They assumed the reservoir size which is regarded as a buffer to balance the high variability of hydrological fluxes in the natural system is estimated as a function of water demand, water input and the length of dry periods. Later on, this method was successfully applied on various cases. In the study of Zhao *et al.* (2016), the MCT was improved by incorporating a snowmelt module, which is removed like 20% of the precipitation in Gao *et al.* (2014). The results of Zhao *et al.* (2016) indicated the plausibility of the improved S_r estimation approach and proved that S_r is most sensitive to evapotranspiration. The research of de Boer-Euser *et al.* (2016) applied water-balance-derived method to study 32 catchments with different climate in New Zealand, using an interception and a root zone storage reservoir to record soil moisture storage deficit from variation in precipitation and transpiration. Nijzink *et al.* (2016) focused on the study of the influence of land cover change for the root zone storage capacity, indicating that temporal variability in climatic conditions and vegetation cover can be taken into account. The root zone storage capacity may be helpful to increase our understanding of the effects of different climates and vegetation covers on the hydrology.

1.2 Problem statement

These studies applying climate-based methods indicate that S_r determines the partitioning between discharge and transpiration, which in turn reveals the significant influence of climate (or the water-balance between precipitation and transpiration) on S_r . This interaction can be reflected through the land cover. It is clear that the ability of vegetation to adjust to different climatic conditions can have an important impact on the hydrology of a catchment. For example, when precipitation decreases, vegetation has to adapt to cope with drier conditions (e.g., Troch *et al.*, 2009; Gentine *et al.*, 2012). On the other hand, if the vegetation is not able to do this, the vegetation cover is likely to change (e.g., Zhang *et al.*, 2001). However, vegetation is not the exclusive representation of climate condition and it is very likely that root development is affected by other factors, including nutrients (e.g. Shahzad and Amtmann, 2017), the survival mechanism of the vegetation (e.g. Christina *et al.*, 2017), or reduced space for root development due to shallow soil layers or high groundwater tables (e.g. Soyly *et al.*, 2014). Thus, it is highly expected to introduce other climate and hydrological factors which can be beneficial to completely understand the relation between S_r , climate, and vegetation conditions.

1.3 Research aim and objectives

This study focuses on the influence of climate and vegetation on root zone storage capacity. This research has therefore the following aim:

Understanding the influences of different catchment characteristics on the climate-derived S_r values and the wider applicability of S_r by comparing it with various climatic, hydrological and vegetation signatures.

In order to achieve the research aim, the following research questions are formulated:

1. How can the climate-derived root zone storage capacity be widely applied in various catchments in Australia?
2. How does root zone storage capacity react to various catchment characteristics?

In order to answer these questions, the following research work plan is developed. The steps are illustrated in Fig 1.2.

- Select and delineate various appropriate catchments in Australia based on hydrological station information and digital elevation model (DEM) data.
- Collect climate data and vegetation data, including discharge, precipitation, maximum and minimum temperature, normalized difference vegetation index (NDVI) and vegetation types.
- Data correction and estimation of areal values for each catchment
- Estimate climate-derived root zone storage capacity.
- Develop a clustering method to classify catchments and analyze the relations between root zone storage capacity and catchment characteristics.

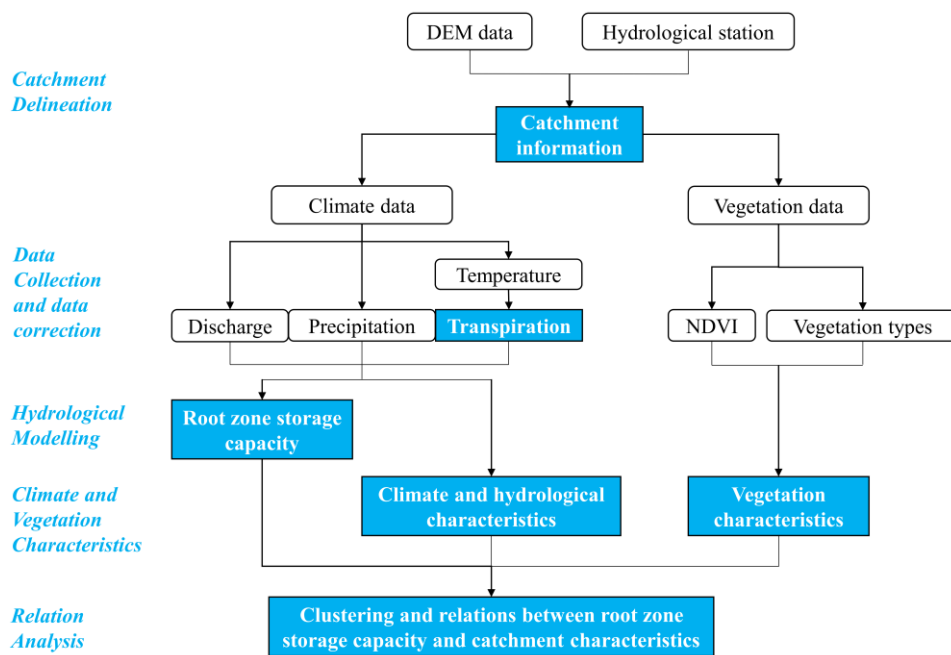


Figure 1.2 Flowchart of solving the research aim.

Study catchments

The catchments used in this study were selected based on the availability of long-term discharge records, the catchment areas, and meteorological data from the catchments. Eventually, a total of 113 catchments were used in this study, spread throughout Australia. In detail, 29 of the total catchments are located in Queensland (QLD), 24 in New South Wales (NSW), 31 in Victoria (VIC), 5 in South Australia (SA), 11 in Western Australia (WA), 8 in Northern Territory (NT) and 5 in Tasmania (TAS), representing different climate and vegetation conditions. Fig 2.1 illustrates the distribution of the study catchments. The catchment delineation is highly related to the obtainable and applicable of data sources, including discharge and climate data. On the other hand, data selection is determined by the result of catchment delineation. Thus, the discharge and climate data sources will be simply introduced in this chapter, whereas the data use and correction will be presented in section 3.

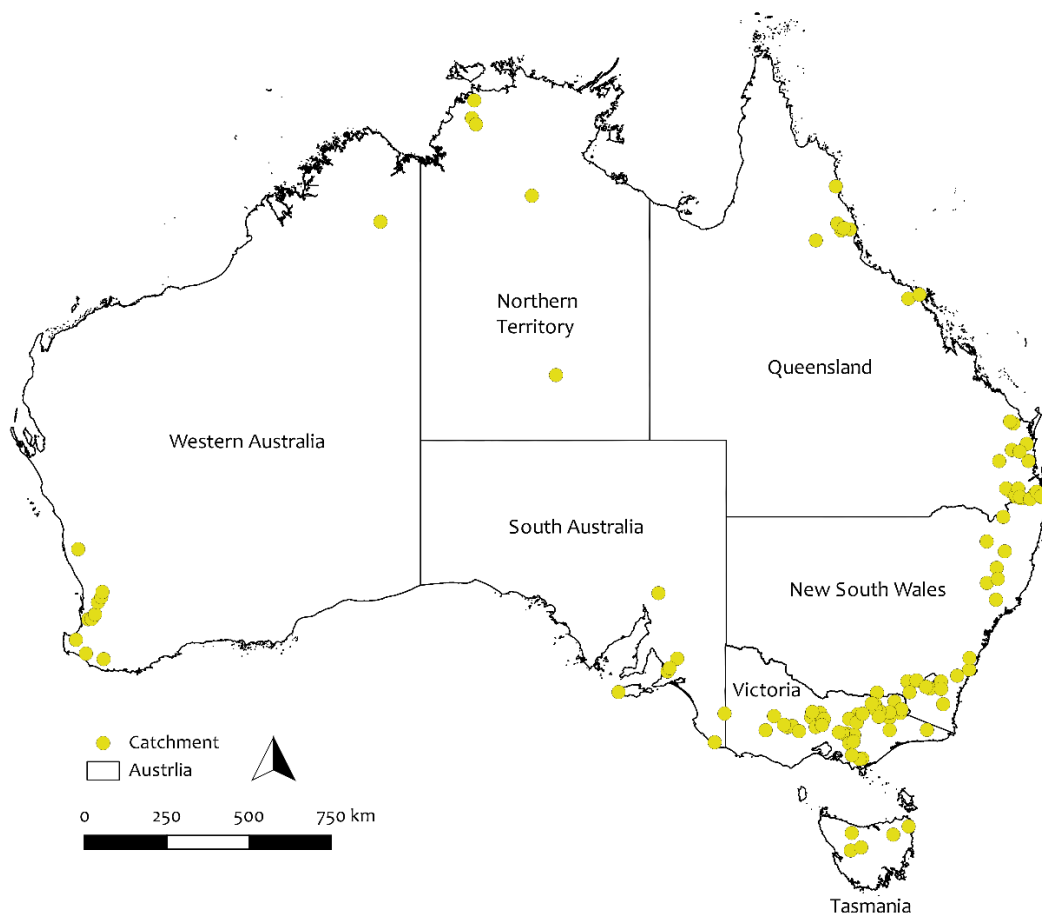


Figure 2.1 Selected study catchments distribution across Australia

2.1 Catchment selection criteria

2.1.1 Long-term discharge data

The long-term discharge daily data is considered as the first selection criterion for catchment delineation since the catchment from which water drains to a common outlet, which the catchment information can be extracted from Digital Elevation Model (DEM) data. Furthermore, discharge is a main input as the estimation of climate-derived root zone storage capacity. The Australian network Hydrological Reference Stations (HRS) (Hydrological Reference Stations (HRS), 2015) of Bureau of Meteorology embraces 222 well-maintained river gauges with high quality, long periods (at least 30 years and end in 2014) of streamflow records managed by Commonwealth, State and Territory water agencies (Zhang et al., 2001). As supplementary, Water Data Online (WDO) (Water Data Online (WDO), 2020) provides free access to nationally consistent current and historical water information that is collected by the Bureau of Meteorology under the Water Regulations (2008). Time series collected from approximately 6000 measurement stations across Australia can be obtained on WDO. Both HRS and WDO enjoy the same hydrological station name and number.

2.1.2 Catchment size

The catchment size is considered as the second selection criterion. In order to moderate the influence of heterogeneity in the signal and magnitude in the signal and magnitude of changes in geology, topography, climate and land cover, both spatially and across months of the year, an appropriate area is highly expected. In this study, for data-rich areas, such as the coastal areas in Queensland, New South Wales, Victoria, an area less than 500 km^2 is selected as the criterion; while for areas with less data, such as most areas in South Australia, Western Australia, Northern Territory and Tasmania, an area less than 800 km^2 is selected. This is because while taking into account the reduction of spatial heterogeneity, it is possible to include as many watersheds with different climatic, hydrological and vegetation signatures as possible. The initial catchment area information is also obtained from HRS, while the practical area applied in following study will be estimated based on DEM data.

2.1.3 Long-term climate data

The long-term meteorological data, precipitation and temperature, which are the input for estimating climate-derived root zone storage capacity, are considered as another selection criterion. The long-term discharge and catchment area identify appropriate catchments, whereas, given the availability of meteorological data, the available catchment will be further reduced. The long-term daily precipitation, maximum and minimum temperature are obtained from Climate Data Online (CDO) (Climate Data Online (CDO), 2020). CDO provides access to a range of statistics, recent weather observations and climate data from Australian Data Archive, a database which holds weather observations dating back to the mid-1800s for some stations. There are tremendous differences among these stations, presenting various gaps in long-term time series datasets. However, in order to estimate the areal value of each catchment, at least two precipitation observation series and one temperature observation series are required. Thus, select at least three raingauge stations located within the catchment or within 30 km from the boundary of the catchment; and at least one temperature stations within or within 50 km from the boundary of the catchment.

According to the three selection criteria, eventually 113 catchments with data period 1980 – 2018 (39 years) are identified. The station information, including discharge, precipitation and temperature with station name, station number and location information (latitude and longitude); the distance between precipitation/temperature and discharge station are summarized in Appendix A.1 and A.2.

2.2 Catchment delineation

According to the above-mentioned selection criteria, 113 catchments including discharge station location information (latitude and longitude) are identified. Catchment delineation is achieved by using the location of the outlet as a reference to extract valid catchment information in Digital Elevation Model (DEM).

2.2.1 Digital Elevation Model (DEM)

The Digital Elevation Model is obtained from 1 second SRTM Derived Hydrological Digital Elevation Model (DEM-H) version 1.0 (Wilson *et al.*, 2011) from ELVIS Portal. It is a 1 arc second (~30 m) gridded digital elevation model (DEM) that has been hydrologically conditioned and drainage enforced. It captures flow paths based on 1 second Shuttle Radar Topography Mission (SRTM) elevations and mapped stream lines, and supports delineation of catchments and related hydrological attributes.

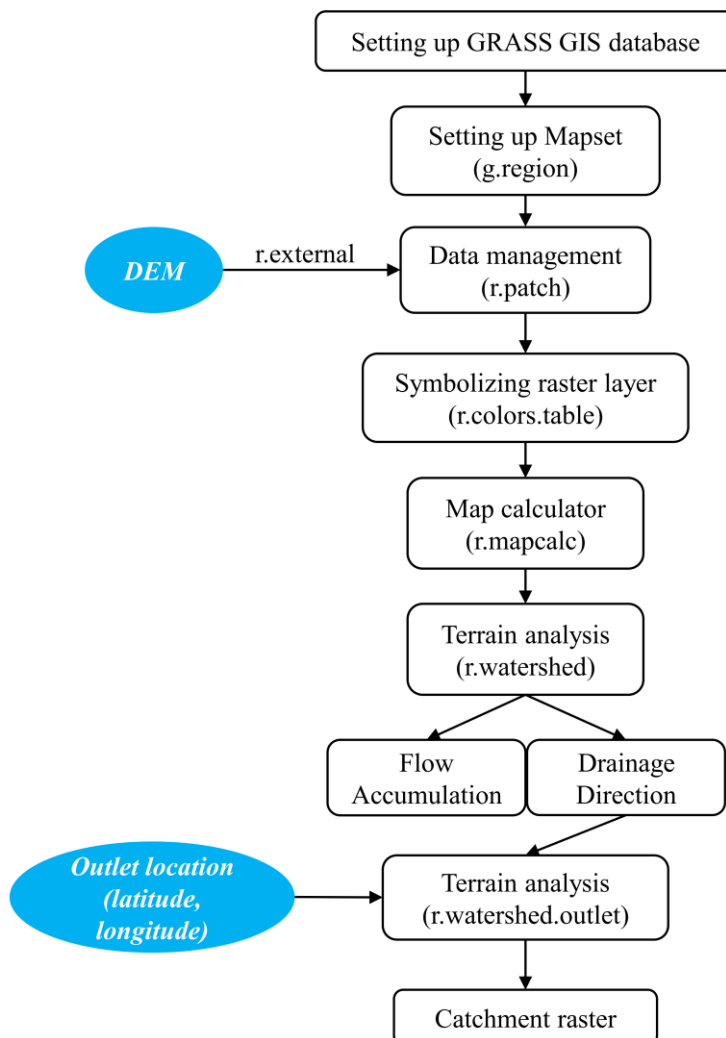


Figure 2.2 Flowchart of catchment delineation

2.2.2 Catchment delineation method

The location information of the outlet and the DEM are combined in this step. The delineation can be achieved by the following steps,

1. In QGIS, the catchment delineation starts from setting a GRASS GIS Database which is simply a set of directories and files with a certain structure.
2. The second step is to determine the location range (study area) based on the catchment location.
3. After successfully setting the Mapset, the DEM data can be added into the Mapset.
4. In the step of terrain analysis, the flow accumulation and the drainage direction can be presented, which means it is clear to see the distribution of stream network and the shape and the size of objective catchment.
5. The last step is to delineating the entire catchment. The location of the outlet truly is the coordinates input to the system, from which the catchment raster layer is obtained.

The flowchart of the methodology is shown in Fig 2.2.

2.2.3 Catchment delineation results

Fig 2.3 presents the map of catchment [QLD_422334A], Kings Creek at Aides Bridge in Barwon-Condamine-Culgoa Rivers Basin, illustrating the outline of catchment, the stream channel and the elevation.

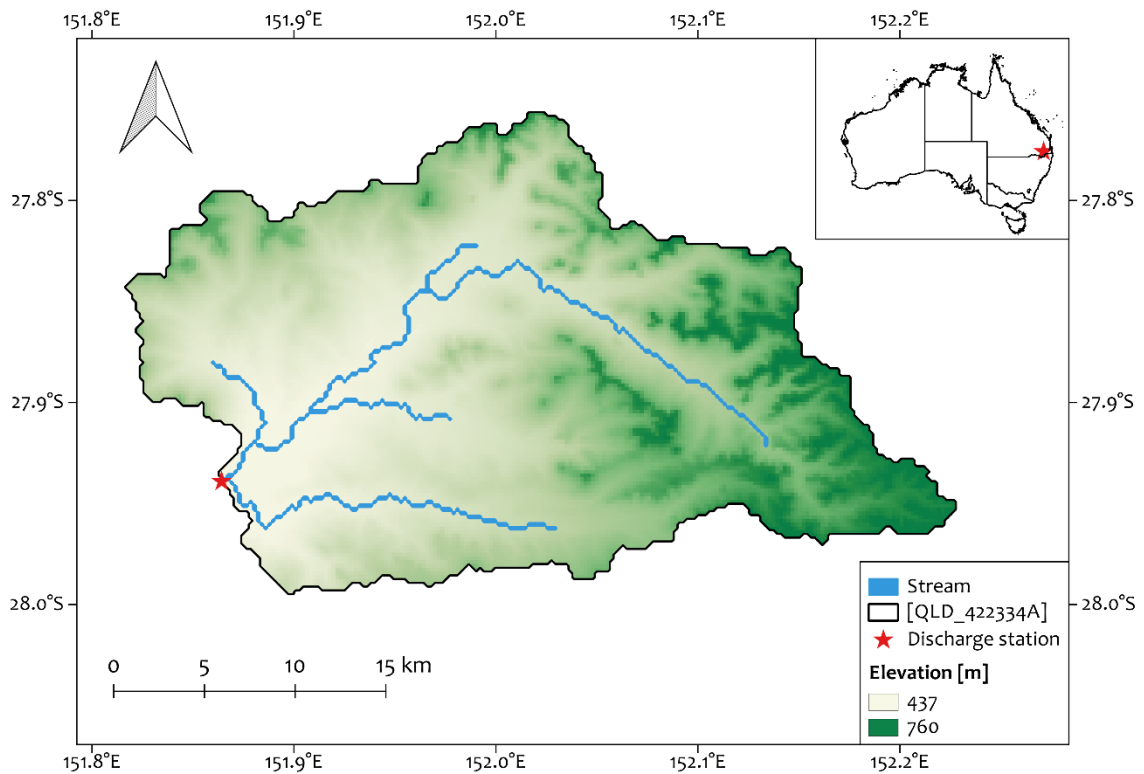


Figure 2.3 The catchment [QLD_422334A] with the location of the discharge station.

2.3 Catchment characteristics

2.3.1 Climate

As these catchments are widespread throughout Australia and Australia has a varied climate, in order to simply describe the catchments, introducing the climate zone identified by the Australian Building Codes Board (Climate zone map: Australia wide, 2015). The catchments with high humidity summer and warm winter, mostly located in north of Queensland and Northern Territory, have annual average air temperature varying from 19 to 28 °C and average precipitation of 800 - 3800 $mm\ y^{-1}$; the catchments with warm humid summer and mild winter, mostly located in south of Queensland (close to the junction of Queensland and New South Wales), have a temperature range from 19 to 21°C and average precipitation of 900 - 1800 $mm\ y^{-1}$; the catchments with hot dry summer, cool winter, mostly located in outback of New South Wales, South Australia and Western Australia (the south of Australia, excluding coastal area) , have a temperature ranging from 12 to 17 °C and average precipitation of 500 to 1200 $mm\ y^{-1}$; the catchments with warm temperate, located in the south of South Australia, the western coastal area of Western Australia and a small part in southern corner of Queensland, the temperature of which changes from 15 to 17 °C and the precipitation changing from 600 to 1200 $mm\ y^{-1}$; the catchments with mild temperate, located in the eastern and southern coastal area of New South Wales, Victoria, and southwestern coastal area of Western Australia, temperature changing from 12 to 16 °C and precipitation of 500 - 1100 $mm\ y^{-1}$; and the catchments with cool temperate, located in the inland closer to the previous zone in Victoria and Tasmania, the annual mean temperature can be lower than 10 and is not higher than 14, and most mean precipitation change from 700 to 1000 $mm\ y^{-1}$. Fig 2.4 present 19 typical catchments which illustrate the climate change throughout Australia. The all catchment climate conditions are presented in Appendix B.

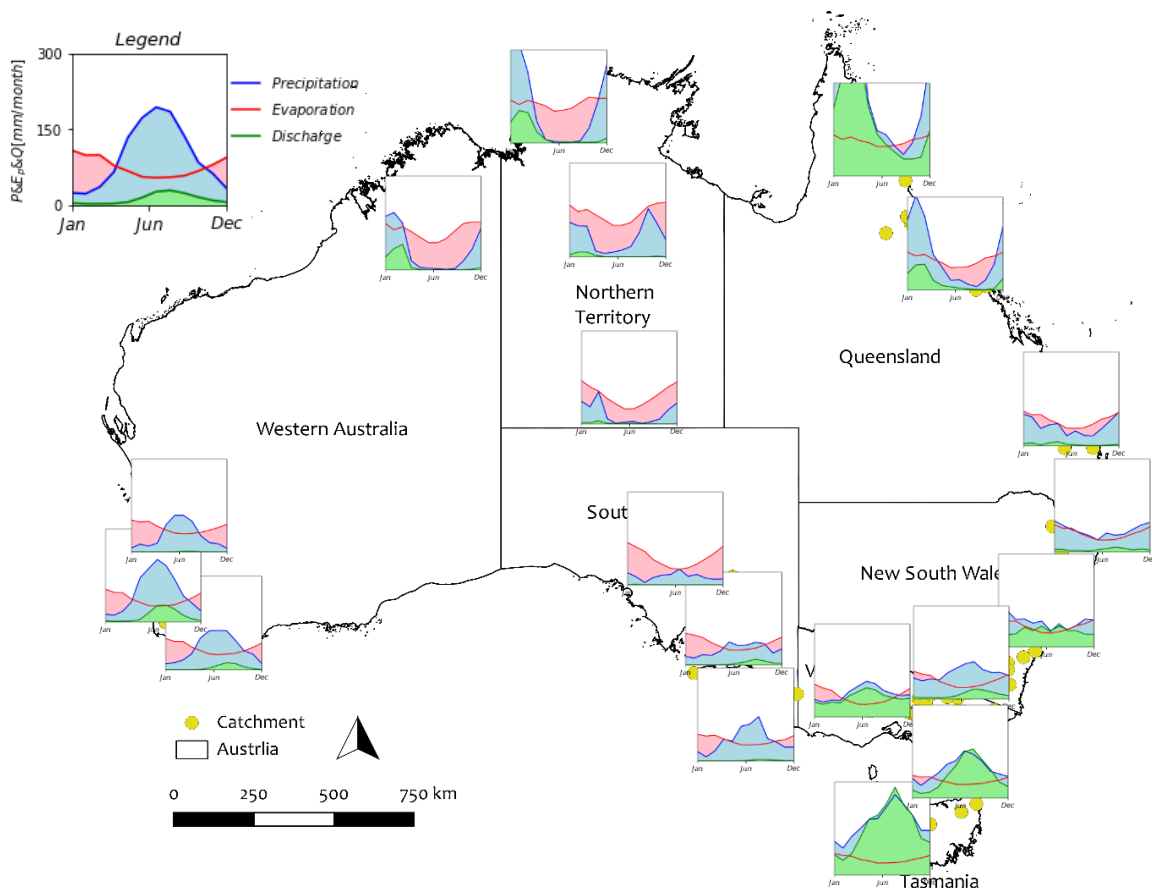


Figure 2.4 Diversity of the climate conditions throughout Australia represented by 19 catchments. Most of the catchments are not displayed can be considered an interpolation of the displayed one. Note that all y axes have the same scale.

2.3.2 Land cover

The surface area of the catchments ranges from 27 to 800 km². The principal land cover in the study catchment is forest, especially numerous catchments are dominated by eucalyptus (the median of total forest proposition is 66% and that of eucalyptus is 55%), and the remaining forests include rainforests and vine thickets, callitris, casuarina, melaleuca, and acacia. Other land cover includes shrublands, grasslands, herblands, inland aquatic and cleared, non-native vegetation, and buildings. The land use information is also visualized and summarized. The land use consists of a) conservation and natural environments, b) production from relatively natural environments, c) production from dryland agriculture and plantations, d) production from irrigated agriculture and plantations, e) intensive uses, and e) water. In addition to climate conditions, land cover is also affected by terrain, topography, soil conditions, and human activities. Although in a relatively wide area, the vegetation distribution and climate classification show an approximately consistent relationship, while the small size of the selected catchments, the difference among them required additional identification.

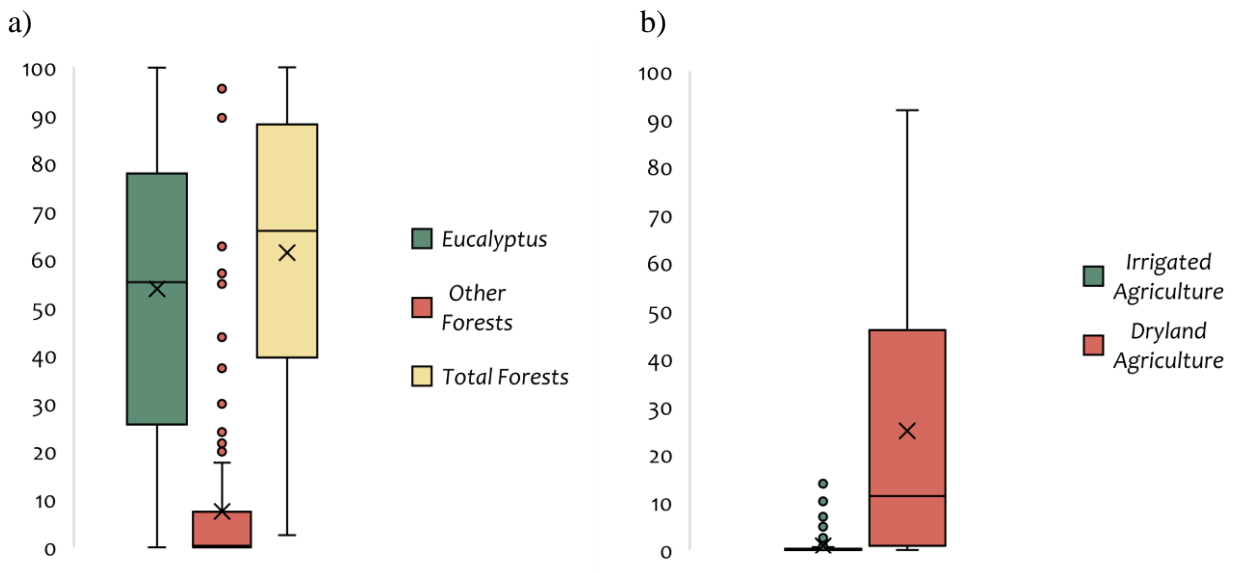


Figure 2.5 a) percentages of eucalyptus, other forests and total forests [%], b) percentages of dryland agriculture and irrigated agriculture [%].

3

Data sources

Two sets of data are used in the study: one for the calculation of climate-derived root zone storage capacity and one to investigate the variation of S_r . It should be noted that the data sources related to calculating S_r have been introduced in section 2.2. In this section, the data is required to be checked for measurement errors caused by gauges and be corrected in operative quality control. For estimating S_r :

- a) Elevation data to assist in estimating the mean catchment areal temperature, which has been introduced in section 2.2.
- b) Discharge data introduced in section 2.1 and will explicitly be described in section 3.1.
- c) Meteorological data, the precipitation, and the potential evaporation which is derived from temperature which also have been introduced in section 2.1 and will be described in section 3.2, 3.3. The method of calculating potential evaporation will be introduced in section 4.

For investigating the variability and relations with catchment characteristics:

- d) Vegetation indices including Vegetation index including Normalized Difference Vegetation Index (NDVI) and Enhanced Vegetation Index (EVI) data for representing the vegetation condition of selected catchment, described in section 3.4.
- e) Vegetation information, described in section 3.5.
- f) Irrigated agriculture, described in section 3.6.

An overview of the above mentioned data sources is given in Table 3.1.

Table 3.1 Overview of consulted data sources during this study.

Data type	Source	Unit	Spatial resolution	Temporal resolution	Temporal availability
Elevation	DEM-H	<i>m</i>	1 arc second	-	-
Discharge	HRS	<i>ML/day</i>	N/A	Daily	Varies station
	WDO	<i>m³/s</i>	N/A	Daily	Varies station
Precipitation	CDO	<i>mm/day</i>	N/A	Daily	Varies station
Maximum and minimum temperature	CDO	°C	N/A	Daily	Varies station
Vegetation indices (NDVI & EVI)	VIP30 v400, LP DAAC	×10000	0.05 Deg	Monthly	1980 - 2014
	MOD13C2 v006, LP DAAC	×10000	500 m	8-day	2002 ongoing
Vegetation information	NVIS Version 5.1	-	100m	-	-
Irrigated Agriculture	ACLUMP	-	50m	-	-

3.1 Discharge data

As introduced in section 2.1.1, the discharge data is obtained from Hydrological Reference Stations (HRS) and Water Data Online (WDO). Since the difference and availability of data records at various stations, and eventually, the period 1980 - 2018 is chosen as the study time span for most catchments. For the missing streamflow data, HRS was filled using the GR4J model (Perrin et al., 2003) which is a daily, lumped, four-parameter rainfall-runoff model that accounts for soil moisture. As for WDO data, validated data has been through the data owner's internal quality assurance processes which include a) removal of spikes and other discrepancies in observation values, b) filling gaps between observations. As the two groups might take different interpolation methods, considering the consistency of data time series, taking the data of the period 1980 – 2014 from HRS and the data of period 2015 – 2018 from WDO.

Unit conversion Since the units of HRS data and WDO data are ML/day and m^3/s , it is required to convert them to mm/day . The unit conversion can be achieved by following functions:

$$Q_{WDO,new}: ML/day \rightarrow mm/day = Q_{WDO,old} \cdot \frac{10^3 \times 10^3}{10^6 A} \quad (3.1)$$

$$Q_{HRS,new}: m^3/s \rightarrow mm/day = Q_{HRS,old} \cdot \frac{10^3 \times 60 \times 60 \times 24}{10^6 A} \quad (3.2)$$

With $Q_{WDO,old}$ and $Q_{HRS,old}$ are the discharges from Water Data Online (WDO) [ML/day] and Hydrological Reference Station (HRS) [m^3/s], $Q_{WDO,new}$ and $Q_{HRS,new}$ are the unit-covered discharges [mm/day], A is the catchment area [km^2].

Take catchment [$QLD_422334A$] as an example, " QLD " is the abbreviation of region Queensland, " $422334A$ " is the discharge station number. The station named Allora is located at Dalrymple Creek in Barwon-Condamine-Culgoa Rivers basin. The station from HRS provides daily discharge data [ML/day] from 1969 to 2014 and that from WDO provides daily discharge data [m^3/s] from 1969 until present. The catchment controlled by this station is $527 km^2$. Fig 3.1 presented the converted long-term discharge time series of HRS and WDO and the final data used in this study.

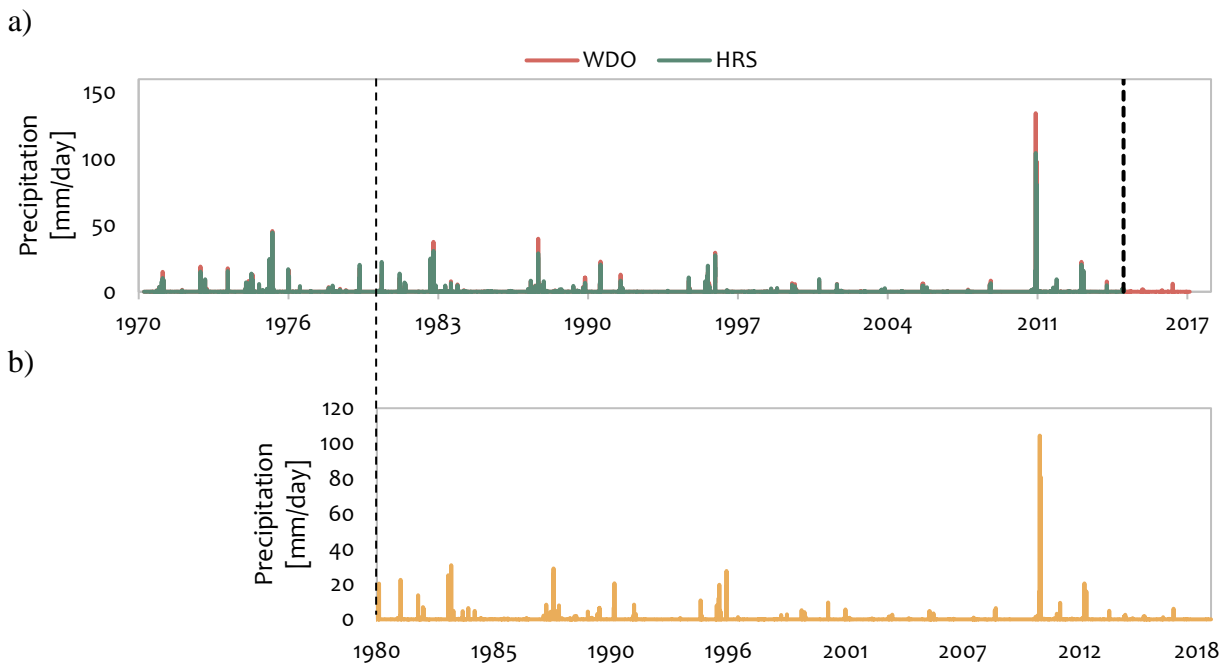


Figure 3.1 a) The unit-converted long-term discharge time series from a) Hydrological Reference Stations (HRS) and b) Water Data Online (WDO) with the unit [mm/day], b) the long-term discharge time series used for the catchment [$QLD_422334A$].

3.2 Precipitation data

As introduced in section 2.1.3, the precipitation data is obtained from Climate Data Online (CDO). For the catchments with different areas, one to three stations were identified as point data for calculating areal precipitation, based on Thiessen Polygon Method. In general, for the smaller catchment, for instance, [QLD_422334A] with an area of 82.79 km^2 which is located at Cochable Creek at Powerline, on Tully-Murray Rivers basin, the raingauge station [P_31168] named Greenhaven was chosen to be the representation of the catchment areal precipitation since the loss of other datasets. However, it depends on whether there are sufficient stations within or near the catchment, not the area of the catchment. For most catchments, at least two are chosen to estimate the areal precipitation.

3.2.1 Precipitation data correction

Before calculating the catchment areal precipitation, it is required to check the measurement errors caused by gauge, manifested as the data loss (or data gap). There are two interpolation criteria applied in this study:

- a) for discontinuous missing single-day data (at most three days), directly use the average of the previous day and the subsequent day as the interpolation to supplement the gap.
- b) for consecutive missing data (up to one month in reality), consider using the data from another station closest to the station; if a nearby station is not available, considering using another station joint to calculate the areal precipitation.

3.3.2 Convert point precipitation to areal precipitation

Thiessen Polygon Method After completing data correction, the long-term point precipitation data can be converted into an areal value over a catchment by using the Thiessen Polygon Method. This method is considered superior to the arithmetical averaging method since some weightage is assigned to each raingauge station. If there are three raingauge stations which form a triangle. Perpendicular bisectors are drawn to each of the sides of the triangle. These bisectors form a polygon around each station. If there are two stations being connected into a line, the perpendicular bisector of the line can directly divide the catchment into two parts.

Here continue to take [QLD_422334A] as an example, where there are three raingauge stations located within the catchment. Fig 3.1 presents the long-term precipitation time series of the selected raingauge stations [P_41018], [P_41256] and [P_41106]. It is noted that from 2013, the available data of [P_41256] ends up with 2012, showing in black dashed line. According to the aforementioned interpolation criteria, the catchment mean long-term precipitation is also presented in Fig 3.2.

Fig 3.3 shows the Thiessen Polygon. The stations P_1, P_2, P_3 divide the catchment into three sub-areas A_1, A_2, A_3 , which are the areas of the respective Thiessen polygons, the average precipitation all over the catchment \bar{P} is computed as

$$\bar{P} = \sum_1^n P_i \cdot \frac{A_i}{A} \quad (3.3)$$

Where \bar{P} is the mean precipitation of the catchment [mm/day], P_i is the observation precipitation for a Thiessen polygon [mm/day], A is the area of the catchment A_i is the area of a Thiessen polygon [km^2], $\frac{A_i}{A}$ is called weightage factor, n is the number of Thiessen polygons.

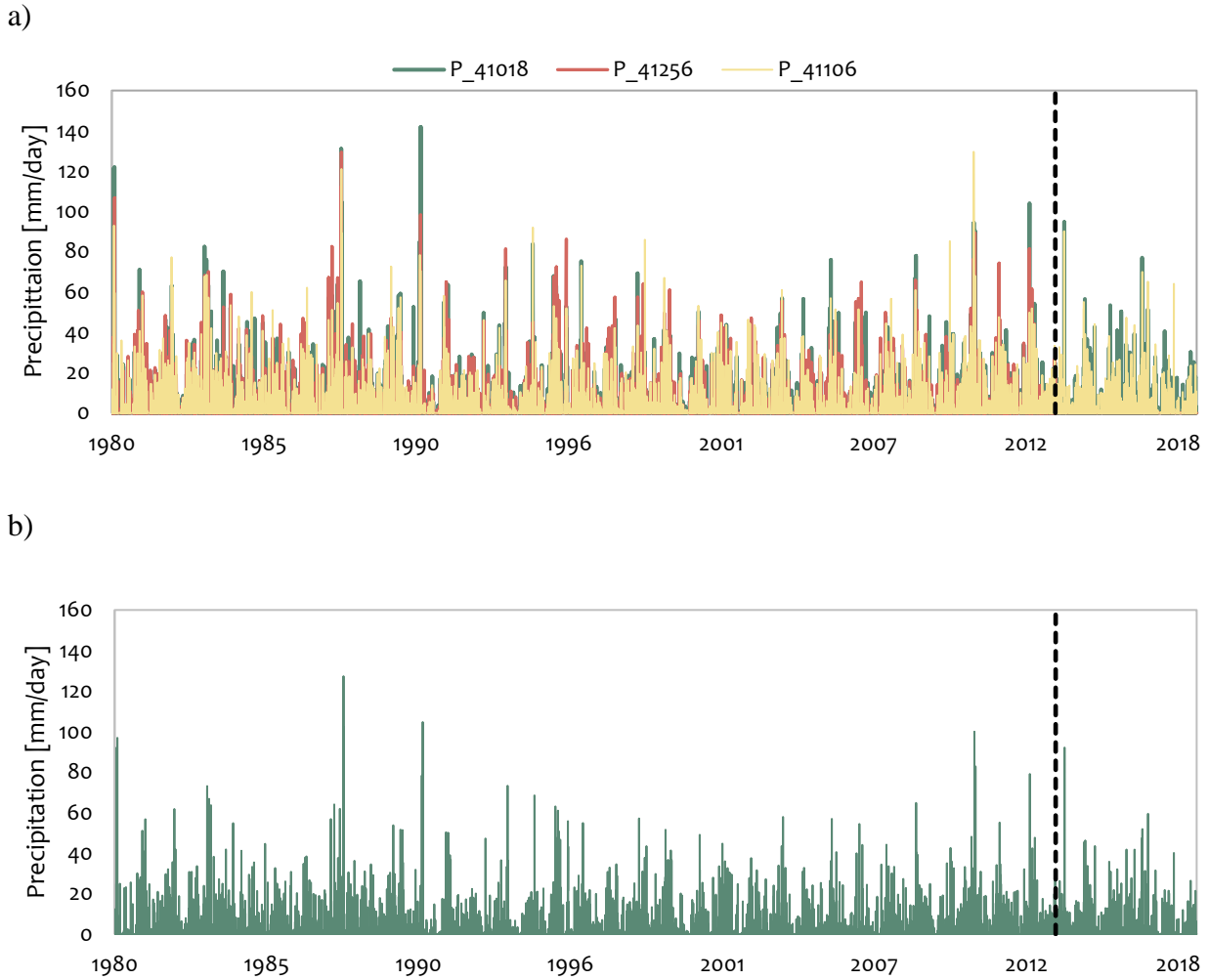


Figure 3.2 a) The original long-term precipitation time series of the selected rain gauge stations [P_{41018}], [P_{41256}] and [P_{41106}] for the catchment [$QLD_{422334A}$]. After the dashed line only two time series data are available, b) The final long-term catchment mean precipitation time series used in following study.

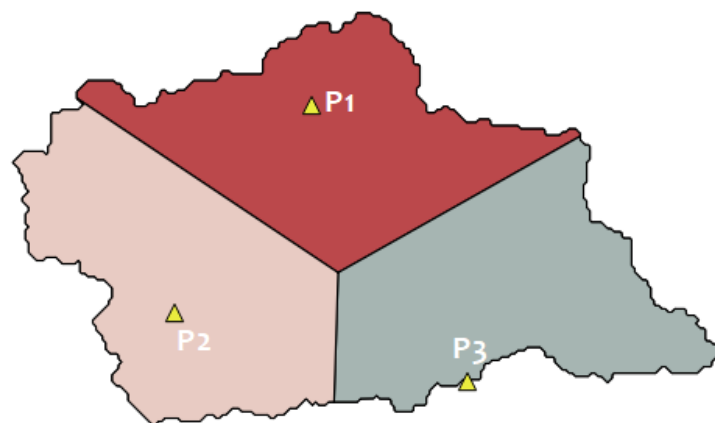


Figure 3.3 Thiessen Polygon for catchment [$QLD_{422334A}$], A_i represents a specific polygon area; P_i represents a rain gauge.

3.3 Temperature data

Same as precipitation, the temperature data is also obtained from Climate Data Online (CDO), whereas they generally are from different meteorological station. Compared with larger heterogeneity of precipitation, the temperature changes slightly with latitude. As a rule of thumb, one degree increase in latitude is roughly equal to a 200 m decrease in elevation, and to a 0.65 °C temperature decrease (Montgomery, 2006). A grid cell of one degree is 111 km × 111 km, which is much larger than the selected catchments in this study. Therefore, the effect of latitude change on temperature is ignored. However, as the elevation of a catchment probably varies from tens to thousands, the elevation correction is required to be considered.

3.3.1 Temperature data correction

The temperature data correction uses the same criterion of precipitation data correction introduced in section 3.1.1. Furthermore, the temperature is influenced by latitude and elevation change, which is required additional processing. The rate of change in temperature observed while moving upward through the Earth's atmosphere. The lapse rate of environmental is highly variable, being affected by radiation, convection and condensation; it averages about 6.5°C/1000m in the lower atmosphere troposphere (The Editors of Encyclopedia Britannica, 2016). The rate of −0.65°C per 100m elevation increase is used in this study.

Data interpolation Continue to take the catchment [QLD_422334A] as an example. The temperature stations used for calculating catchment mean values are [T_40082] and [T_40004] with the elevations 89 m and 24 m, respectively. It is noted that there are some dots located in the zero line (in the black box), which are the data losses and are interpolated by the criteria shown in section 3.2.1. The original and corrected long-term time series are presented in Fig 3.4.

Elevation correction The second step is to divide the objective catchment into various elevation sections. According to every specific catchment with different elevation condition, a various interval 50 – 100 m is applied (generally the catchment is divided into five or sub-sections). The median value is regarded as the representation of each section, such as 100 m for range [50, 150] m. The average elevation of the basin is obtained based on the area proportion of each sub-section. The elevation changes from 436 m to 811m, taking an interval 65 m. The catchment is divided into five parts. Fig 3.5 illustrated the sub-sections, highlighted in red.

The catchment mean areal temperature is calculated by following formulas,

$$\bar{H} = \sum_1^n H_i \cdot \frac{AH_i}{AH} \quad (3.4)$$

With \bar{H} is the mean elevation of the catchment [m], H_i is the mean elevation of a particular elevation sub-section [m], AH is the area of the catchment [km²], AH_i is the area of a particular elevation sub-section [km²].

The areal temperature is achieved. As the selected temperature station generally has a different elevation from the mean value, it is significant to adjust the temperature data, based on the lapse rate criterion. The maximum and minimum temperature of the catchment are both derived from:

$$\bar{T} = T_{old} \cdot \left(1 + \frac{H_{old} - \bar{H}}{100} \times 0.65 \right) \quad (3.5)$$

With \bar{H} is the mean elevation of the catchment [m], H_{old} is the elevation of a temperature station, [m], T_{old} is the observation temperature from the station [°C], \bar{T} is the mean temperature of the catchment [°C].

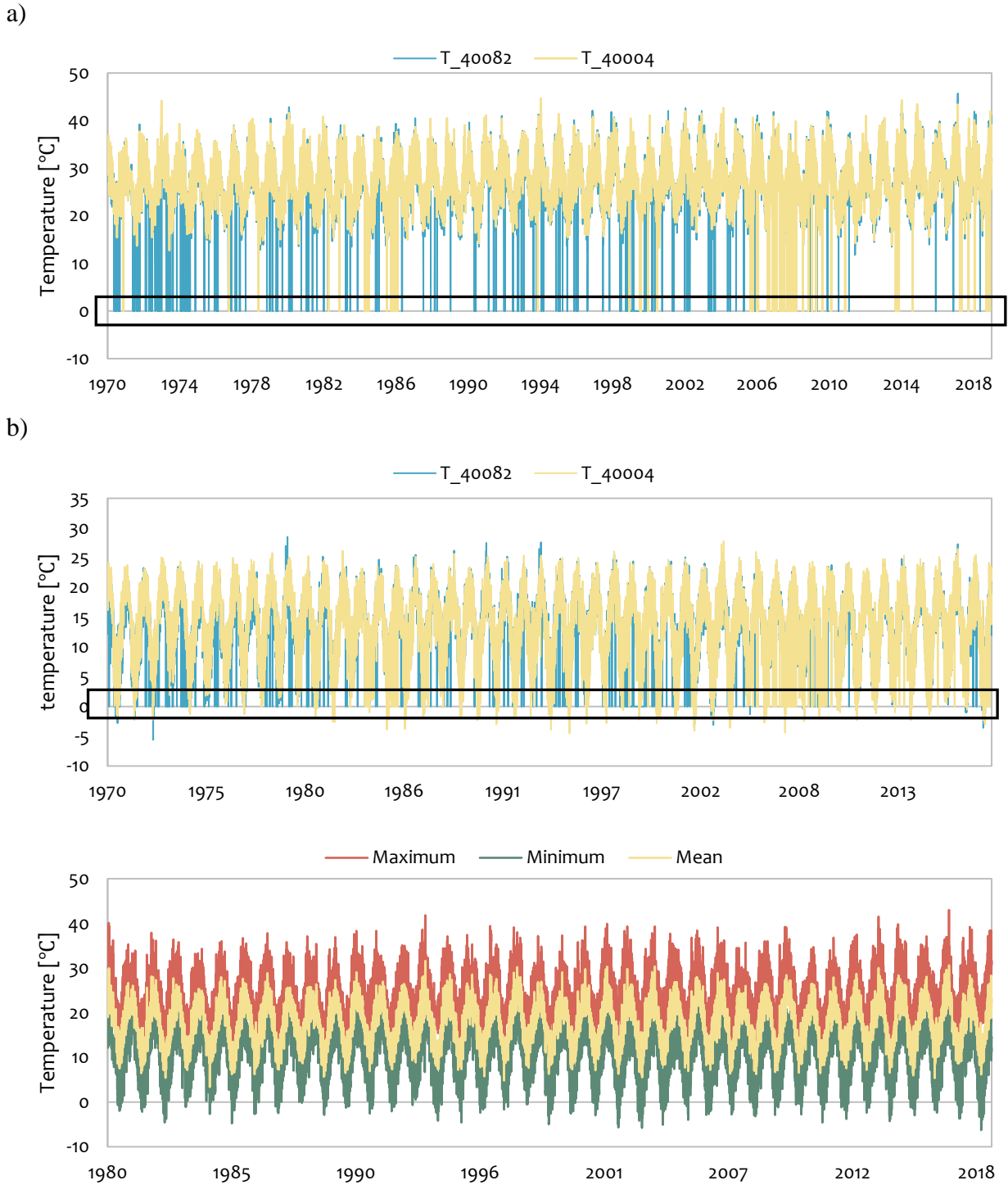


Figure 3.4 a) The original maximum temperature time series, b) the original minimum temperature time series, c) the corrected maximum, minimum and mean temperature time series for the catchment [QLD_422334A].

3.3.2 Convert point temperature to areal temperature

Same as section 3.2.2, using Thiessen Polygon Method to calculate the areal temperature. It is noted that the mean temperature is the average of the maximum and minimum temperature.

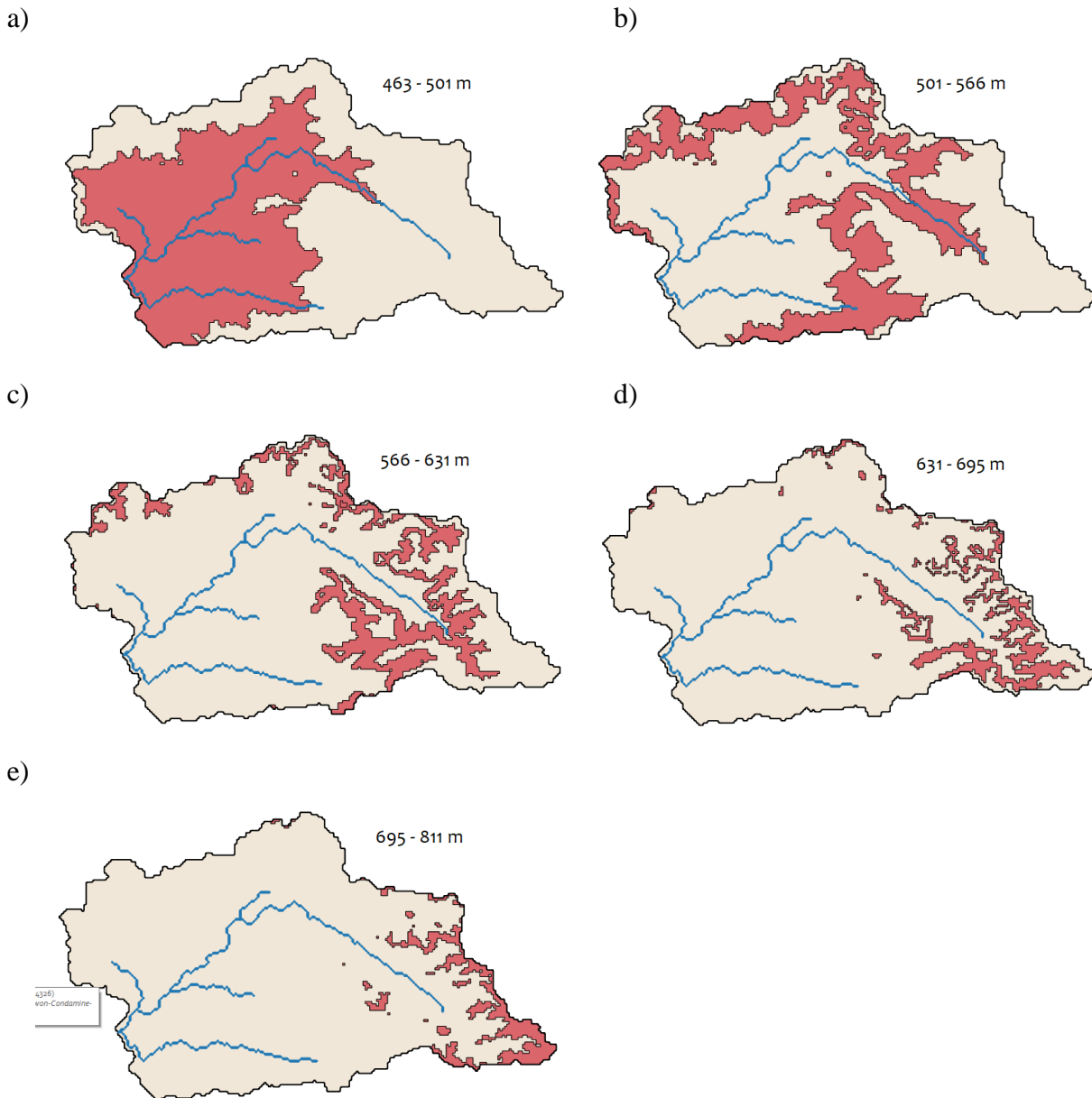


Figure 3.5 The elevation sub-sections of the catchment [QLD_422334A]. The elevation range a) 436 – 501 m, b) 501 to 566 m, c) 566 – 631 m, d) 631 – 695 m, e) 695 – 811 m. The sub-section is highlighted in red.

3.4 Vegetation indices (NDVI and EVI)

The NDVI and EVI data are acquired from VIP30 v004 and MODIS MOD13C2 v006. VIP30 global datasets were created using AVHRR N07, N09, N11, and N14 datasets (1981 - 1999) and MODIS/Terra MOD09 surface reflectance data (2000 - 2014). Both the two data products are provided monthly at 0.05-degree (5600 m) spatial resolution in geographic (latitude and longitude) grid format.

Vegetation indices, Normalized Difference Vegetation Index (NDVI) and the Enhanced Vegetation Index (EVI), were derived to reflect the spectral signature of vegetation status and have been widely applied in all kind of studies (Rouse et al., 1974; Huete et al., 2002; Miura et al., 2001; Wang et al., 2007). Previous studies have found links between NDVI and root zone storage capacity (Adegoke and Carleton, 2002); and NDVI and EVI can be used to estimate root zone storage capacity (Schnur et al. 2010). The NDVI was proposed by Rouse et al. (1974) based on differences in pigment absorption features in red and near-infrared regions of the electromagnetic spectrum (Eq. (3.6)). The EVI is a modified index combining blue, red and near-infrared (Eq. (3.7)) to minimize atmospheric and canopy background effects on NDVI. The EVI is an 'optimized' vegetation index designed to enhance the vegetation signal with improved sensitivity in high biomass regions and improved vegetation monitoring through a de-coupling of the canopy background signal and a reduction in atmosphere influences (Huete et al., 2002; Schnur et al. 2010). While the NDVI is chlorophyll sensitive, the EVI is more responsive to canopy structural variations, including leaf area index (LAI), canopy type, plant physiognomy, and canopy architecture (Terrestrial Biophysics and Remote Sensing Lab, TBRs, 2008).

$$NDVI = \frac{NIR - Red}{NIR + Red} \quad (3.6)$$

$$EVI = G \times \frac{NIR - Red}{NIR + C_1 \times Red - C_2 \times Blue + L} \quad (3.7)$$

where NIR/Red/Blue are atmospherically-corrected or partially atmosphere corrected (Rayleigh an ozone absorption) surface reluctances, L is the canopy background adjustment that addresses non-linear, differential NIR and read radiant transfer through a canopy, and C_1, C_2 are the coefficients of the aerosol resistance term, which uses the blue band to correct for aerosol influences in the red band. The coefficients adopted in the MODIS-EVI algorithm are; $L = 1, C_1 = 6, C_2 = 7.5$, and (gain factor) $G = 2.5$ (Terrestrial Biophysics and Remote Sensing Lab, TBRs, 2008)

3.5 Vegetation types

The vegetation information is obtained from Australia - Present Major Vegetation Groups - NVIS Version 5.1 (National Vegetation Information System V5.1). It provides the latest summary information on Australia's present (extant) native vegetation, which has been classified into Major Vegetation groups and has a 100m x 100m cell size and a format of ESRI Grid/ArcGIS File Geodatabase raster. The data represent on-ground dates of up to 2006 in Queensland, 2001 to 2005 in South Australia (depending on the region) and 2004/5 in other jurisdictions, except NSW. NVIS data was partially updated in NSW with 2001-09 data, with extensive areas of 1997 data remaining from the earlier version of NVIS. Major Vegetation Groups (33 in total) were identified to summaries the type and distribution of Australia's native vegetation. The classification contains different mixes of plant species within the canopy, shrub or ground layers, but are structurally similar and are often dominated by a single genus.

Considering the areas dominantly covered with forest, which can, due to the deeper root zone of forest, be expected that the zoot zone storage capacity is larger than the other vegetation types. However, as the vast distribution of eucalyptus in Australia, it is essential to consider the effect of eucalyptus. Previous studies have found that many tree species can grow roots to depths of more than 10 m (Jackson et al., 1996; Davidson et al., 2011; Eamus et al., 2015) with maximum rooting depths reaching about 60 m for Eucalyptus trees (Stone and Kalisz 1991). A deep rooting profile increases the amount of water available for plant growth and provides a buffering role of deep soil layer through the storage of water during wet season, further withdrawn during dry seasons (Oliveira et al. 2005; Nardini et al. 2015). Furthermore, Eucalyptus with fast root growth capacity, its roots can reach the groundwater table at a depth of 12 m after 2 years and the proportion of water taken up near the groundwater table was much higher during dry periods (Christina et al., 2017). In a word, deep rooting can increase the amount of water available for the trees and provide a significant role for large amounts of water stored in wet season which can be used in dry season, resulting in high transpiration and eventually a higher estimation of root zone storage capacity. It is reasonable to separately analyze the influence of eucalyptus forest and other kinds of forests. The forest types considered in this study is summarized in Table 3.2.

Table 3.2 Forest and woodland classifications with number and name considered in this study.

<i>Eucalyptus</i>		<i>Other Forests and Woodlands</i>	
MVG number	MVG name	MVG number	MVG name
2	Eucalypt Tall Open Forests	1	Rainforests and Vine Thickets
3	Eucalypt Open Forests	6	Acacia Forests and Woodlands
4	Eucalypt Low Open Forests	7	Callitris Forests and Woodlands
5	Eucalypt Woodlands	8	Casuarina Forests and Woodlands
11	Eucalypt Open Woodlands	9	Melaleuca Forests and Woodlands
12	Tropical Eucalypt Woodlands	10	Other Forests and Woodlands
		30	Unclassified Forest

3.6 Irrigated agriculture

Previous studies have found that irrigation has large impacts on terrestrial water balances especially in regions with extensive irrigation. Surface water-fed irrigation decreases runoff and increases water table, while groundwater-fed irrigation increases water table depth and increases or decreases runoff depending on the pumping station (Leng et al., 2017). On the other hand, the climate-derived root zone storage capacity takes the precipitation as the input to the hydrological model, while the irrigation increases the infiltration into root zone. Thus, it is significant to allow for the influence of irrigation on root zone storage capacity.

The dataset is the obtained from the Australian Collaborative Land Use and Management Program (ACLUMP) (Australian Collaborative Land Use and Management Program, 2018) which is the most current national compilation of catchment scale land use data for Australia (CLUM), replacing the Catchment Scale Land Use of Australia (Catchment Scale Land Use of Australia, 2018). It provides a high resolution of $50\text{ m} \times 50\text{ m}$ raster dataset. Land use is classified according to Australia Land Use and Management (ALUM) Classification version 8, a three-tiered hierarchical structure. There are five primary classes, the fourth class "Production from Irrigated Agriculture and Plantations" provides the Irrigation information, including irrigated plantation forests, grazing irrigated modified pastures, irrigated cropping, irrigated perennial horticulture, irrigated seasonal horticulture and irrigated land in transition.

4

Methodology

This study can be simplified in five steps described in Fig 1.2, including 1) catchment delineation, 2) data collection and correction, 3) estimation of climate-derived root zone storage capacity, 4) definition of climate and hydrological signatures, and vegetation signatures, 5) principal component analysis and k-means clustering for relation analysis between root zone storage capacity and catchment characteristics, and grouping catchments into various clusters. The detailed schematization of the steps involved in this study is presented in Fig 4.1.

4.1 Potential evaporation

Before estimating the climate-derived root zone storage capacity, the first objective is to calculate long-term potential evaporation. Hamon Evapotranspiration method is used. Hamon (1963) developed a simple equation to estimate the potential evapotranspiration (E_p) given mean air temperature and day length, without including the effects of humidity wind speed and land cover. It is widely applied spatiotemporally as the less requirement for data inputs. The potential evapotranspiration does not become zero when the mean air temperature is lower than zero. Furthermore, Previous studies (Federe et al., 1996, Vörösmarty et al. (1998)) found that the Hamon model was comparable to more input-detailed models. The potential evaporation is estimated as:

$$P_E = k \cdot 0.165 \cdot 216.7 \cdot N \cdot \left(\frac{e_s}{\bar{T} + 273.3} \right) \quad (4.1)$$

With P_E is the potential evaporation, [mm/day]; k is proportionality coefficient = 1^1 , unitless; N daytime length, [-]; e_s is saturation vapor pressure [mb] and is derived by Murray (1967), allowing air temperature to fall below $0^\circ C$; \bar{T} is mean temperature;

This should be solved with the constitutive relations:

$$e_s = 6.108e^{\left(\frac{17.27T}{T+237.3}\right)} \quad (4.2)$$

$$N = \frac{24}{\pi} \cdot \omega \quad (4.3)$$

$$\omega = \cos^{-1}[\tan(\delta) \tan(\varphi)] \quad (4.4)$$

$$\delta = 1 + 0.033 \cos\left(\frac{2\pi}{365} \cdot J\right) \quad (4.5)$$

With ω is the sunset hour angle, [$radians$]; φ is latitude [$radians$]; δ is the declination [$radians$]; J is the Julian Day fo the year. It is noted that when the sun does not rise ω is set equal to 0, when the sun does not set ω is set equal to π , which is accomplished by taking only the real portion of the result of the equation calculating ω (Allen et al., 1998).

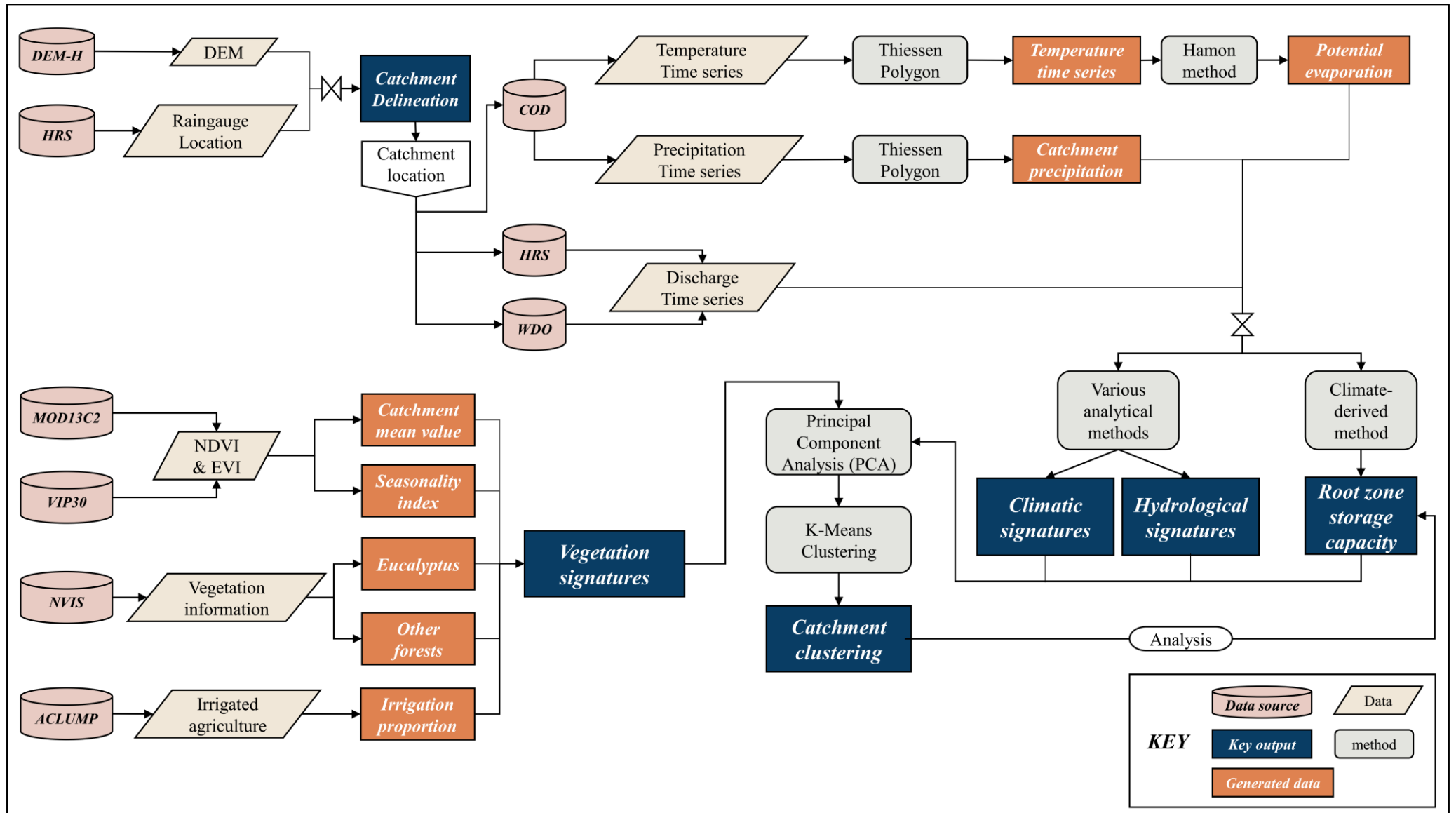


Figure 4.1 Schematization of implemented methodology

4.2 Climate-derived root zone storage capacity

The climate-derived root zone storage capacity S_r was identified based on the methods suggested by Gao et al. (2014) and was successfully tested and developed by de Boer-Euser et al. (2016), Zhao et al. (2016), Wang-Erlandsson et al. (2016) and Nijzink et al. (2016). The principle of this method is that vegetation can develop a buffer storing water to overcome drought period with a specific return period. In a word, the long-term water balance determines the amount of water storage and actual mean transpiration. Following the method of Nijzink et al. (2016), the root zone storage capacity can be derived through five steps: a) Estimation of effective precipitation, P_e b) Estimation of actual transpiration, E_t c) Estimation of root zone storage capacity, S_r d) Removing long drought period, e) Frequency analysis (Gumbel distribution).

4.2.1 Estimation of effective precipitation

The principle of the first step is to follow the water balance for interception storage:

$$\frac{dS_i}{dt} = P - E_i - P_e \quad (4.6)$$

With S_i is the interception storage, [mm], P is the precipitation, [mm/day], P_e is the effective precipitation, [mm/day]; E_i is the interception evaporation, [mm/day]. This is solved by:

$$E_i = \begin{cases} E_p & \text{if } E_p dt < S_i \\ \frac{S_i}{dt} & \text{if } E_p dt > S_i \end{cases} \quad (4.7)$$

$$P_e = \begin{cases} 0 & \text{if } S_i \leq I_{max} \\ \frac{S_i - I_{max}}{dt} & \text{if } S_i > I_{max} \end{cases} \quad (4.8)$$

With E_p is the potential evaporation, [mm/day]; I_{max} is the interception capacity, [mm]. Thus, it is essential to determine the value of interception capacity I_{max} , further to estimate the effective precipitation P_e . Here, following Monte Carlo sampling method, setting the range of I_{max} is [1, 5] mm (Nijzink, 2016) and taking 1000 samples. Then the upper limit and lower limit of E_i can be derived, eventually resulting in upper and lower values for P_e .

4.2.2 Estimation of actual transpiration

Following the long-term water balance, assuming no additional gains or losses (irrigation, capillary and deep percolation), storage changes and/or data errors, the long-term mean actual transpiration can be calculated:

$$\bar{E}_t = \bar{P}_e - \bar{Q} \quad (4.9)$$

With \bar{E}_t is the long-term mean actual transpiration, [mm/day], \bar{P}_e is the long-term mean effective precipitation, [mm/day], \bar{Q} is the long term mean discharge, [mm/day]. The actual mean transpiration is scaled by the ratio of the long-term mean daily potential evaporation \bar{E}_p to the annual mean potential evaporation \bar{E}_p , taking into account the seasonality.

$$E_t = \frac{\bar{E}_p}{E_p} \times \bar{E}_t \quad (4.10)$$

4.2.3 Estimation of root zone storage capacity

The cumulative water deficit between actual transpiration and precipitation over time can be estimated by means of an "infinite-reservoir", meaning that the daily water deficit is cumulated from T_0 (at the time the cumulative deficit is zero), as long as precipitation minus transpiration is less than zero, until the total deficit returns to zero, ending at T_1 . The maximum deficit in this period is the representation that the water demand that satisfies vegetation survival and growth throughout that time:

$$S_r = \max \int_{T_0}^{T_1} (E_t - P_e) dt \quad (4.11)$$

Where S_r is the root zone storage capacity of time period from T_0 to T_1 . Fig 4.2 presents an example of a water year (1980 March to 1981 February) for the catchment [QLD_422334A].

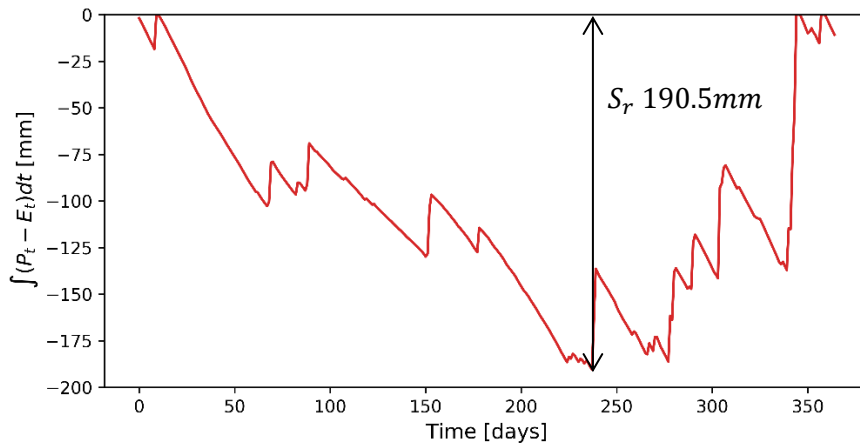


Figure 4.2 Derivation of root zone storage capacity (S_r) for a water year (1980 March to 1981 February) in the catchment [QLD_422334A] as difference between the cumulative precipitation (P_e) and the cumulative effective transpiration (E_t).

4.2.4 Gumbel distribution

Removing long drought period For a long-term time series, many S_r values can be obtained. Ideally, each water year can present a similar graphical example of Fig 4.2. For instance, the catchment [TAS_302214], located in Tasmania, illustrates a relatively ideal situation, showing in Fig 4.3 (a). However, due to the non-negligible influence of El Niño's events which are often associated with drier than normal conditions across eastern and northern Australia, the climate-derived method (based on water balance) cannot be entirely achieved during long drought periods. According to statistics, the years of El Niño in this study include: 1982-1983, 1988-1988, 1991-1992, 1993-1994, 1994-1995, 1997-1998, 2002-2003, 2006-2007, 2009-2010, 2015-2016 (Australian Government, 2015). When the precipitation cannot meet the water requirement for vegetation growth, vegetation will obtain water from other sources, such as by capillary from groundwater. It turns out that in this study, the cumulative water deficit continuously increases and cannot return to zero in two water years. Taking two catchments as example: the previous study objective [QLD_422334A], located in the east coastal area, and the catchment [NSW_401009], located the southeast corner. Fig 4.3 (b) illustrates the original S_r values. It is clear that there are several drought periods. In order to reduce the unidentifiable influence from other water sources, removing the long drought period (water deficit cannot return back to zero within 2 water years) and then re-calculating the S_r series, seen Fig 4.3 (c). The locations of the three catchments are heightened in Fig 4.4.

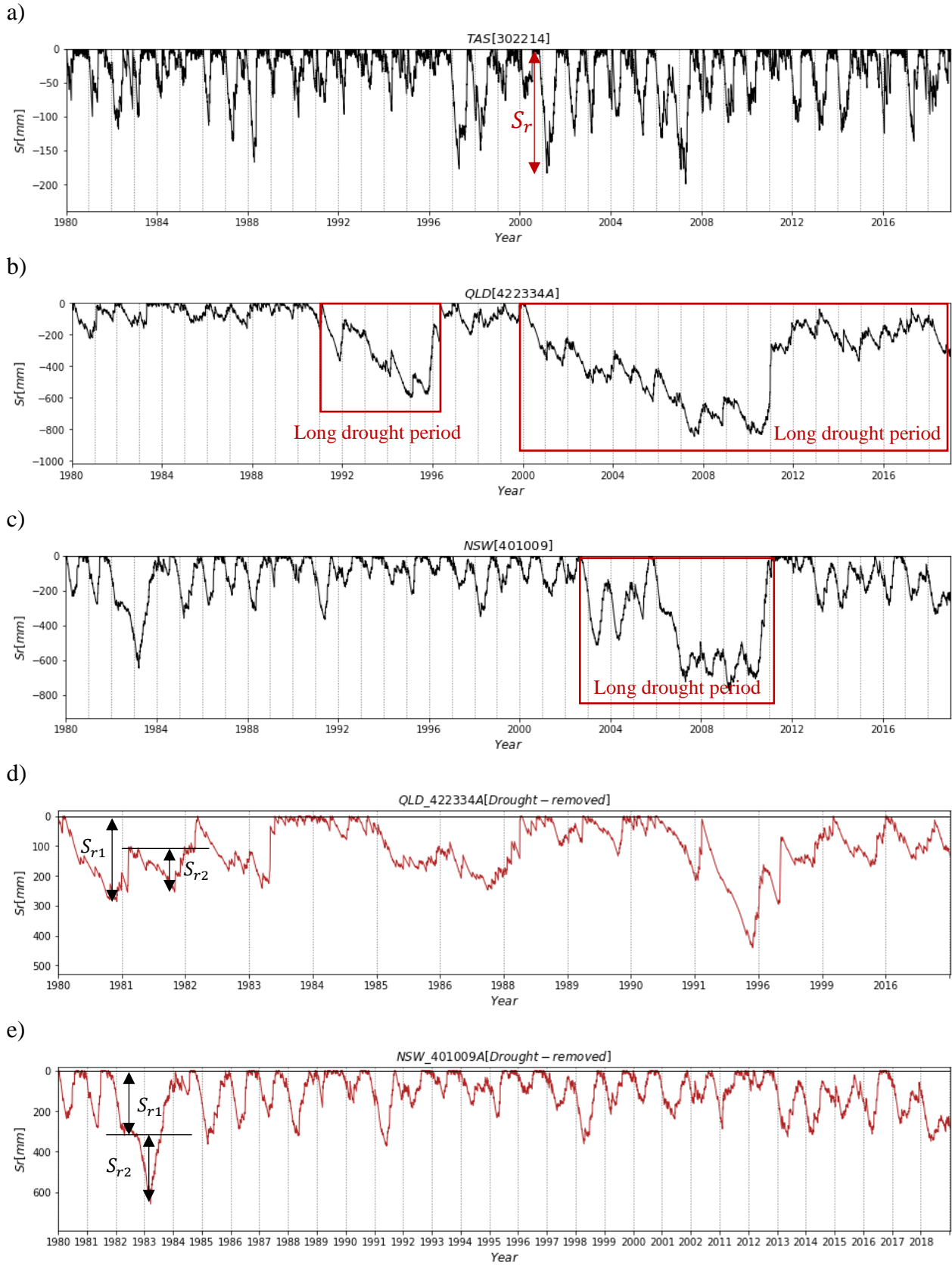


Figure 4.3 The original S_r results for the catchment a) [TAS_302214], b) [QLD_422334], c) [NSW_401009]; S_r results removing long drought period for d) [QLD_422334] and e) [NSW_401009]. It is noted that if the water deficit returns back to zero within one year, shown in a), the S_r is the maximum value, if not, the S_{r2} of the second year is calculated based on the value of last year, shown in c) and d).

Gumbel distribution The Gumbel distribution (Gumbel, 1941), frequently used for estimating hydrological extremes, was used to standardize the frequency of drought occurrence. It allows the estimation of the S_r required to overcome droughts with certain return periods, such as droughts with return periods of 10, 20, and 40 years. Gumbel uses the reduced variate y as a function of the return period T of annual S_r estimates.

$$y = -\ln(-\ln(1 - 1/T)) \quad (4.12)$$

y is defined as a function of X (S_r):

$$y = a(X - b) \quad (4.13)$$

$$b = X_m - s \cdot \frac{y_m}{s_y} \quad a = \frac{s_y}{s} \quad (4.14)$$

$$X = X_m + \frac{(y - y_m)s}{s_y} \quad (4.15)$$

With X_m and y_m are the mean values of X and y , s and s_y are the standard deviation of X and y .

The $S_{r,20}$ for drought return periods of 20 years is identified as the ultimate root zone storage capacity since previous work suggested that vegetation designs S_r to satisfy deficits caused by dry periods with return periods of approximately 10-20 years (Gao et al., 2014; de Boer-Euser et al., 2016; Nijzink et al., 2016). Thus, the drought-removed S_r series which can be obtained based on aforementioned approach, are fitted to Gumbel extreme value distribution to estimate $S_{r,20}$. Fig 4.4 provides an example, the catchment [TAS_302214] of using Gumbel distribution, the red dots represent the root zone storage capacity with a drought return period of 5, 10, 20, 40, 60 and 100 years.

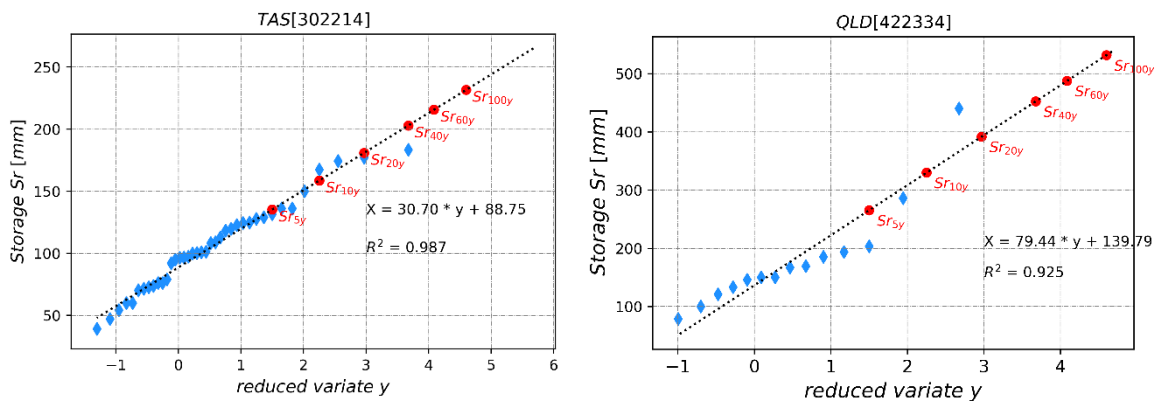


Figure 4.4 Root zone storage capacities S_r related to different drought return periods as estimated using the Gumbel distribution for the catchment [TAS_302214] and [QLD_422334]. Blue dots indicate the annual S_r obtained by climate-derived S_r , red dots indicate different return periods of S_r . The Gumbel distribution of all catchments are presented in Appendix B.

4.3 Climate signatures

The climate-derived S_r are not a linear combination of the characteristics and thus the influence of these are not straightforward. Therefore, the S_r values are compared with several signatures to figure out which one strongly affect S_r . The method used to derive S_r is based on climate data, so it is expected that climate has a strong influence on the derived S_r values. The climate signatures can be derived from the climate data sources (discharge, precipitation, temperature and potential evaporation). Below the applied signature are described.

4.3.1 Long-term mean annual precipitation and potential evaporation

The long-term mean annual precipitation \bar{P} , temperature \bar{T} and potential evaporation \bar{E}_p are directly calculated by mean of the mean values of selected data. The long-term mean values provide an primary description for the catchments. The long-term mean values provide a primary description of the catchments. Higher precipitation provides sufficient water for vegetation's survival and growth, therefore, a relatively lower requirement for the water storage. While a higher discharge means part of surface water directly flows into rivers and part of water infiltrating the root zone can flow fast, where vegetation need higher storage. As for the temperature and potential evaporation, as the latter is derived from the former, higher temperature leads to larger transpiration, and subsequently, more storage is expected by vegetation. The long-term mean value can be calculated by the following formula.

$$\bar{P} = \frac{\sum_{i=1}^n P_i}{n} \quad (4.22)$$

Where \bar{P} can be changed with \bar{T} and \bar{E}_p , is the long-term mean value, P_i is the value of the i th day, n is the total number of selected period.

4.3.2 Seasonality index of precipitation and potential evaporation

Previous studies have found that the seasonality of precipitation is also a determining factor (Gao et al., 2014). The higher the rainfall seasonality index, the larger a S_r is required. It is reasonable to take the seasonalities of other climate factors. The unstable water input and output to the root zone might result in a higher tolerance of storage capacity for vegetation requirements.

$$IS_P = \frac{1}{\bar{P}} \sum_{m=1}^{12} \left| \overline{P_m} - \frac{\bar{P}}{12} \right| \quad (4.23)$$

With $\overline{P_m}$ is the long-term mean monthly precipitation, \bar{P} is the long-term mean annual precipitation. The seasonality index potential evaporation E_p can also be estimated in this way. IS_P and IS_{E_p} present the seasonality indexes of precipitation, discharge and potential evaporation.

4.3.3 Aridity index

The dimensionless aridity index is estimated by Budyko (1974) as:

$$AI = \frac{\bar{E}_p}{\bar{P}} \quad (4.29)$$

With the ratio between long-term mean potential evaporation and precipitation. AI can range from 0 to infinity.

4.3.4 Similarity index

The similarity index governing the seasonality and timing of precipitation. The seasonality index has been independently estimated, while it is expected to see whether or not the precipitation is in phase with potential evaporation and the temperature regimes (Berghuijs et al., 2014). To allow

simple forms for this, assuming that the seasonal variability of precipitation and temperature can be modeled as simple sine curves (Milly, 1994).

$$P(t) = \bar{P}[1 + \delta_p \sin(2\pi(t - s_p)/\tau_p)] \quad (4.24)$$

$$T(t) = \bar{T} + \Delta_T \sin(2\pi(t - s_T)/\tau_T) \quad (4.25)$$

With t is the time, [days], s is the phase shift, [days], τ is the duration of the seasonal cycle, [days], δ is dimensionless seasonal amplitude, Δ is the seasonal amplitude, and P and T stand for precipitation and temperature [mm/day], the duration τ is one year (365 days). Considering there are lots of drought period without precipitation in Australia, the restriction that the maximum seasonality of precipitation which has an upper bound $\delta_p = 1$ is removed (Berghuijs et al., 2016). In the case that $\delta_p = 1$, a correction factor C_r is introduced:

$$P(t) = \max(0, \bar{P} \cdot [1 + C_r + \delta_p \sin(\frac{2\pi(t-s_p)}{\tau})]) \quad (4.26)$$

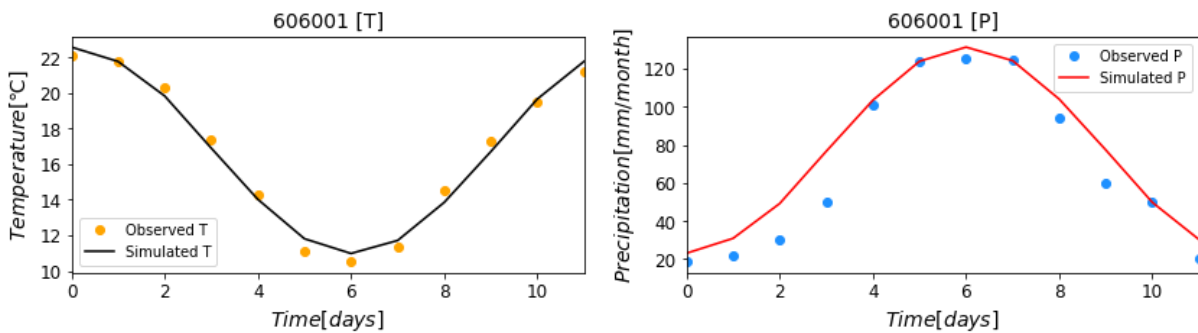
$$C_r = -0.001 \cdot \delta_p^4 + 0.026 \cdot \delta_p^3 - 0.245 \cdot \delta_p^2 + 0.2432 \cdot \delta - 0.038 \quad (4.27)$$

Using a least squares optimization, the coefficients of the equations for all individual catchment can be determined. The similarity index is defined as:

$$\delta_p^* = \delta_p \cdot \text{sgn}(\Delta_T) \cdot \cos(2\pi(s_p - s_T)/\tau) \quad (4.28)$$

δ_p^* ranges from -1 to 1, when $\delta_p^* = -1$, the strongly winter-dominant precipitation is out of phase with temperature; $\delta_p^* = 0$, uniform precipitation throughout the year; $\delta_p^* = 1$, the strongly summer-dominant precipitation is in phase with temperature. Fig 4.5 gives two examples of the observed and simulated precipitation, for precipitation is out of and in phase with temperature.

a)



b)

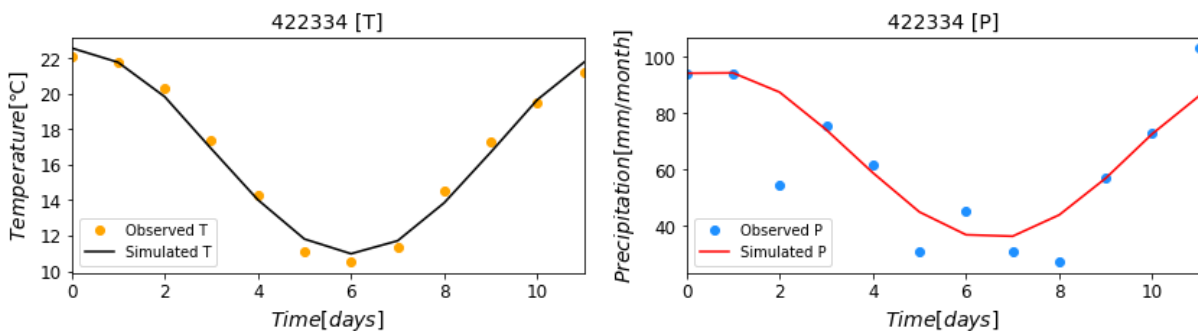


Figure 4.5 Conceptual description of monthly climate. a) example of a precipitation regime that the precipitation is out of phase with the temperature, [WA_606001], b) example of a precipitation regime that the precipitation is in phase with the temperature, [QLD_422334A]

4.4 Hydrological signatures

The hydrological signatures can also be derived from the climate data sources (discharge, precipitation, temperature and potential evaporation), and the observed hydrograph, and most signatures are represented by one value. All the signatures are calculated for the selected period removing long drought years, and for specific signatures, the low flow period (summer or winter for different catchments), are additionally taken into account. Below the applied signature are described.

4.4.1 Long-term mean annual discharge and the seasonality index

The long-term mean discharge \bar{Q} is also directly calculated by the mean of the mean values of selected data with the same method of estimating precipitation and potential evaporation. The calculation method is the same as formula 4.22.

4.4.2 Seasonality index of discharge

The seasonality index IS_Q is calculated with the same method of estimating the seasonality index of precipitation and potential evaporation. The calculation method is the same as formula 4.23.

4.4.3 Runoff Coefficient

Runoff coefficient (RC) refers to the ratio of the long-term mean runoff to the long-term mean precipitation during the same period. It describes the ratio of precipitation to runoff, comprehensively reflecting the influence of natural geographical factors on precipitation - runoff relationship in a catchment.

$$RC = \frac{\bar{Q}}{\bar{P}} \quad (4.30)$$

With \bar{Q} and \bar{P} are long-term mean discharge and precipitation, respectively.

4.4.4 Autocorrelation coefficient

The autocorrelation coefficient (AC) reflects the degree of correlation of the same event in two different periods, which can be explained by the impact of the past on the present. For this study, it is a measure for the smoothness of a hydrography (Euser et al., 2013). The autocorrelation coefficient with a one-day lag for a hydrograph is calculated (Winsemius et al. 2009). A one-day lag means the data point is compared with the previous data point within a hydrograph, reflecting the timing of the peaks.

$$AC = \frac{\sum(Q_i - \bar{Q})(Q_{i+1} - \bar{Q})}{\sum(Q_i - \bar{Q})^2} \quad (4.31)$$

With AC is the autocorrelation coefficient, Q_i and Q_{i+1} are the discharges for two consecutive days, \bar{Q} is the long-term mean discharge.

Low flow period (AC_{low}) The low flow period is taken into account to investigate whether this signature can be used to evaluate a quick response of a catchment on rain events. Note that for the selected more than 100 catchments, the low flow periods are different. In several catchments, there is no clear low flow period, which might be highly correlated with the autocorrelation coefficient of the total period.

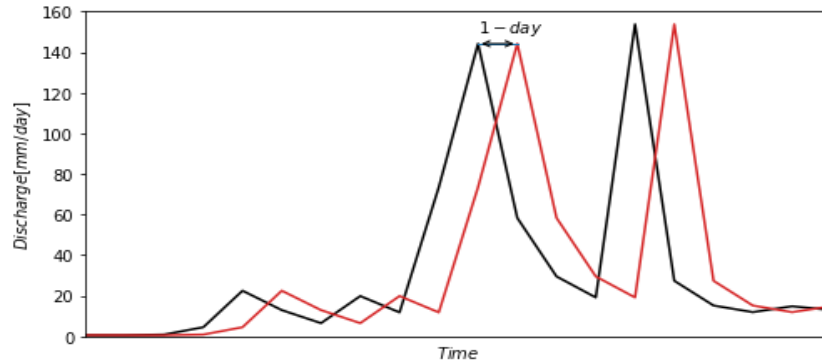


Figure 4.6 Schematic example of autocorrelation (AC), derived from streamflow hydrograph of the catchment [QLD_108003], 1980 January.

4.4.5 Declining limb density

Like the autocorrelation, this declining limb density (DLD) is an indication of the smoothness of the hydrograph. The DLD describes the ration between the number of peaks (N_{pk}) and the total declining limbs of the hydrograph (Shamir et al., 2005). Therefore, the DLD is the mean time of recession limbs. Together with DLD also RLD which reflects the inverse of the mean time to peak can be used for catchment classification.

$$DLD = \frac{N_{pk}}{T_d} \quad (4.32)$$

With N_{pk} is the number of peaks, T_d is the cumulative duration of declining limb.

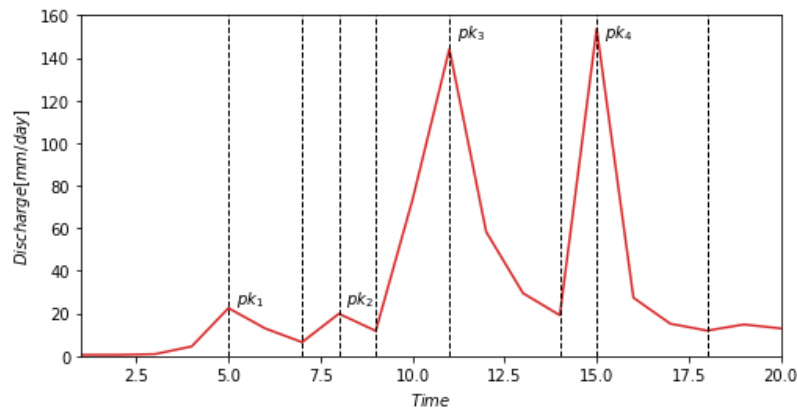


Figure 4.7 Schematic example of declining limb density (DLD), derived from streamflow hydrograph of the catchment [QLD_108003], 1980 January.

4.4.6 Peak distribution

The peak distribution (PD) presents whether the peak discharges are of equal height, of which the peak discharges are exclusively considered (Euser et al., 2013). After removing extreme floods, a flow duration curve just taking these peak flows into account is illustrated, and the average slope between the 10th and 50th percentile is regarded as the representation of this signature. By means of the slope of the flow duration curve, only the peak heights of hydrograph are compared.

$$PD = \frac{Q_{10} - Q_{50}}{0.9 - 0.5} \quad (4.33)$$

With Q_{10} and Q_{50} are the flow exceeded in 10% and 50% of the peaks, respectively.

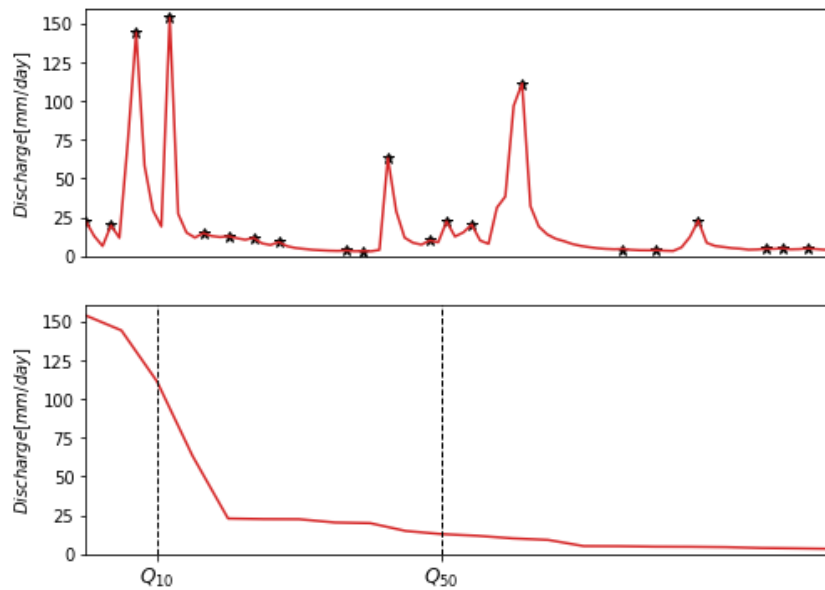


Figure 4.8 Schematic example of peak flow distribution (PD), derived from streamflow hydrograph of the catchment [QLD_108003], 1980 January.

Low flow period (PD_{low}) The peak distribution during the low flow period is again taken into account to investigate whether it can identify the peaks in the discharge during the low flow period. 10th and 50th percentiles are used for estimating this signature. Note that for the selected more than 100 catchments, the low flow periods are different. In several catchments, there is no clear low flow period.

4.5 Vegetation signatures

The climate-derived S_r is originally a parameter for conceptual hydrological models and for that purpose it is expected to reflect a representative storage capacity in a catchment. For catchment scale, the vegetation condition cannot be represented by a single type. The characteristics used for the correlation analysis between vegetation and S_r have been introduced in section 3.3, 3.4 and 3.5: NDVI, EVI, vegetation types and irrigated agriculture. Obviously, they are not all vegetation signatures, while can reflect the vegetation condition to some extent.

4.5.1 Catchment NDVI and EVI

In principle, the mean NDVI or EVI value of a specific catchment can be directly calculated as the average value of the gridded data located in the catchment. However, since the cell is relatively large (5.6 km x 5.6 km) and the area of the catchment is small, the edge of the catchment is not matched perfectly with the edge of the cell, which means that some of the cells are partly inside the catchment and partly outside. Therefore, it is necessary to provide each cell a specific weightage, which depends on the ratio of the area of the cell in the catchment and the whole cell area. Same as aforementioned, [QLD_422334A] is still the sample. Fig 4.9 illustrated the NDVI distribution and the two types of cells with different weightages.

The mean NDVI of the catchment can be calculated through:

$$\overline{NDVI} = \frac{\sum_i^n (NDVI_i \times \frac{A_{Ci}}{A_C})}{n} \quad (4.34)$$

$$\overline{EVI} = \frac{\sum_i^n (EVI_i \times \frac{A_{Ci}}{A_C})}{n} \quad (4.35)$$

With \overline{NDVI} and \overline{EVI} are the catchment mean values, $NDVI_i$ and \overline{EVI}_i are the values of a specific cell, A_{Ci} is the corresponding area of that cell, A_C is the standard cell with a fixed area, n is the cell number that the catchment covers.

4.5.2 Seasonality index of NDVI and EVI

Similar to the climate signatures, the vegetation condition changing throughout a year reflects to the change vegetation water demand.

$$IS_{NDVI} = \frac{1}{\overline{NDVI}} \sum_{m=1}^{12} \left| \overline{NDVI}_m - \frac{\overline{NDVI}}{12} \right| \quad (4.36)$$

$$IS_{EVI} = \frac{1}{\overline{EVI}} \sum_{m=1}^{12} \left| \overline{EVI}_m - \frac{\overline{EVI}}{12} \right| \quad (4.37)$$

With \overline{NDVI}_m and \overline{EVI}_m is the long-term mean monthly value, \overline{NDVI} and \overline{EVI} is the long-term mean annual value.

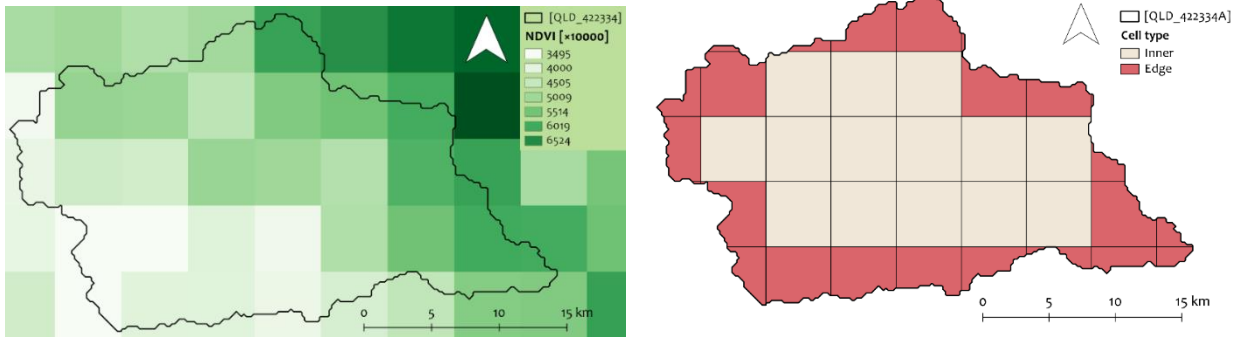


Figure 4.9 NDVI distribution of the catchment [QLD_422334A], (b) two types of cells with different weightage values. The cells in yellow are the edge with smaller weightages, the cells in pink are the inner with a weightage of one.

4.5.3 Vegetation types

Different vegetation types and their corresponding land covers occur in different climates and ecosystems and can have different survival mechanisms. The transpiration is undeniable to be affected by the change of vegetation types, and subsequently the hydrological of catchment will change. The NVIS data contains vegetation types and areas. Each major vegetation specie is represented by a specific color. The ultimate objective of data processing is to obtain the area proportion of different vegetation types in a specific catchment. Here continue taking the catchment [QLD_422334A] as the sample. Fig 4.10 illustrates the distribution of the major vegetation species, in which eucalypt open forests, eucalypt open woodlands and eucalypt woodlands account for 5.89%, 4.56% and 10.42, respectively. The eucalyptus takes up 20.87% in total and there is no any other forest species. For other catchments, the proportions of two main forest types, eucalyptus and other forests are calculated according to the catchment vegetation conditions.

$$R_E = \frac{A_E}{A} \quad (4.38)$$

$$R_{OF} = \frac{A_{OF}}{A} \quad (4.39)$$

$$R_{TF} = \frac{A_F}{A} \quad (4.40)$$

With R_E , R_{OF} and R_F are the proportions of eucalyptus, other forests and total forests including the former two, A_E , A_{OF} and A_F are the area of eucalyptus, other forests and total forests, and A is the catchment area.

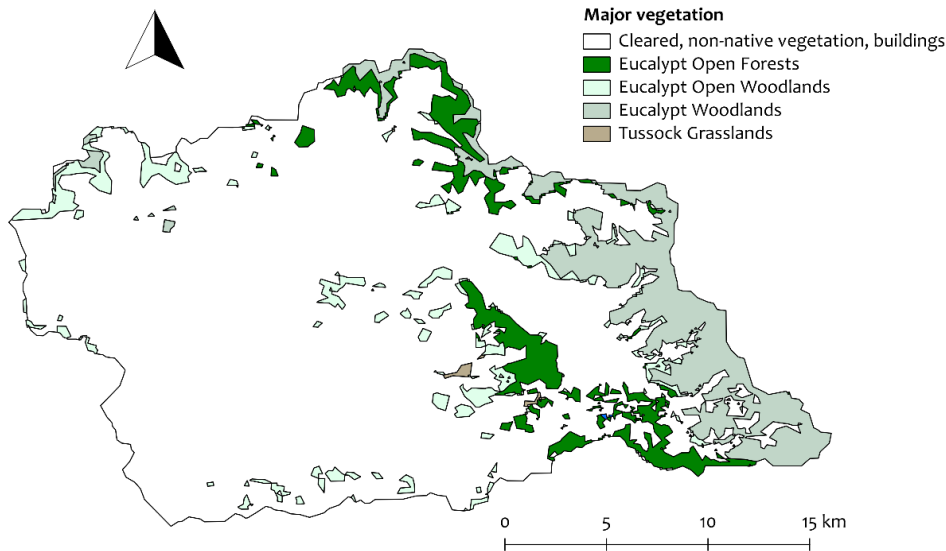


Figure 4.10 The distribution of the major vegetation species in catchment [QLD_422334A]. The eucalyptus of this catchment contains eucalypt open forests, eucalypt open woodlands and eucalypt woodlands.

4.5.4 Irrigation condition

The method to visualize the land cover types is the same with that is used in section 4.4.3, the method to delineate vegetation information. The land use distribution of the example catchment [QLD_422334A] is shown in Fig 4.11. It is important to note that there are six kind land use types: a) Conservation and natural environments, b) Production from relatively natural environments, c) Production from dryland agriculture and plantations, d) Production from irrigated agriculture and plantations, e) Intensive uses, f) Water. The irrigation of [QLD_422334A] accounts for 4.9%.

$$R_I = \frac{A_I}{A} \quad (4.41)$$

With R_I is the proportion of irrigated agriculture, A_I and A are the areas of irrigated agriculture and the catchment.

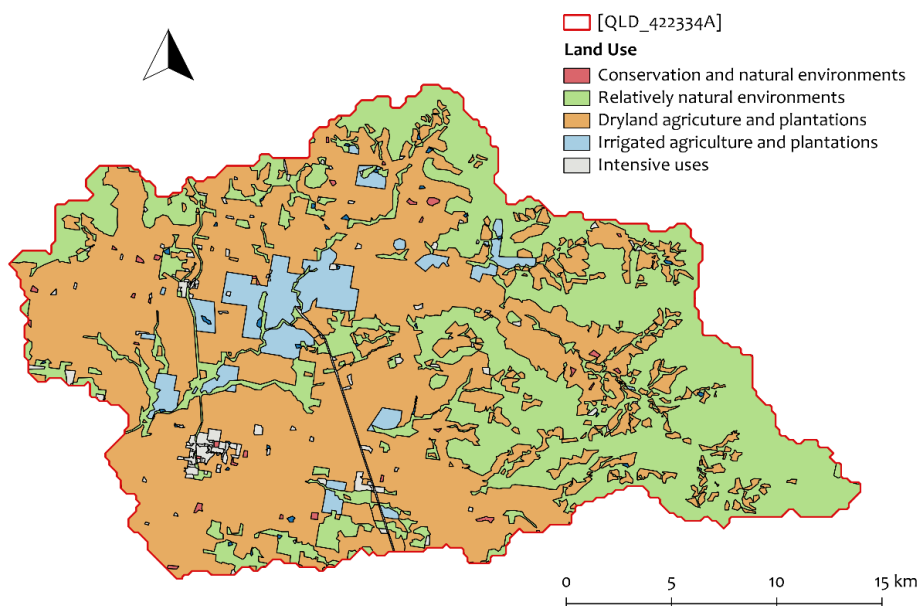


Figure 4.11 The land use distribution of the catchment [QLD_422334A]. The irrigation area is colored with blue, which takes up 4.9% of the total catchment.

4.6 Principal component analysis (PCA)

The method of principal component analysis (PCA) is based upon the early work of Pearson with the specific adaptations to principal component analysis suggested by the work of Hotelling (1933). PCA is a statistical tool which can be used to reduce the dimensions of multivariate problem. The correlation indicates that some of the information contained in one variable is also contained in some of the other remaining variables (Singh et al., 2019). Note that the original variables present various units, thus, they are expected to express in standard form so that the sample variance is one. Then the analysis is made on the correlation matrix, with the total variance equal to the number of variables. The inputs for PCA in this study are various characteristics, including climate signatures, hydrological signatures and vegetation signatures which are introduced in section 4.3 and 4.4.

4.6.1 PCA and processing

The PCA consists of several steps, which are listed below. For better understanding of the method, two cases are presented: the root zone storage capacity S_r and the long-term mean annual temperature \bar{T} , and S_r and runoff coefficient RC as the inputs for PCA.

Step 1. Calculation of the correlation matrix, C. Identifying the variables as the input for PCA. The first step is to calculate the matrix of standardized variables, and then the correlation matrix can be derived, following the formula below.

$$X = (x_j^{(i)} - \mu_j) / S_j \quad (4.16)$$

$$C = \frac{1}{m} X^T X \quad (4.17)$$

With x denotes the matrix standardized variables, $x_j^{(i)}$ is the i th observation on j th variable, μ_j is the mean value of the j th variable, S_j is the standard deviation of the j th variable. X^T is the transpose of the standardized matrix. (Table 4.1)

Table 4.1 Correlation matrix of two cases

	<i>Case 1</i>		<i>Case 2</i>	
	S_r	T	S_r	RC
S_r	1	0.507	S_r	1
T	0.507	1	RC	-0.324
				1

Step 2. Calculation of the eigenvalues and eigenvectors of the correlation matrix. The eigenvectors are orthogonal and the eigenvector with the largest eigenvalue describes the largest amount of variance in the data. (Table 4.2)

Table 4.2 Eigenvectors and eigenvalues of two cases

	<i>Case 1</i>		<i>Case 2</i>	
	<i>PC1</i>	<i>PC2</i>	<i>PC1</i>	<i>PC2</i>
<i>Eigenvectors</i>	0.707	-0.707	0.707	0.707
	0.707	0.707	-0.707	0.707
<i>Eigenvalues</i>	1.520	0.497	1.335	0.682

Step 3. Selection of the amount of principal components (PCs) (the eigenvalues). By transforming the original variables, a linear combination which contributes a maximum to their total variance is generated, which is the first principal component. The second principal component not related to the first one occupies the largest residual variance, and so on until the total variance is analyzed. This selection is determined by the variance explained by each PC. The explained variance per PC is the eigenvalue of that PC divided by the sum of all eigenvalues.

Step 4. Calculation of principal component loading matrix. The principal component loading matrix which reflects how much a particular parameter is correlated with different factors, is obtained by premultiplying eigenvector with the square root of the eigenvalues. The loading matrix can be derived from:

$$A = Q \times D^{0.5} \quad (4.18)$$

With A is the loading matrix, Q is the eigenvector and D is the eigenvalue.

4.6.2 Interpretation of PCAs

The catchment characteristics are compared with S_r are very likely to be correlated, making it difficult to assess their individual relation with S_r . PCA is used to explore the dependencies between the characteristics, by means of the configuration of the vectors of the PCA. It can be explained that if the vectors present the same or similar direction the characteristics which the vectors represent are highly dependent and positively correlated; if the vectors show an inverse direction, it means that the characteristics are negatively correlated; whereas if the vectors present an orthogonal or similar orthogonal shape, the characteristics are highly uncorrelated. These three configurations are illustrated in Fig 4.13. It is noted that the longer a vector is, the higher the loadings, and thus the more influence the vector has on the total analysis. Furthermore, as a PCA only shows the relative similarities and differences within the data used for the PCA, only the relative directions of the vectors and the relative length differences of the vectors are important (de Boer-Euser et al., 2019).

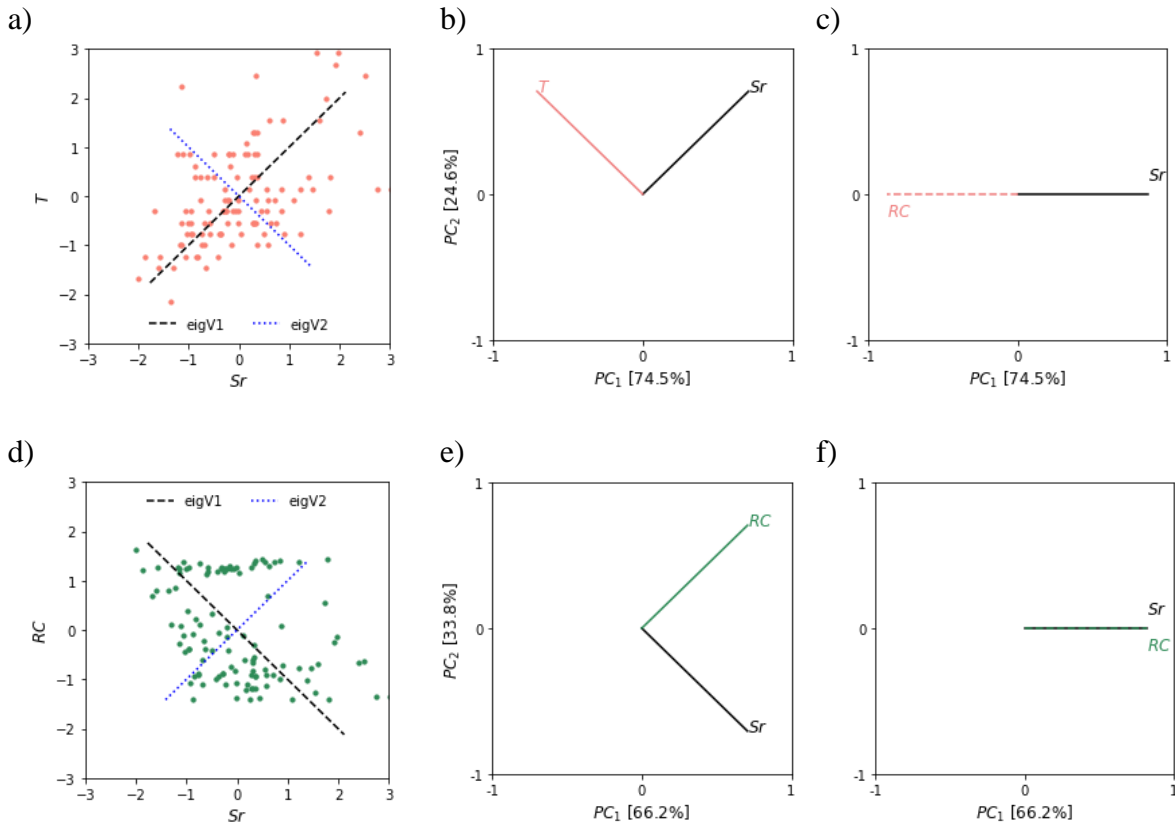


Figure 4.12 Examples showing the PCA processing. The three graphs a, b, c (in red) present the relation between S_r and T , and c, d, e (in green) present the relation between S_r and RC . a) and d) present variables (dots) with eigenvectors (dashed lines); b) and e) present PCA results; c) and f) present the loading values for PC1.

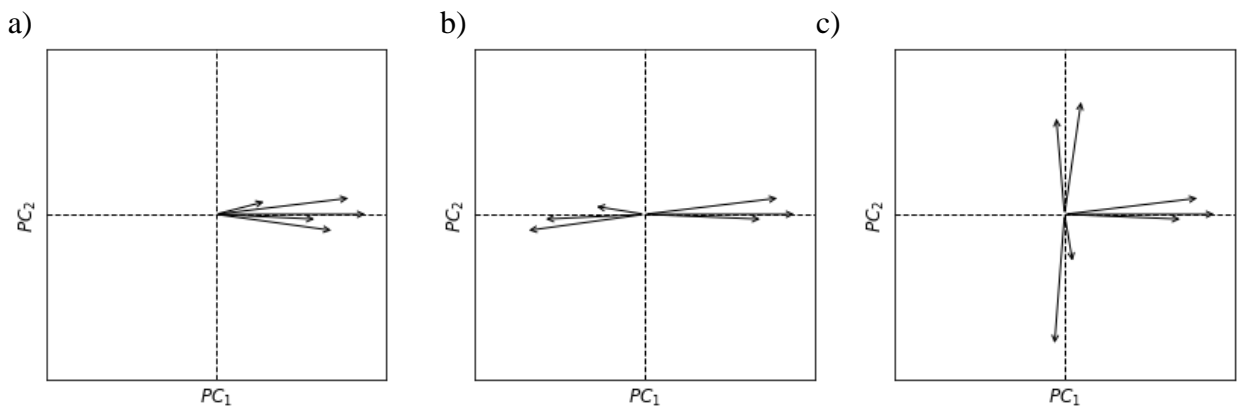


Figure 4.13 Illustration of possible relationships for PCA results: each vector represents a characteristic. The axes are formed by the first two components (PCs). a) highly dependent and positive correlated, b) highly dependent and negative correlated, c) highly uncorrelated. Note that the three diagrams just illustrate relatively ideal conditions.

4.7 K-Means clustering

The objective of clustering algorithm is to group the catchments into several clusters such that the catchments within a cluster are similar while there is dissimilarity between the catchments in different clusters. K-Means clustering (MacQueen, 1967) is a method commonly used to automatically partition a data set into k clusters. For a dataset $X = \{x_1, x_2, \dots, x_n\}$ that contains n dimensional data values, where $x \in R^d$, and the number of data subsets k which are expected to be generated, the K-Means clustering algorithm organizes the data objectives into k clusters. Each cluster has a centroid. Calculate the sum of the squared distances of the data points in the cluster to the cluster centroid, selecting Euclidean distance as the similarity and the criterion to identify the distance.

$$J(c_k) = \sum_{x_i \in C_k} \|x_i - \mu_k\|^2 \quad (4.19)$$

The objective of clustering is to find the minimum sum of distance $J(C) = \sum_{k=1}^K j(c_k)$.

$$J(C) = \sum_{k=1}^K j(c_k) = \sum_{k=1}^K \sum_{x_i \in \mu_k} \|x_i - \mu_k\|^2 = \sum_{k=1}^K \sum_{i=1}^n \|x_i - \mu_k\|^2 \quad (4.20)$$

$$d_{ki} = \begin{cases} 1, & \text{if } x_i \in c_i \\ 0, & \text{if } x_i \notin c_i \end{cases} \quad (4.21)$$

With u_k is the mean value of each cluster. The K-Means clustering algorithm starts with an initial k clusters, and then assigns each data to various clusters to reduce the total sum of squares of distances. Since the total sum of squares of distances in the K-Means algorithm tends to decrease with the increase of the number of clusters (when $k = 0, J(c) = 0$). Therefore, the total sum of squared distances can only reach the minimum value under a certain number of k . The K-Means algorithm is an iterative process which includes four steps (Isik and Singh, 2008).

- 1) divide the data into k initial clusters,
- 2) calculate the means or centroids of the k clusters,
- 3) for each case, calculate its distance to each center and assign it to the closest center,
- 4) repeat Step 2 and 3 until no cases are reassigned

In this study, the data as the input for K-Means is derived from PCA results. The transformed catchment characteristics, including climate and hydrological signatures, and vegetation signatures. They are introduced in section 4.3 and 4.4.

5

Results

In this chapter, the results obtained by Hamon potential evaporation method, climate-derived root zone storage capacity, catchment characteristics and Principal Component Analysis (PCA) combined with K-Means clustering will be discussed. The results of potential evaporation are derived with the methodology described in Section 4.1. Then the long-term discharge, precipitation, potential evaporation time series are used for estimating root zone storage capacity, and the climate signatures are together discussed in section 5.1. Furthermore, the climatic data and vegetation data are used to calculate hydrological signatures and vegetation signatures, using the methodology presented in section 4.4. Subsequently these characteristics are compared with root zone storage capacity by means of PCA method, and the correlation between them will be discussed in section 5.1. Finally, the catchments will be grouped into several clusters with specific characteristics, shown in section 5.3. These outputs can be summarized into two parts: 1) estimation of climate-derived root zone storage capacity, 2) analysis of the relation between S_r and catchment characteristics.

5.1 Root zone storage capacity and climate signatures

The climate-derived root zone storage capacity (S_r) is estimated based on long-term daily discharge, precipitation and potential evaporation time series. Fig 5.1 provides an overview of the long-term mean annual values. The precipitation (P), in general, catchments located in coastal areas have higher precipitation whereas those located in inland areas with lower values. In southeast, the southeast trade wind and a warm current provide more precipitation and higher temperature; in eastern Australia, the southeast monsoon blows in summer and there is more precipitation, winter is in the opposite, and the warm current also leads to more rainfall; in southeast Australia, it is affected by the mid-latitude westerly wind, there is mild temperature and precipitation; in southwestern Australia, the Mediterranean climate controls this area and the precipitation is sufficient. In the middle and south Australia, where there is affected by high pressure and southeast trade wind, the precipitation is relatively low. The potential evaporation (E_p) is calculated by means of Hamon Evapotranspiration method. In general, the potential evaporation distribution is consistent with latitude, and is influenced by the the Pacific Ocean, the Indian Ocean and the monsoon (southeast coastal area), the potential evaporation decreases from north to south and from west to east. It can be seen that the catchments in Tasmania (TAS) enjoy the most minimum E_p , and although the catchments in the south of Queensland (QLD) and Northern Territory (NT) are located in similar latitude, those in NT present higher level, compared with those in QLD.

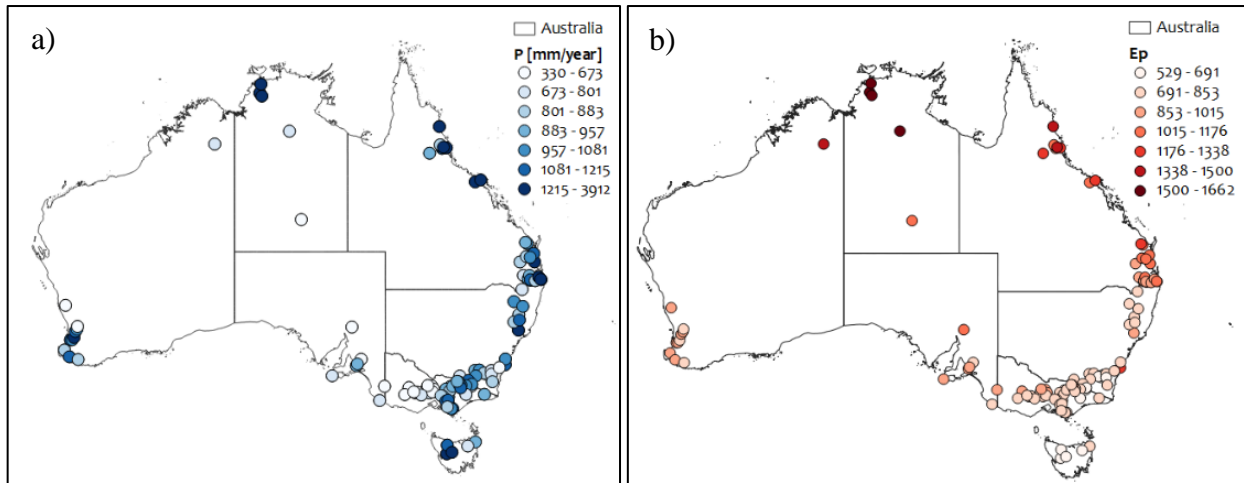


Figure 5.1 Map with study catchment and a) mean annual precipitation, b) mean annual potential evaporation. Light colors mean lower values and dark colors mean higher values for all.

Focusing first on the relation between S_r and the absolute difference, Fig. 5.2 (a) shows the spatial patterns of S_r and aridity index. According to the regions, the S_r values can be divided into (I) north in Northern Territory, (II) northeast in Queensland, (III) east in the junction between Queensland and New South Wales, (IV) southeast in New South Wales, Victoria and Tasmania, (V) south in South Australia, and (VI) southwest in Western Australia. It is clear that S_r values in east to southeast (II, III, IV) have lower values than those in north and southwest (I, VI). Note that the six catchment classes just rely on the locations, which is convenient for description. For the catchments in north (I), South (V) and southwest (VI) regions larger S_r generally coincide with smaller AI , but for the north and east pattern this is less clear. The same can be observed from Fig 5.3, the classes VI and V show negative relations between S_r and AI , whereas for other three classes, there is no clear trend.

Second, similarity index δ presents seasonality and the timing of precipitation. The values equal 1 (the value larger than one represents long term drought period without any precipitation) means precipitation is in phase with potential evaporation, -1 means precipitation is out of phases with potential evaporation and 0 means uniform precipitation throughout of the year. It can be seen from Fig 3.2 (b), the values generally decrease from north and northeast to south and southwest, meaning that in north and east high precipitation and high potential evaporation occurs in the same months (summer), whereas in south and west, high precipitation occurs in winter and potential evaporation in summer. Fig 3.3 (b) offers numerable description. It is convinced that the catchments are divided into two categories of which the values in north and east (I, II, III) present positive relation between S_r and δ , and negative relation in south and west. This indicates that the consistence of P and Ep have a strong correlation with S_r .

As supplements, separate seasonality index of precipitation IS_P , potential evaporation IS_{Ep} are also derived, shown in Fig 5.2 (d, e). From the map Fig 5.2 (c, d), it seems that high S_r is consistent with high IS_P , especially in north, east and southwest, while the relation between S_r and IS_{Ep} does not present clear results. Although high S_r values coincide with lower IS_{Ep} in north (NT) and east (QLD and NSW) and lower S_r values with higher IS_{Ep} in southwest (WA), however, there is no obvious correspondence for the catchments located in the south. From Fig 5.3 (c, d), in general, for all study catchments, the seasonal precipitation results in high root zone storage, whereas the seasonal potential evaporation is not significant, thus, this signature will not be taken into account for analysis for PCA. Combined with Fig 5.3 (e) the long-term mean temperature, which indicates that the absolute values of potential evaporation are more correlated with S_r .

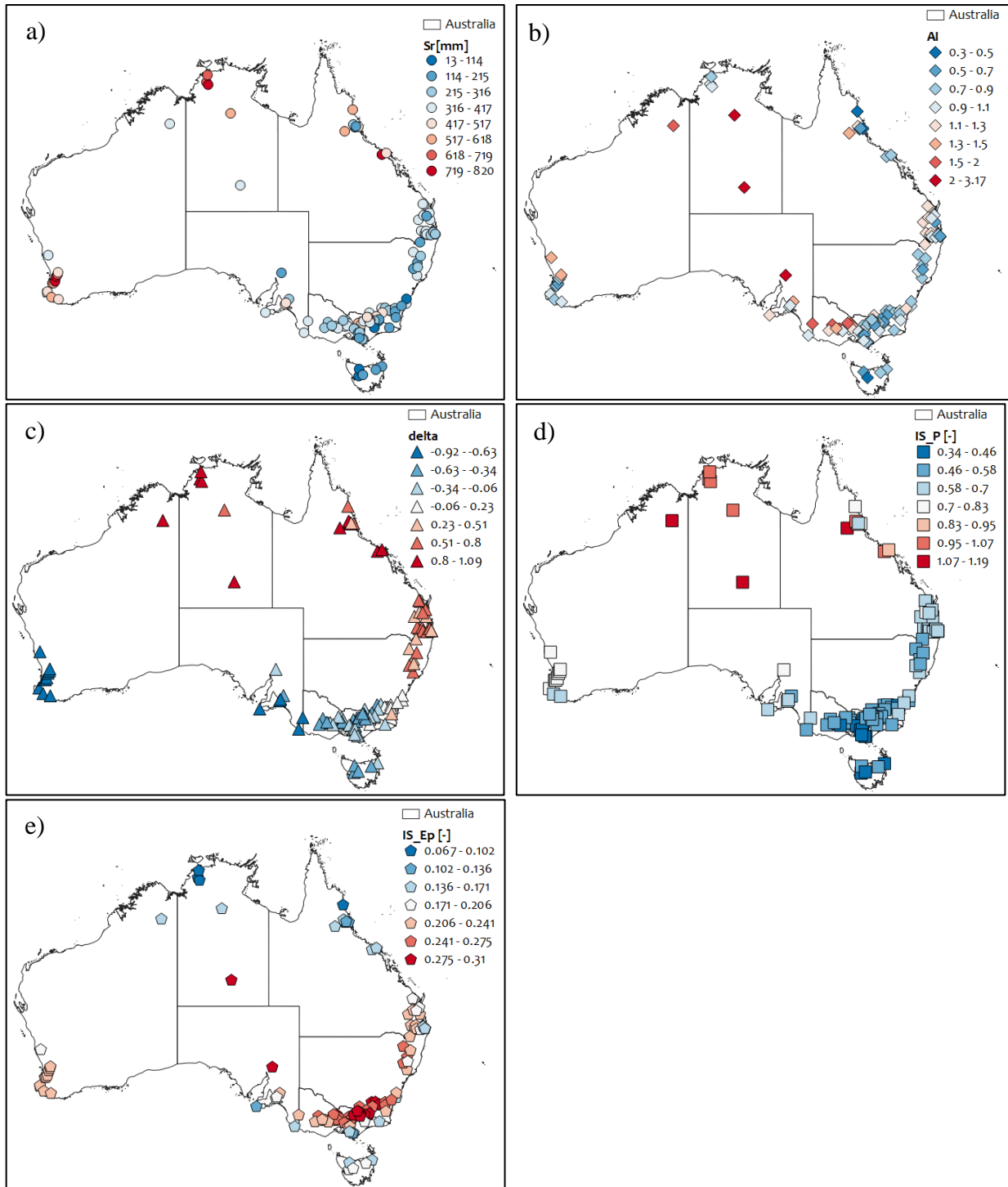


Figure 5.2 Map with study catchments and a) climate-derived root zone storage capacity S_r [mm], b) aridity index AI [-], c) similarity index δ [-], presenting the timing of precipitation, d) seasonality index of precipitation IS_p [-], e) seasonality index of potential evaporation IS_{Ep} [-]. The color changing from blue to white to red means the specific value ranges from lower to higher.

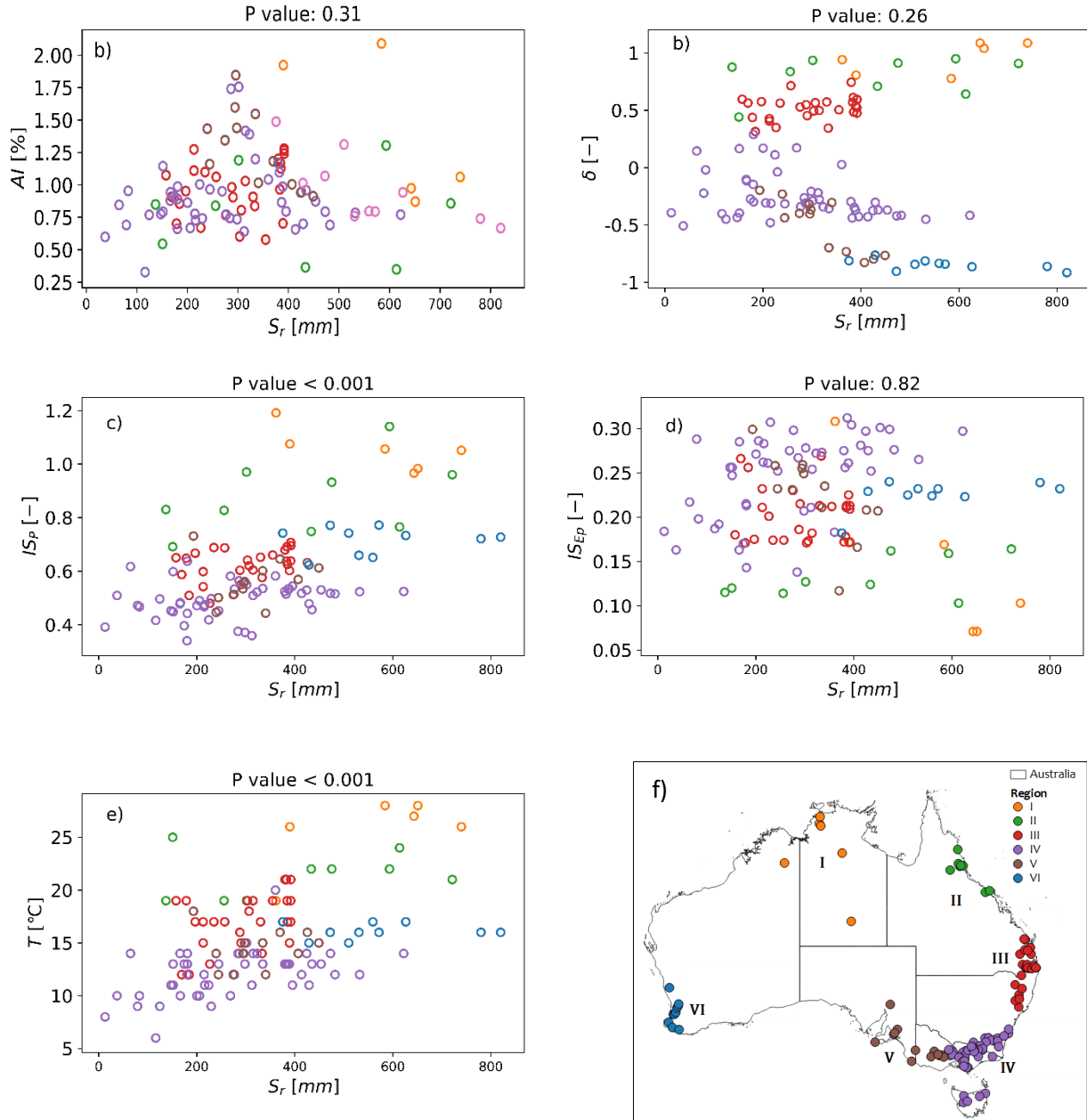


Figure 5.3 Root zone storage capacities and a) climate-derived root zone storage capacity S_r [mm], b) aridity index AI [-], c) similarity index δ [-], presenting the timing of precipitation, c) seasonality index of precipitation IS_p [-], d) seasonality index of potential evaporation IS_{Ep} [-], e) mean annual temperature T [°C], and f) a region-based classification for the catchments. **Note that this is a roughly climate-based and region-based classification in order to conveniently illustrate the relations between S_r and various signatures in the following sections.** The titles of the sub-plots show the Spearman's correlation coefficients of the whole catchments (significant correlation for $p < 0.05$).

5.2 Root zone storage capacity and hydrological signatures

Estimated root zone storage capacities are compared with hydrological signatures in the study catchments. Fig 5.4 S_r is compared with the various hydrological signatures, including the long-term mean annual discharge, the seasonality index of discharge, autocorrelation coefficient throughout the entire period and in low flow period, declining limb density, peak distribution of the entire period and of the low flow period. These signatures are generally reflecting the characteristics of discharge.

S_r is not significantly correlated with autocorrelation coefficients AC , AC_{low} and density declining limb DLD (Fig 5.4 c, d, f), both of which are representing the smoothness of hydrograph, although S_r values of the catchments in the north (Region I, orange dots) show a positive correlation with these signatures. Therefore, for a long-term discharge time series, a vast change in the discharge values cannot lead to a consistent larger root zone storage capacity. The correlation between S_r and runoff coefficient RC is pretty interesting, Fig 5.4 e. It is clear that for all catchments, there is a relatively negative correlation between the two, while the relation in different regions presents an entirely different trend. For the catchments in the north (Region I, orange dots), larger S_r values are consistent with larger RC ; for the catchments in the east, large S_r values coincide with smaller RC but for the northeast and southwest the relation is unclear. The most interesting is the obvious difference in the southeast to the south region (Region IV and V, purple and brown dots), the catchments are divided into two groups, one presents a negative correlation between S_r and RC , another one has high RC and is weakly correlated. Actually, the southeast region is dominated by a cool temperate or alpine climate. The monsoon from Pacific Ocean, the middle-latitude westerlies, and the terrain conditions together act in this region, showing large differences, subsequently resulting in the catchments cannot be simply grouped based on locations.

S_r is compared with peak distribution PD and peak distribution in low flow period PD_{low} , Fig 5.4 e) and f). Overall, for PD throughout the entire period, the distinction between the north (Region I, II) and the south (Region IV and V, purple and brown dots) is conspicuous. It can be seen that S_r is positively correlated with PD in the north, while weakly correlated in the south. However, it is different from the similar result of AC and AC_{low} , the PC_{low} presents apparently different relation compared with PD . For these catchments located in the north, peak distribution is no longer critical, while for those in the south, higher peak distribution in low flow period (generally in summer period for this region) can lead to lower S_r . As for the east and southwest, the peak distribution is not an important signature.

Eventually, according to Spearman's correlation coefficient and the visualization results, the runoff coefficient RC and the peak distribution during low flow period PD_{low} are considered to be the input signatures for PCA and K-Means clustering. The map of root zone storage capacity compared with RC and PD_{low} are presented in Fig 5.5. It is a supplement for Fig 5.4, which visualized the value distribution of S_r and hydrological signatures. For most catchments, the discharge (Q), it can be seen from Fig 5.5b that the high discharges are mostly distributed in the eastern coastal area, especially in the northeast in QLD, the southeast in Victoria (VIC) and in TAS, the middle and western area present lower levels. Fig 5.5c and d, high S_r values and low RC co-occur in the north, the east and southwest (Region I, II, III and VI, orange, green, red and blues dots). S_r in the southeast to the south, part of catchments mainly located in VIC and TAS have present opposite values between S_r and RC , in contrast, others in NSW and SA present coincident values between S_r and RC . As for the relation with PD_{low} , clear opposite values can be observed in the north, east and southwest (Region I, II, III and VI, orange, green, red and blues dots). The condition in southeast is complicated, catchments present opposite results in TAS and consistent results in SA, while noncommittal results in VIC and the south of NSW.

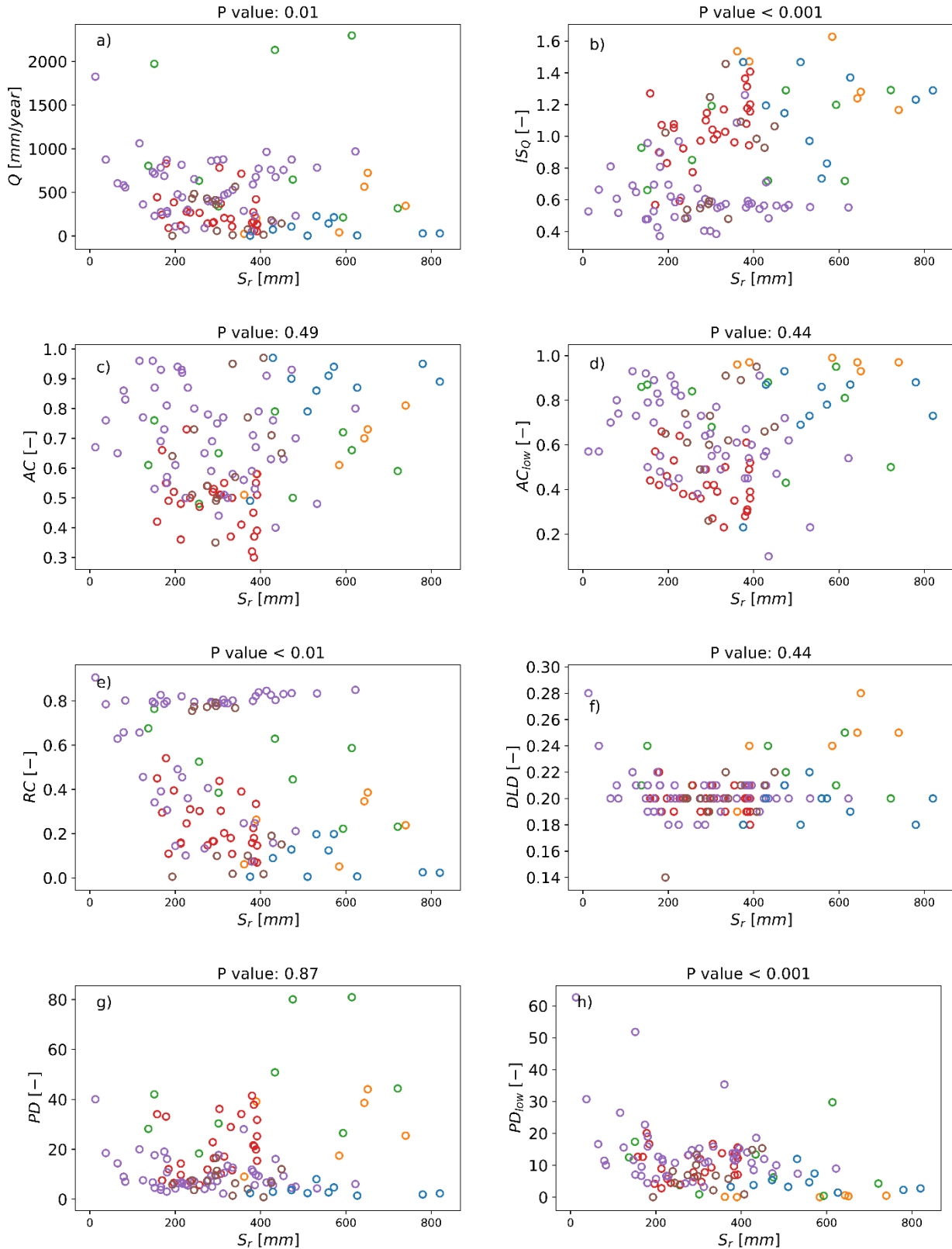


Figure 5.4 Root zone storage capacities and a) long-term mean discharge Q [mm], b) seasonality index of discharge IS_Q [-], c) autocorrelation coefficient AC [-], d) autocorrelation coefficient in low flow period AC_{low} [-], e) runoff coefficient RC , f) declining limb density DLD [-], g) peak distribution PD [-], h) peak distribution in low flow period PD_{low} [-]. The titles of the sub-plots show the Spearman's correlation coefficients of the whole catchments (significant correlation for $p < 0.05$).

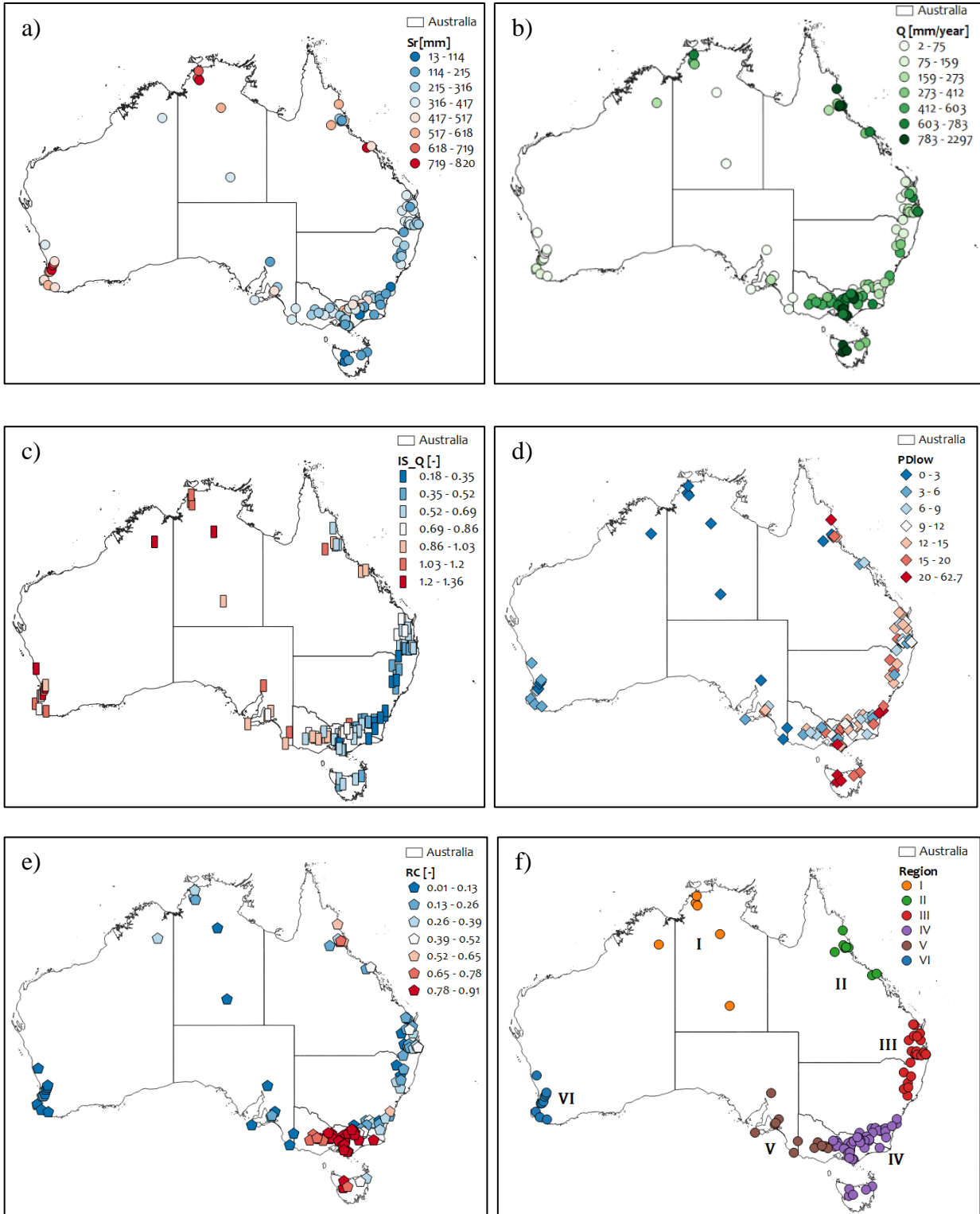


Figure 5.5 Map with study catchments and a) root zone storage capacity S_r [mm], b) mean annual discharge Q [mm], c) seasonality index of discharge IS_Q [-], d) runoff coefficient RC [-], e) peak distribution in low flow period PD_{low} , f) region classification. The color from blue to white to red represents an increase in value.

5.3 Root zone storage capacity and vegetation signatures

The climate-derived root zone storage capacities are compared with characteristics of the vegetation in the study catchments. It should be noted that the vegetation signatures in this study are not simply a description of vegetation themselves, but include land cover and land use types in a broader sense. In summary, the vegetation signatures include NDVI and EVI, the seasonality index of NDVI and EVI, vegetation types and irrigated agriculture conditions.

5.3.1 NDVI and EVI

Fig 5.6 S_r is compared with NDVI, EVI and the seasonality index of the two IS_{NDVI} and IS_{EVI} . Continue to follow the region classification described in Fig 5.3 g. Mean annual NDVI and EVI are negatively correlated with S_r when considering all catchments, while NDVI provides stronger correlation compared with EVI. The seasonality of NDVI and EVI present an extremely similar pattern, generally a positive correlation with S_r for all catchments. In terms of the catchments in different regions, S_r values of the catchments in the north (Region I and II, orange and green dots) and the southwest (Region VI, blue dots) show a positive correlation, whereas of the catchments from east to southeast to south, the correlation is insignificant. The condition with EVI presents a similar but less conspicuous correlation, except Region I (orange dots). For the seasonality index, as the two have a similar pattern, taking the seasonality index of NDVI for detailed explanations. For these location-based classes, there is no clear trend between S_r and any class. The visualization results are presented in Fig 5.5, high S_r coincides with high NDVI in the southwest, while low NDVI in other regions. In the north, the east and the southeast (the junction area between NSW and VIC, and TAS), higher S_r is consistent higher IS_{NDVI} , while in the southwest and the south (the region from VIC to SA), S_r and IS_{NDVI} present opposite results. As the results of NDVI and EVI present relatively consistent pattern and the correlation of NDVI is higher than EVI, eventually only the mean annual NDVI and the seasonality index of NDVI IS_{NDVI} are used for PCA.

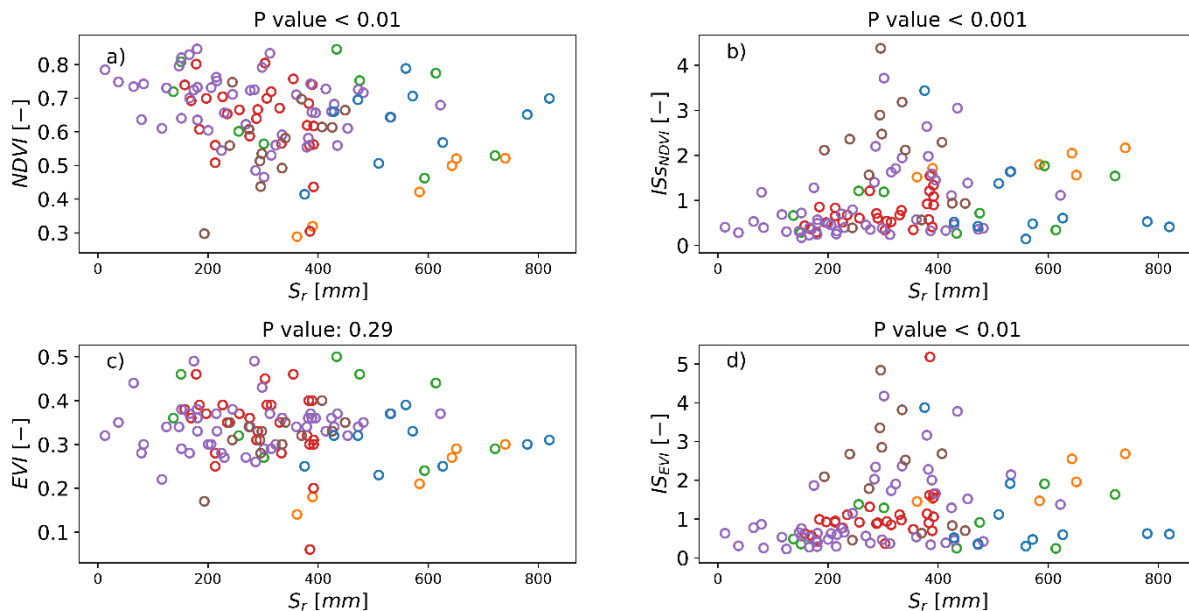


Figure 5.6 Root zone storage capacity S_r and a) mean annual NDVI, b) seasonality index of NDVI IS_{NDVI} , c) long-term mean annual EVI, d) seasonality index of EVI. The titles of the sub-plots show the Spearman's correlation coefficients of the whole catchments (significant correlation for $p < 0.05$). The six classes with different colors are the same with the classification shown in Fig 5.3.

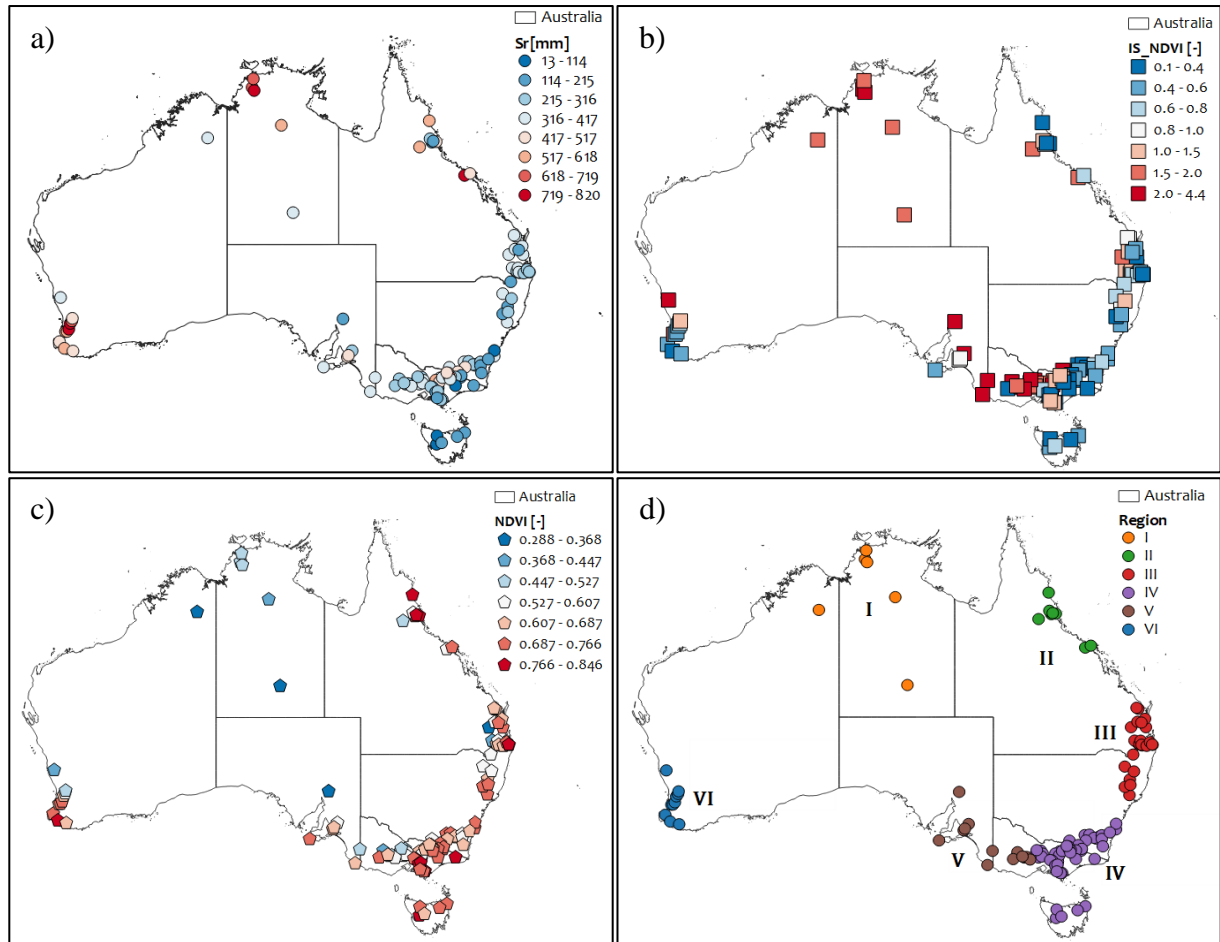


Figure 5.7 Map with study catchments and a) root zone storage capacity S_r [mm], b) runoff coefficient RC [-], c) peak distribution in low flow period PD_{low} , d) region classification. The color from blue to white to red represents an increase in value.

5.3.2 Land cover and land use

The land cover, vegetation types can also have a significant influence on the climate-derived S_r , mainly because different vegetation types have various transpiration patterns and survival strategies. Furthermore, land use, especially for agricultural purposes, which artificially changes the natural vegetation patterns. The irrigated agriculture can change the input and output of the water system, meaning that additional water is added to the root zone from groundwater or the extraction of runoff for irrigation, both of the surface water irrigation or groundwater irrigation can break the long-term water balance. Thus, irrigated agriculture is also considered.

Fig 5.8 comparing root zone storage capacity S_r and total forests R_{TF} , eucalypt forests R_E , other forests R_{OF} and irrigated agriculture R_I . The first three figures (a, b, c) illustrate the vegetation area distribution in different catchments. It is recognized that eucalyptus has a very broad distribution in Australia. Except for the catchments in the northeast (Region II, green dots) that are mostly dominated by rain forests, most of the other forests in the catchments account for no more than 40%, and most of them are less than 20%. Even R_{OF} in many catchments are almost negligible, especially in the southwest, part of the southeast (Region IV, V and VI; purple, brown and blue dots). According to the few data available for analysis, S_r is negatively correlated with other forests, especially for the Region II (rainfall forests-dominated), larger other forests area leads to lower S_r values. As for eucalypt, firstly the S_r values are not highly correlated with eucalypts, and secondly, there is no obvious relation between S_r and eucalypt when considering all catchments. A positive correlation exists in the north (Region I, II and VI; orange, green and blue dots), whereas for other regions, the correlation tends to be negative. Fig 5.8 d) presents comparing S_r and irrigated agriculture. It can be seen that for most catchments, the irrigation area is zero, the catchments with non-zero values show a positive correlation for S_r and R_I . Considering the zero-value might affect the precision, this signature is not taken into account for PCA. As supplementations, Fig 5.9 provides another illustration. Here all sub-figures show the total forests versus S_r . For the five sub-figures, the circle in the same location means the same catchment. It is figured out that the catchments with larger eucalypt forests have less other forests as well as irrigated agriculture. Fig 5.10 provides the distribution map, comparing S_r and these characteristics.

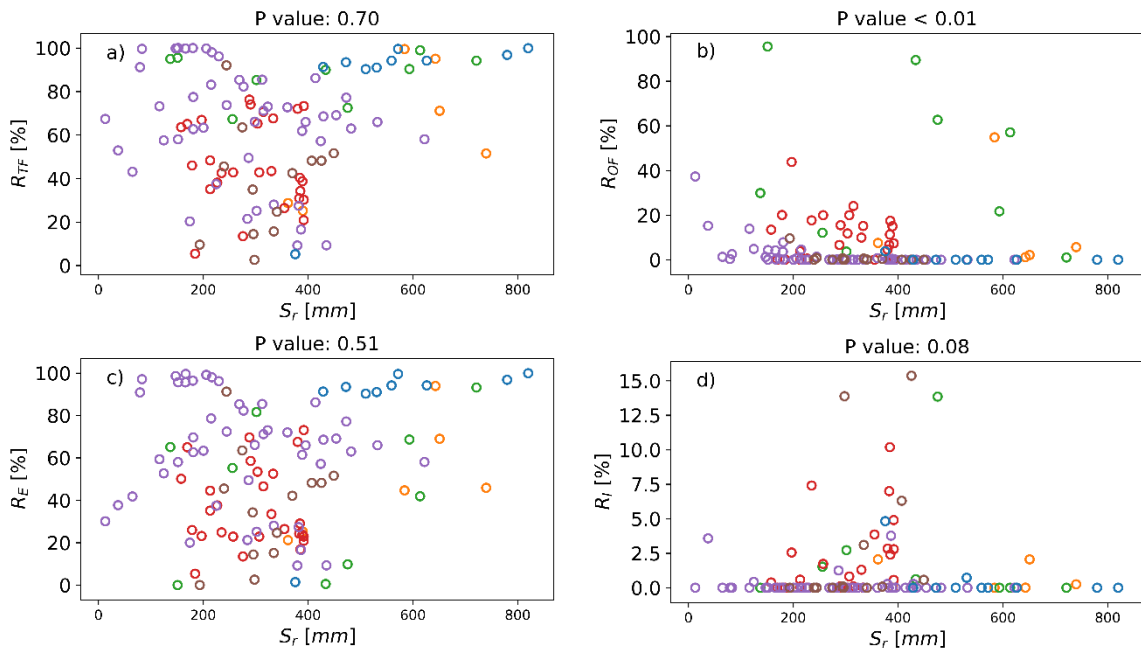


Figure 5.8 Root zone storage capacity S_r and a) total forests R_{TO} [%], b) eucalypt forests R_E [%], c) other forests R_{OF} [%], and d) irrigated agriculture R_I [%]. Note that these values are the proportion of vegetation in the study catchments.

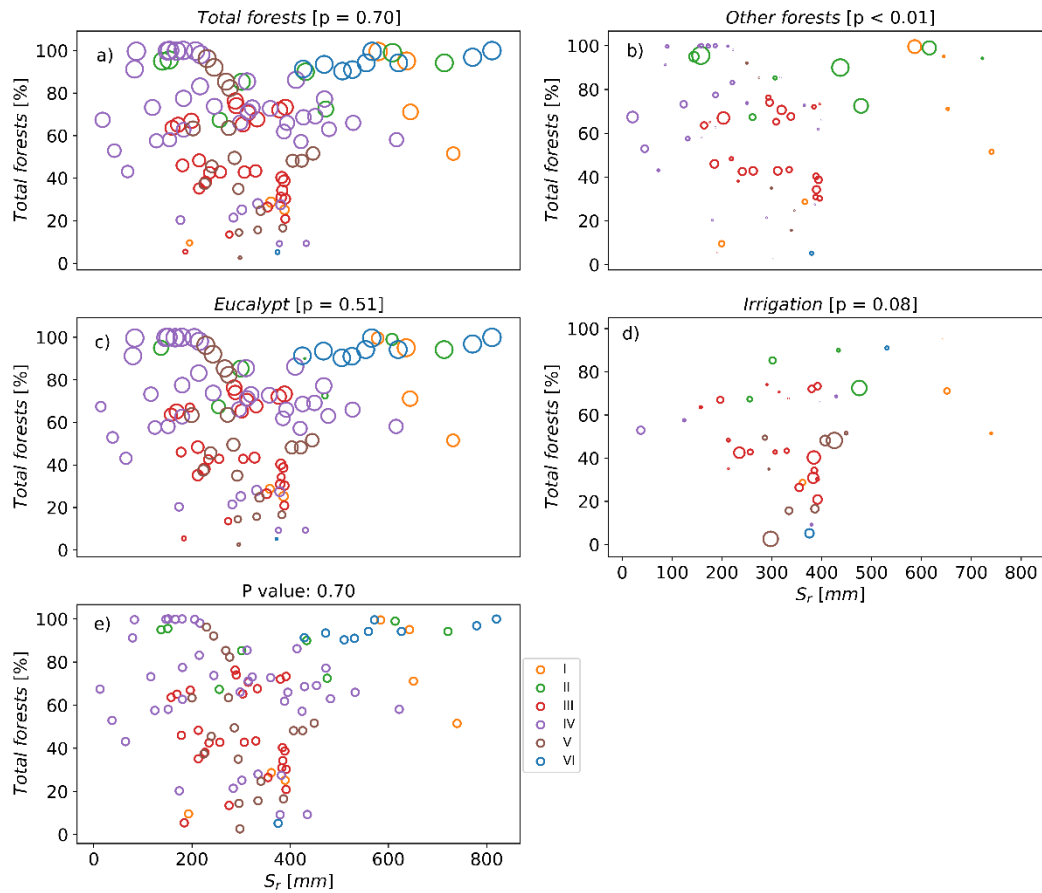


Figure 5.9 Total forests versus root zone storage capacity S_r . Larger circle means higher percentage of vegetation type or land use type for a) eucalypt forests [%], b) other forests proportion [%], c) total forests, the sum of eucalypt and other forests [%], d) irrigated agriculture [%]; and e) present the relationship between S_r and total forests. The titles of the sub-plots show the specific types with the Spearman's correlation coefficients of the whole catchments (significant correlation for $p < 0.05$).

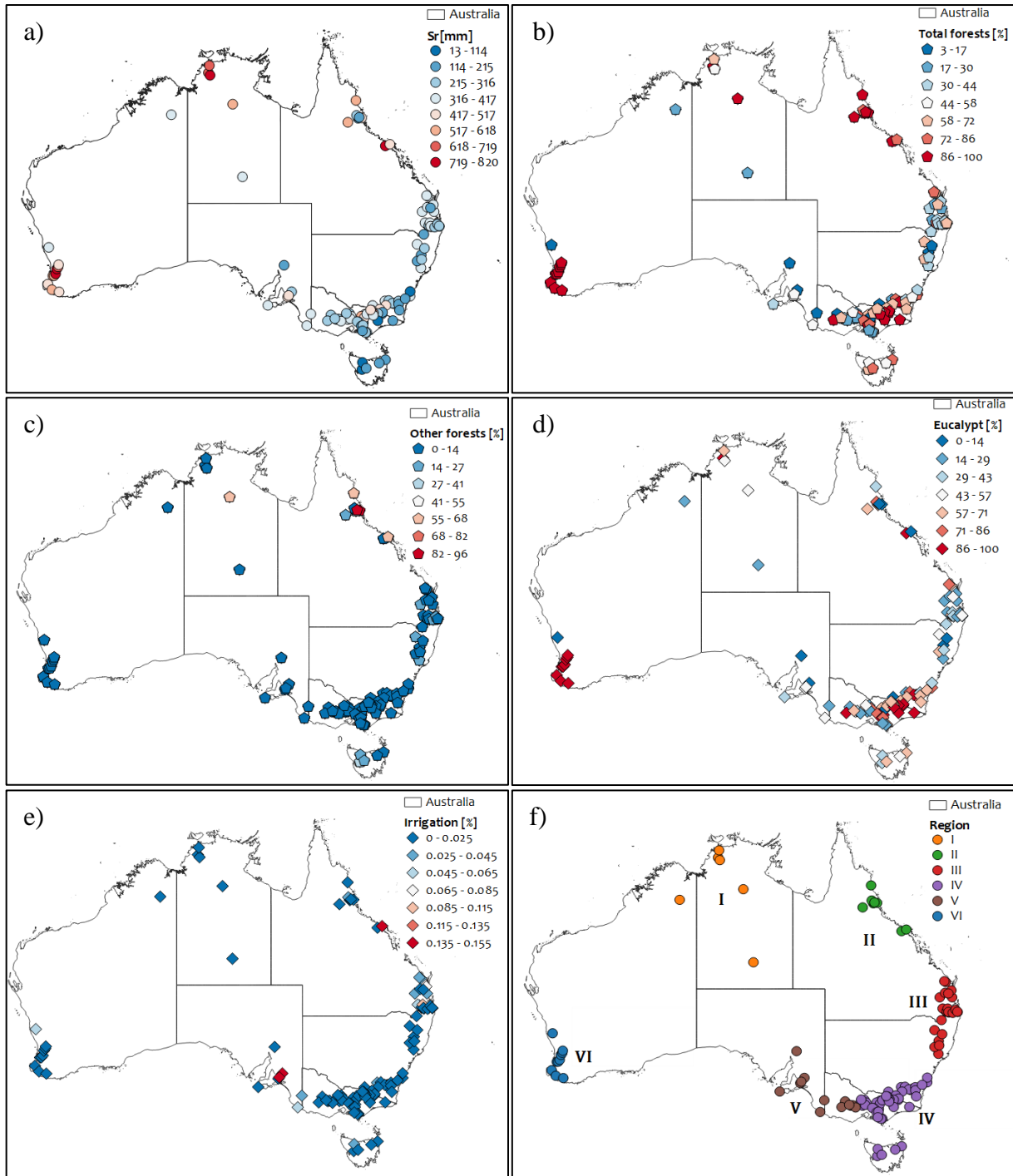


Figure 5.10 Map with study catchments a) root zone storage capacity S_r [mm], b) total forests R_{TO} [%], c) eucalypt forests R_E [%], d) other forests R_{OF} [%], and e) irrigated agriculture R_I [%], f) region classification. The color from blue to white to red represents an increase in value.

5.4 Principal component analysis (PCA)

5.4.1 Input for PCA

Based on the results of the aforementioned, the signatures as input for PCA are identified, including:

- a. Root zone storage capacity (S_r).
- b. The climate signatures: long term mean annual precipitation (P), discharge (Q), potential evaporation (E_p) and temperature (T); the seasonality index of precipitation (IS_P), potential evaporation (IS_{E_p}) and discharge (IS_Q); and the similarity index (δ).
- c. Hydrological signatures: Runoff coefficient (RC), peak distribution (PD) and peak distribution in low flow period (PD_{low}).
- d. Vegetation signatures: Normalized difference vegetation index $NDVI$, the seasonality index of $NDVI$ (IS_{NDVI}), eucalyptus (R_E), other forests (R_{OF}) and total forests (R_{TF})

5.4.2 PCA results

The PCA results are derived from the correlation matrix of the signatures. To illustrate what the PCAs results are based on, the correlation matrix is presented in Table 5.1. According to the principal component loading matrix obtained from correlation matrix reveals that the first three components together account for about 70.8% of the total explained variance. Here the eigenvectors and eigenvalues are presented in Table 5.2 and the first three component loading values are listed in Table 5.3. The PCA results for the catchments of all signatures are shown in Fig 5.11.

The first component is strongly correlated (loadings of more than 0.8) with long-term mean temperature (or potential evaporation derived from temperature), the seasonality index of precipitation, and moderately (loadings of more than 0.6) correlated with the seasonality index of potential evaporation and discharge, the similarity index and peak distribution. It can be seen that S_r and temperature; the seasonality index of precipitation and discharge and the similarity index have a strong positive correlation; S_r and the seasonality index of potential evaporation are negatively correlated. Other signatures do not show a high influence on the first component. The first component can be regarded as climate-dominated. Thus, the change in climate conditions might lead to a higher S_r value. The second component is strongly correlated with a long term mean annual discharge, $NDVI$, and precipitation, and moderately influenced by runoff coefficient and other forests, as well as the seasonality of $NDVI$. In this component, the climate signatures and hydrological signatures separately show correlation with inner characteristics, but the relationship with S_r is not clear. The third component is strongly related to forests index, especially the eucalypt plays as a significant role, and moderately correlated with the seasonality index of $NDVI$. This component can be regarded as vegetation-dominated.

Three components are considered. For the first two components Fig 5.11 a, which presents the most important relationships among all of the signatures. For each climatic signature, the majority are positively correlated with each other and S_r , but negatively correlated with potential evaporation seasonality. For hydrological signatures, both higher runoff coefficient and peak distribution in low flow period result in lower S_r , while higher peak distribution throughout the entire period is consistent with higher S_r . For vegetation signatures, there is a clear difference between eucalypt forests and other forests, the former is negatively related to S_r and the latter is positively related to S_r . The total forests, compromise considering the effects of eucalypts and other forests located in the middle. $NDVI$ which reflects the whole vegetation condition is plausibly presenting a similar pattern with eucalypt forests. according to the loading values of S_r for PC_1 , PC_2 and PC_3 are 0.46, -0.26, and 0.39 respectively. Although the third component takes up a lower explained ratio, while

it is higher related to S_r , compared with the second component. Fig 5.11b present the most relevant components (PC_1 and PC_3), it is clear that the climate signatures and vegetation signatures are less correlated, especially temperature, potential evaporation, precipitation and the seasonality index of three are present an approximate orthogonal relationship with eucalypt, total forests, $NDVI$ and $NDVI$ seasonality. Only other forests show a positive correlation with these climatic signatures, except for potential evaporation seasonality, and discharge is positively correlated with $NDVI$ seasonality but negatively correlated with others. The interesting is S_r just located in the middle between climate signatures and vegetation signatures, which means climate change and vegetation change can significantly lead to the change of S_r , although they do not present a direct correlation, S_r can be the bridge. At the same time, the hydrological signatures, runoff coefficient, and peak distribution in the low flow period, show a negative correlation with S_r , whereas peak distribution of the entire period a positive correlation.

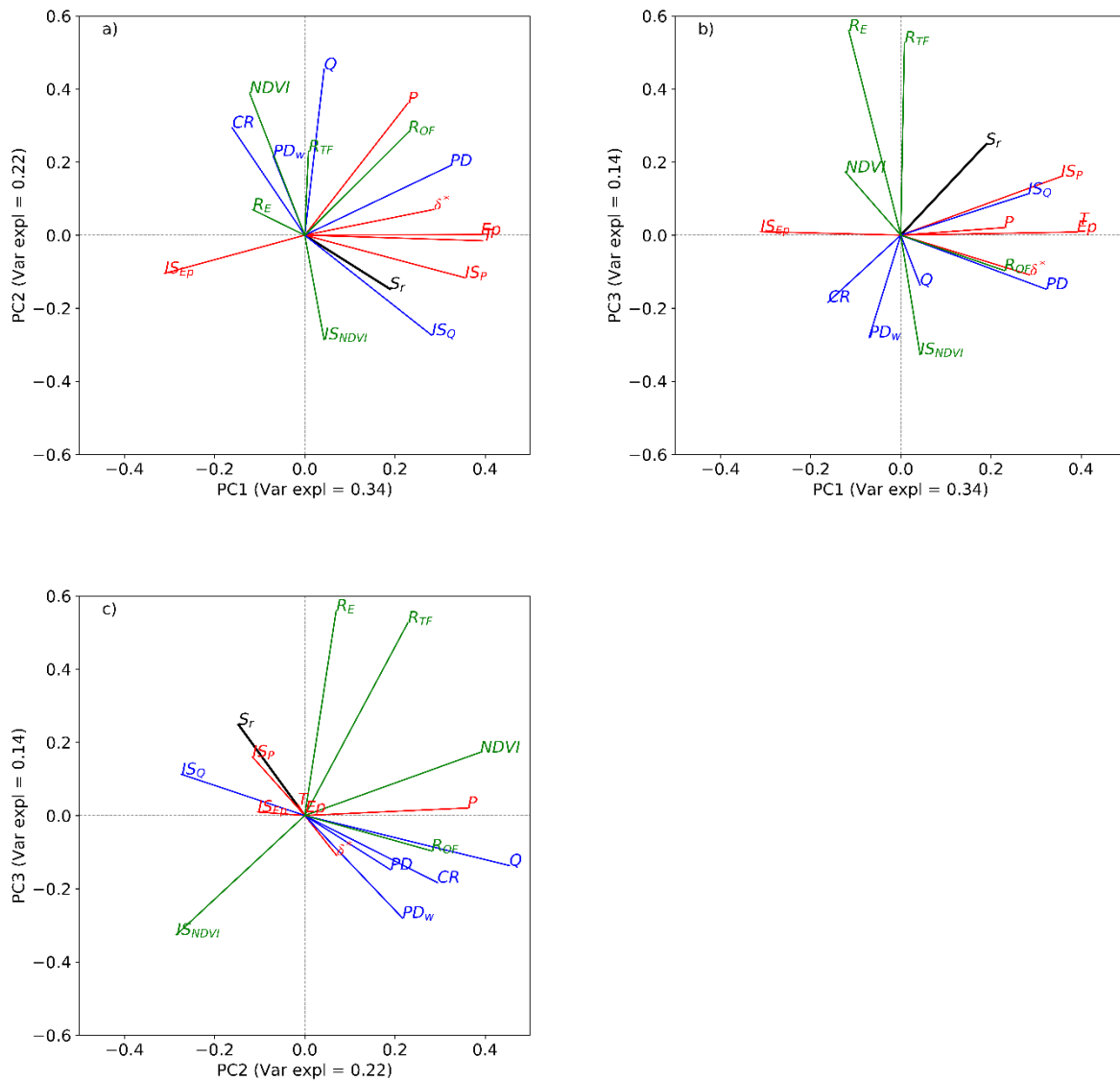


Figure 5.11 Principal component analysis with the catchment characteristics and S_r in this study. S_r and catchment characteristics with their loading on, a) PC_2 versus PC_1 , b) PC_3 versus PC_1 and d) PC_3 versus PC_2 . The signatures shown in different colors: S_r (black), climate signatures (red), hydrological signatures (blue) and vegetation signatures (green).

Table 5.1 Correlation matrix of the selected signatures

	S_r	T	P	Ep	Q	IS_P	IS_{Ep}	IS_Q	δ	RC	PD	PD_{low}	$NDVI$	IS_{NDVI}	R_E	R_{OF}	R_{TF}
S_r	1	0.50	0.25	0.48	-0.11	0.55	-0.11	0.41	-0.06	-0.32	0.16	-0.35	-0.28	0.21	0.14	-0.03	0.13
T	0.50	1	0.46	0.98	0.08	0.84	-0.70	0.62	0.60	-0.31	0.69	-0.22	-0.27	0.13	-0.22	0.47	0.04
P	0.25	0.46	1	0.47	0.73	0.28	-0.49	0.02	0.34	0.06	0.69	0.20	0.39	-0.34	-0.09	0.68	0.29
Ep	0.48	0.98	0.47	1	0.13	0.81	-0.67	0.57	0.62	-0.24	0.71	-0.18	-0.28	0.15	-0.21	0.47	0.04
Q	-0.11	0.08	0.73	0.13	1	-0.13	-0.21	-0.51	0.10	0.70	0.44	0.33	0.49	-0.19	-0.06	0.56	0.25
IS_P	0.55	0.84	0.28	0.81	-0.13	1	-0.57	0.70	0.51	-0.43	0.51	-0.33	-0.41	0.15	-0.02	0.31	0.15
IS_{Ep}	-0.11	-0.70	-0.49	-0.67	-0.21	-0.57	1	-0.42	-0.53	0.18	-0.60	0.08	-0.01	0.05	0.18	-0.46	-0.07
IS_Q	0.41	0.62	0.02	0.57	-0.51	0.70	-0.42	1	0.33	-0.80	0.33	-0.25	-0.49	0.14	-0.15	0.09	-0.10
δ	-0.06	0.60	0.34	0.62	0.10	0.51	-0.53	0.33	1	-0.17	0.67	-0.06	-0.16	-0.10	-0.27	0.42	-0.05
RC	-0.32	-0.31	0.06	-0.24	0.70	-0.43	0.18	-0.80	-0.17	1	-0.03	0.25	0.33	0.07	0.08	0.04	0.11
PD	0.16	0.69	0.69	0.71	0.44	0.51	-0.60	0.33	0.67	-0.03	1	0.27	-0.06	0.00	-0.26	0.52	0.02
PD_{low}	-0.35	-0.22	0.20	-0.18	0.33	-0.33	0.08	-0.25	-0.06	0.25	0.27	1	0.25	-0.13	-0.18	0.10	-0.13
$NDVI$	-0.28	-0.27	0.39	-0.28	0.49	-0.41	-0.01	-0.49	-0.16	0.33	-0.06	0.25	1	-0.73	0.30	0.19	0.41
IS_{NDVI}	0.21	0.13	-0.34	0.15	-0.19	0.15	0.05	0.14	-0.10	0.07	0.00	-0.13	-0.73	1	-0.40	-0.18	-0.52
R_E	0.14	-0.22	-0.09	-0.21	-0.06	-0.02	0.18	-0.15	-0.27	0.08	-0.26	-0.18	0.30	-0.40	1	-0.33	0.85
R_{OF}	-0.03	0.47	0.68	0.47	0.56	0.31	-0.46	0.09	0.42	0.04	0.52	0.10	0.19	-0.18	-0.33	1	0.21
R_{TF}	0.13	0.04	0.29	0.04	0.25	0.15	-0.07	-0.10	-0.05	0.11	0.02	-0.13	0.41	-0.52	0.85	0.21	1

Table 5.2 Eigenvectors and eigenvalues

	S_r	T	P	Ep	Q	IS_P	IS_{Ep}	IS_Q	δ	RC	PD	PD_{low}	$NDVI$	IS_{NDVI}	R_E	R_{OF}	R_{TF}	Eigenvalues
PC_1	0.19	0.40	0.23	0.39	0.04	0.36	-0.31	0.28	0.29	-0.16	0.32	-0.07	-0.12	0.04	-0.12	0.23	0.01	5.88
PC_2	-0.15	-0.02	0.36	0.00	0.45	-0.12	-0.10	-0.27	0.07	0.29	0.19	0.22	0.39	-0.28	0.07	0.28	0.23	3.85
PC_3	0.25	0.03	0.02	0.01	-0.14	0.16	0.01	0.11	-0.11	-0.18	-0.15	-0.28	0.17	-0.33	0.56	-0.10	0.53	2.42

Table 5.3 The first three principal component loading matrix of the selected signatures.

	S_r	T	P	Ep	Q	IS_P	IS_{Ep}	IS_Q	δ	RC	PD	PD_{low}	$NDVI$	IS_{NDVI}	R_E	R_{OF}	R_{TF}	Eigenvalues
PC_1	0.46	0.96	0.55	0.95	0.10	0.86	-0.75	0.68	0.69	-0.39	0.78	-0.17	-0.30	0.10	-0.28	0.56	0.02	5.88
PC_2	-0.29	-0.03	0.71	0.00	0.89	-0.23	-0.21	-0.54	0.14	0.58	0.37	0.42	0.76	-0.56	0.14	0.55	0.45	3.85
PC_3	0.39	0.05	0.03	0.01	-0.21	0.25	0.02	0.18	-0.17	-0.28	-0.23	-0.44	0.27	-0.51	0.87	-0.15	0.82	2.42

5.5 K-Means clustering

5.5.1 Catchments clustering results

For K-Means clustering method, the transformed signatures, that are, the eigenvector values of the first three component from PCA are the input to the model. According to the region-based classification which is illustrated in section 5.1 (Fig 5.3g) and several adjustments, four outlets have been removed, the 109 catchments are divided into eight clusters, which means $k = 7$ for K-Means model. The clustering results are presented in Fig 5.11 with a three-dimension plot including all the first three principal components and three two-dimensional diagrams, which present the projections of PC_1 and PC_2 , PC_1 and PC_3 , PC_2 and PC_3 , respectively. Fig 5.13 provides the root zone storage capacities distribution throughout Australia. Note that in all the figures below, the same color represents a specific catchment cluster.

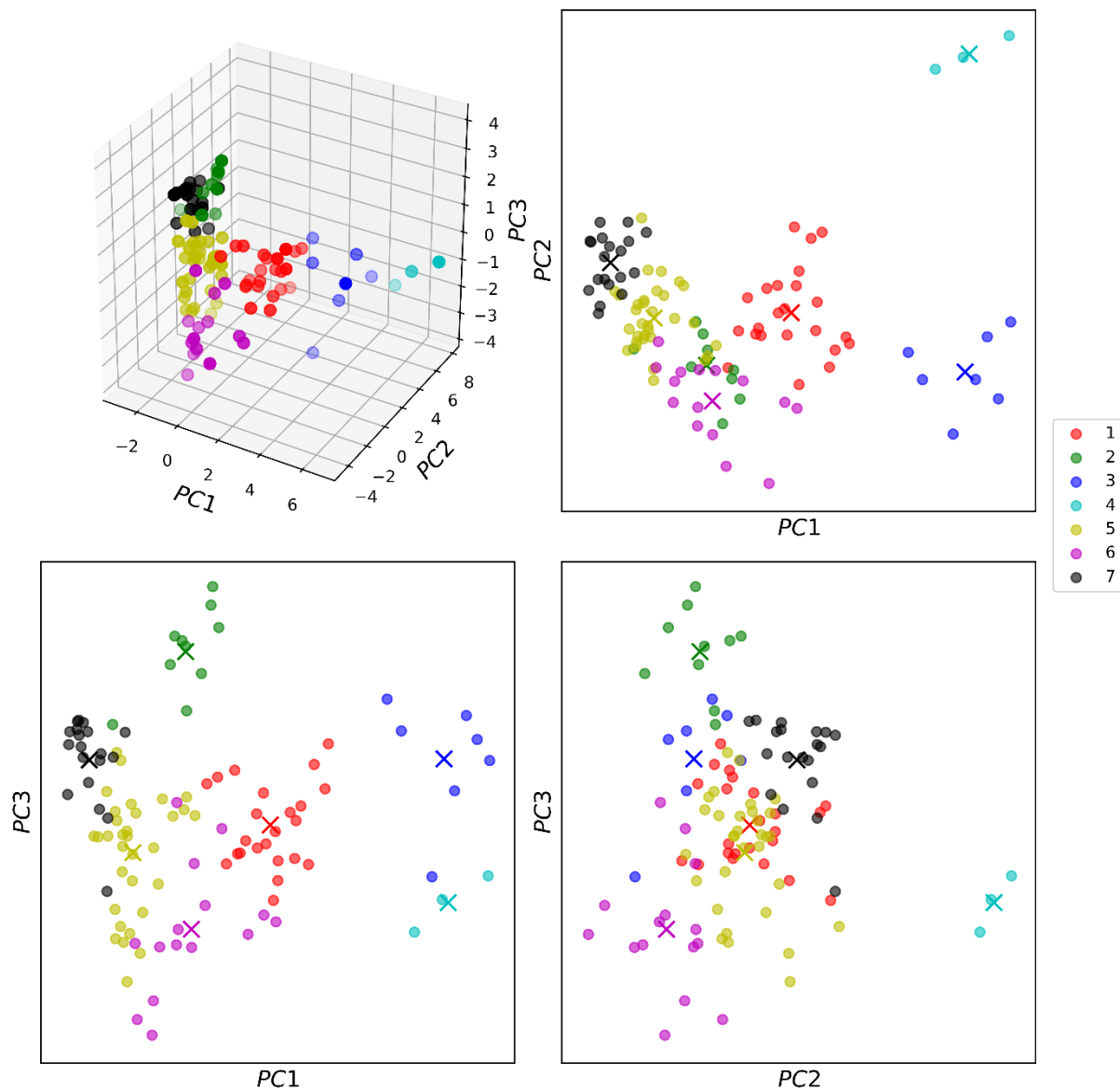


Figure 5.12 K-Means clustering results on S_r and catchments signatures (PCA-reduced data) for a) three-dimension plot including the first three principal components, b) PC_2 versus PC_1 , c) PC_3 versus PC_1 and d) PC_3 versus PC_2 . The catchments are divided into seven clusters, each cluster is specified with the same color in all four sub-figures.

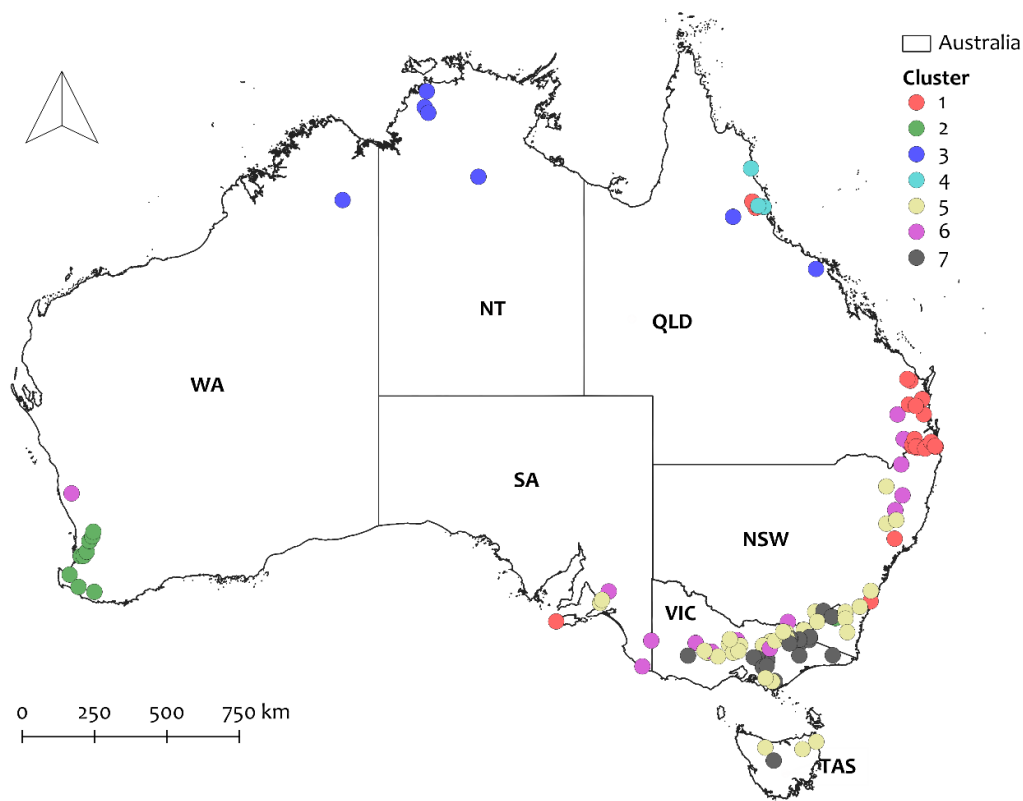


Figure 5.13 Map with root zone storage capacity in seven clusters of the selected catchments throughout Australia.

5.5.2 Catchment clusters characteristics

In order to figure out the specific characteristics of each catchment cluster, plot the results of PCA and K-Means clustering, shown in Fig 5.15; and the climatic signatures, hydrological signatures and vegetation signatures are re-calculated based on the new classification, shown in Fig 5.15.1 and 5.15.2. The characteristics of each cluster are described below.

Cluster 1 (red dots) The catchments in Cluster-One are dominantly distributed in the east of Australia, close to the junction of Queensland and New South Wales, are spread across the coastal area from Bundaberg to Brisbane. Besides, three catchments are located in Herber River, in the north of Queensland; two scattered in the southeast coastal area of New South Wales, in Clyde River - Jervis Bay and Hunter River; and one in Kangaroo Island, in South Australia. S_r in this cluster ranges from 137 to 391 mm, with annual mean temperature varying from 15 to 21 °C and mean precipitation of 747 to 1212 mm. From Fig 5.15, it can be seen that this cluster is highly climate-related and is relatively eminently correlated with root zone storage capacity. The long-term mean annual temperature T (potential evaporation E_p), the similarity index δ , precipitation P , the seasonality index of precipitation IS_p and discharge IS_Q from climatic signatures (Fig 5.15 (1), (2), (5) – (7)), and the other forests index R_{OF} (Fig 5.15 (9)) and peak distribution PD (Fig. 5.14 (10)) collectively affect S_r values. From Fig 5.15, it can be seen that S_r have a relatively smaller range, compared with other clusters. As most catchments in this cluster are partially covered by other forests, Fig 5.15 (15) reveals that the S_r is negatively correlated with R_{OF} .

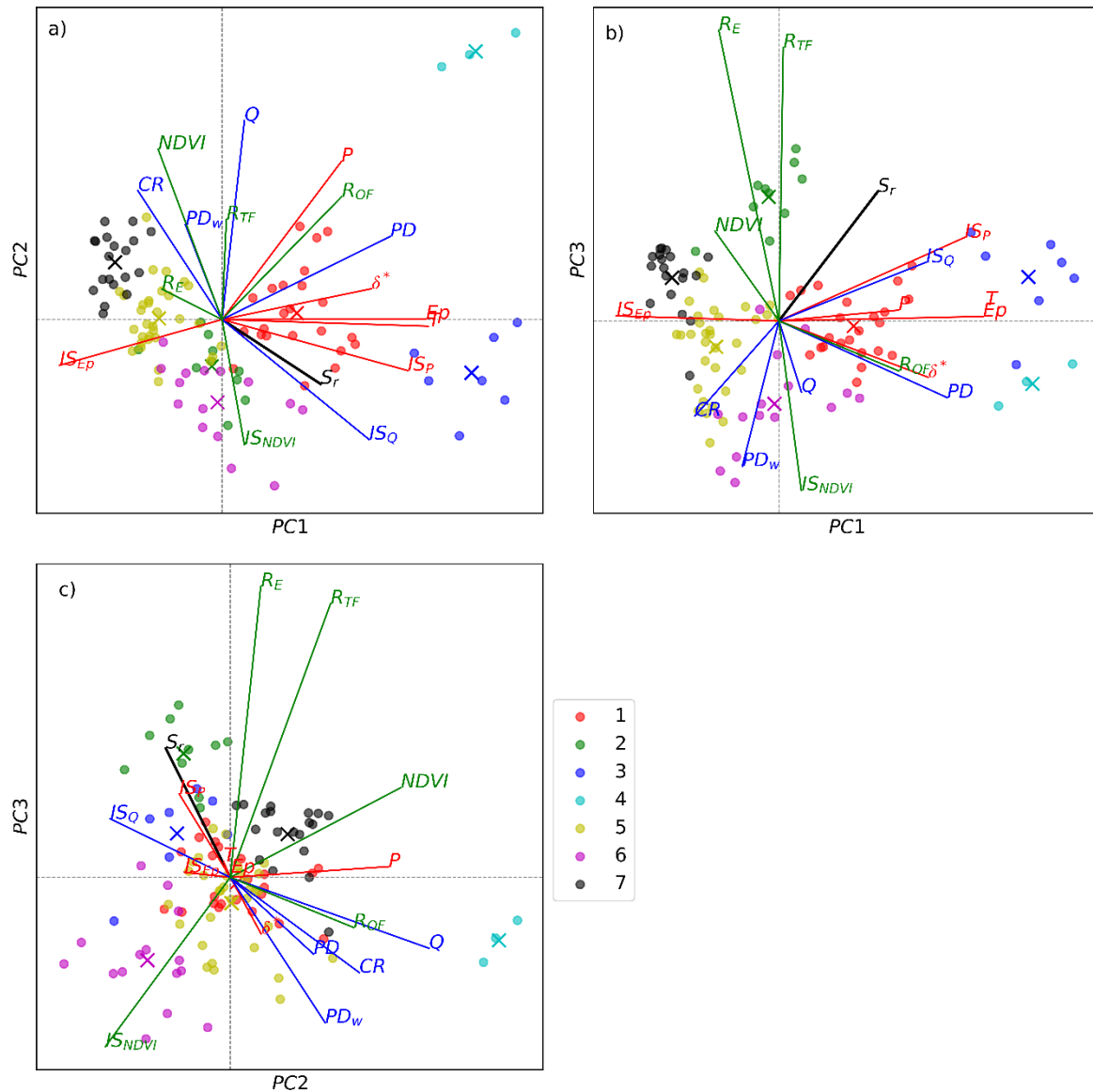


Figure 5.14 The results of PCA and K-Means clustering for a) PC_2 versus PC_1 , b) PC_3 versus PC_1 and c) PC_3 versus PC_2 . It is a combination of Fig 5.10 and 5.11.

Cluster 2 (green dots) S_r values of Cluster 2 ranges from 269 to 820 mm . The annual average temperature and precipitation range of this cluster are 10 - 17 $^{\circ}C$ and 623 - 1277 mm . The catchments in this cluster are all located in the southwest coastal area in Western Australia, along the coast from Perth to Albany, nearly consistent with the Region VI in region-based classification (Fig 5.3g), and a special catchment is located in Tasmania. The fundamental characteristics have been described above. From Fig 5.3, it is clear that this cluster is mainly influenced by vegetation signatures. The NDVI seasonality index IS_{NDVI} , long-term mean annual $NDVI$, eucalypt forests index R_E present dominant influence on this cluster. Additionally, it is also affected by the seasonality index of precipitation IS_P and discharge IS_Q . In general, although the S_r values present the large difference between these catchments, From Fig 5.15, it can be seen that the climatic signatures and hydrological signatures of this cluster show an approximate horizontal trend except

what has mentioned above, The eucalypt presents the highest level, compared with other clusters, nearly taking up the whole catchment; and in contrast, there are no other forests. It is different from other signatures, the NDVI values present a relatively large range, changing from 0.5 to 0.79. It is reasonable to speculate different eucalyptus species or the coverage density (forest and woodland) can cause significant different root pattern, which subsequently leads to different root zone storage capacity. With regard to seasonal variations in precipitation and discharge, it is evident that seasonality means the existence of more dry periods, which leads to the requirement for more water storage in the catchments dominated by eucalypts to overcome the drought.

Cluster 3 (blue dots) S_r values range from 390 to 740 mm with annual average precipitation of 774 - 1872 mm and temperature of 21 - 28 °C. The catchments in this cluster include those in Region I of region-based classification, the north in Northern Territory. Besides, two catchments in Northern Queensland are also included, which are located in the Flinder-Norman River basin and Don River basin. From Fig 5.13, this cluster is simply dominated by climatic signatures, the long-term temperature T (potential evaporation E_p), seasonality index of precipitation IS_p and discharge IS_Q . The cluster is close to the equator, where the temperature is at a high level and the temperature difference is small. In contrast, the difference during the year of precipitation and discharge is gigantic, summer rainfall can be larger than 300 mm per month while there is no rainfall in winter. The high level of seasonal change can be seen from Fig 5.15 (5) and (7), it is interesting that S_r is negatively correlated with the seasonality index both for precipitation and discharge, whereas positively correlated with the similarity index. It means the larger the difference of precipitation or discharge during a year the lower S_r values, but if the wet period and high potential evaporation level tend to be consistent, in another word, precipitation is in phase of potential evaporation, there will be larger S_r .

Cluster 4 (cyan dots) This cluster just contains three catchments, all of the three are located on the Northeast coast, one is located in Bloomfield River, one in Fisher Creek and another in Coachable Creek. The S_r for these is 151, 433 and 613 mm respectively; average annual precipitation is 2583, 3391 and 3912 mm, and the corresponding annual average temperatures are 25, 22 and 24 °C. Note that since the number of samples is small, the characteristics illustrated here possibly lack of representation. On the other hand, due to an obvious clustering result shown in Fig 5.13, it is representative to some extent. It can be seen that this cluster is governed by long-term mean annual precipitation P and other forests proportion R_{OF} . Additionally, the similarity index, peak distribution, and long-term mean discharge can also together play a role. As the limitation of sample size, for most catchment signatures, a correlation between S_r and them can be illustrated. However, Fig 5.15 (2) and (10) and presents a noticeable positive correlation between S_r and P , PD . Furthermore, Fig 5.15 (14) and (15) separately show that S_r is negatively correlated with eucalypt forests and positively correlated with other forests. In fact, all of the three catchments are covered by rainforests and vine thickets, which results in less requirement for water storage. The catchments are in tropical rainy climate, abundant precipitation as well as peak flow, combined with the regulating effect of rainforests, there is no need to develop a huge water storage zone to overcome drought period.

Cluster 5 (yellow dots) S_r values in this cluster range from 37 to 622 mm, with average temperature varying from 9 in Tasmania to 16 in South Australia and average precipitation of 496 to 1139 mm. The catchments are extensively distributed in the southeast coastal area from New South Wales to Victoria, additionally two in South Australia, close to Adelaide, and three in Tasmania, close to the bass strait. Fig 5.13 shows that this cluster is primarily dominated by the seasonality index of potential evaporation IS_{E_p} , eucalypt forests R_E , runoff coefficient RC . As the supplementation, NDVI and NDVI seasonality index IS_{NDVI} are synergistically affect S_r . From Fig 5.15, in terms of the seasonality index of potential evaporation, it is clear that higher S_r values are

consistent with higher IS_{Ep} . The runoff pattern is quite interesting, the catchments are divided into two sections, one with low runoff coefficient values is less correlated with S_r , another with relatively lower runoff coefficient values presents negative correlation with S_r . In fact, the RC with high values are tightly located in Victoria. As the precipitation presents a small range, the large difference among the discharges causes to the well-defined two classes RC values. On the other hand, this cluster has a wide eucalypt forests values distribution, showing a small positive correlation with S_r . In addition to the uncertainty of data sources, the influence of eucalypts is expected further study.

Cluster 6 (purple dots) S_r values in this cluster range from 184 to 435 mm, the average annual precipitation and temperature respectively range from 465 to 969 mm, and 12 to 17 °C. The catchments are widely distributed the coastal areas. Four catchments are located in the junction between Queensland and New South Wales, several scattered in Victoria, three in the southeast area of South Australia where there is close to Victoria, one in Tasmania and one in Western Australia (different from Cluster 3, relatively more northern). Fig 5.13 shows the most significant signature is the NDVI seasonality index IS_{NDVI} , then affected by the seasonality index of potential evaporation IS_{Ep} and discharge IS_Q , long-term mean annual discharge Q and peak distribution in low flow period PD_{low} to varying degrees. This explains to a certain extent why the catchments in this cluster are widely distributed in different regions under different climatic conditions. From Fig 5.15, combine the vegetation signatures, it is clear that these catchments have a low level of forest coverage, the “cleared, non-native vegetation and buildings” are the main land cover type. Because of the artificial influence, the rainfall-runoff pattern has been entirely changed, the low level of infiltration into the root zone leads to a high level of surface runoff, resulting in higher seasonality index of NDVI. High seasonality indicates that the annual change in vegetation is obvious, leading to a higher requirement for vegetation to develop a large storage capacity to overcome the drought period. It also can be seen that the cluster has moderate seasonality index of precipitation, it is similar to Cluster 5, the catchments in Victoria present high runoff coefficients and low seasonality index of discharge, in contrast, other catchments present opposite results. This reflects that the cluster is less affected by climatic characteristics and more depend on the vegetation condition.

Cluster 7 (black dots) S_r values of this cluster range from 79 to 473 mm, with annual average precipitation varying from 623 to 1615 mm and an average temperature of 6 to 14 °C. The catchments in this cluster are concentrated in Victoria and Tasmania, most of them with higher altitudes present obvious alpine climate. Fig 5.13 shows this cluster is correlated with eucalypt forests R_E , the seasonality index of potential evaporation IS_{Ep} and $NDVI$, and slightly influenced by runoff coefficient RC . It is similar to Cluster 5 but less affected by climatic and hydrological signatures. From Fig 5.15, the vegetation signatures indicate that the catchments are dominantly covered by eucalypt forests, which is negatively correlated with S_r . Since several catchments are partially covered by other forests, the seasonality index of potential evaporation provides a positive correlation with S_r , reflecting on $NDVI$, there is no clear correlation with S_r . As for runoff coefficient, except for those might be artificially reformed, it presents a clear negative correlation with S_r .

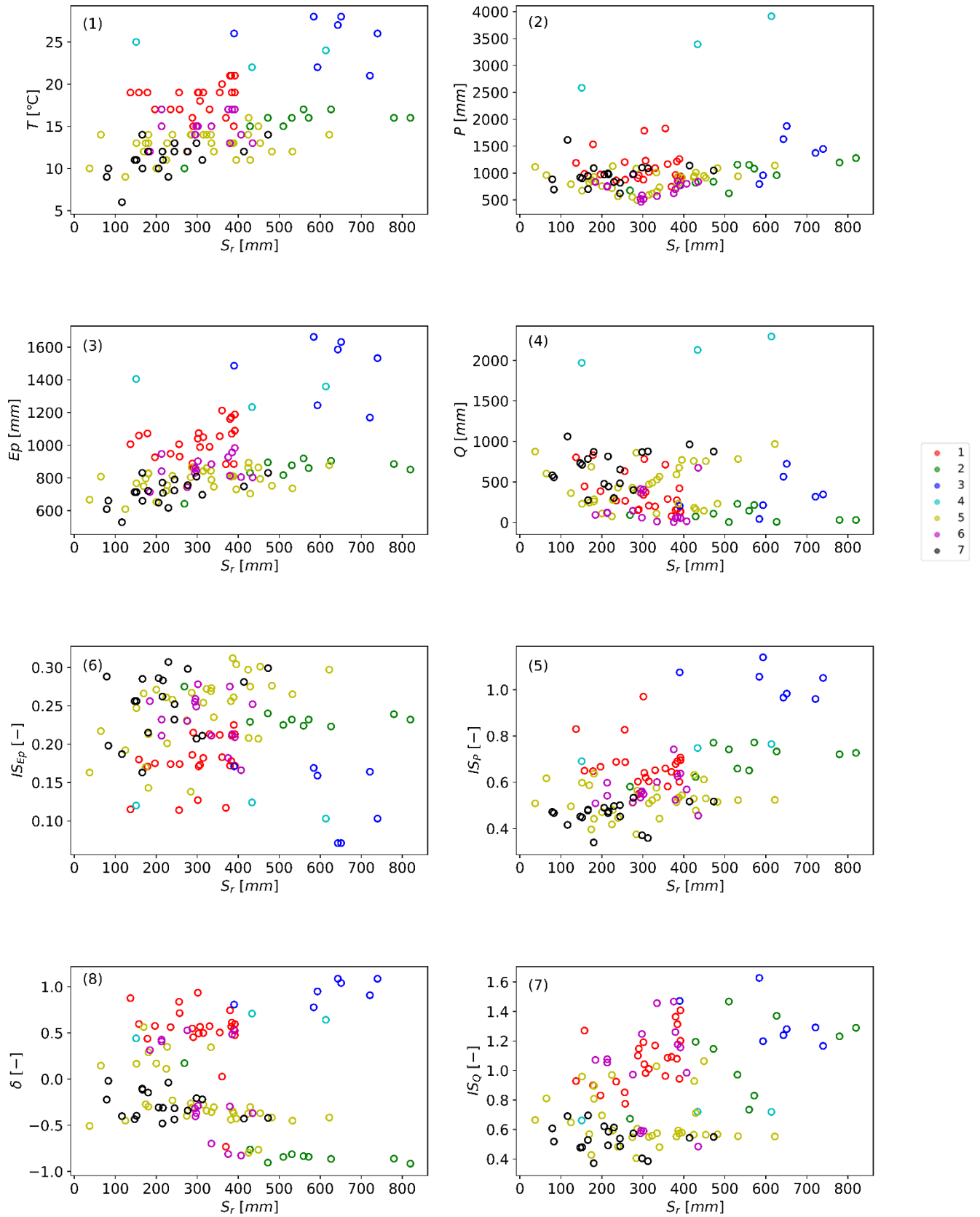


Figure 5.15.1 Root zone storage capacity S_r and long-term mean annual (1) temperature T , (2) precipitation P , (3) potential evaporation E_p , (4) discharge Q ; seasonality index of (5) precipitation IS_P , (6) potential evaporation IS_{E_p} , (7) discharge IS_Q ; (8) similarity index δ , reflecting the timing of precipitation.

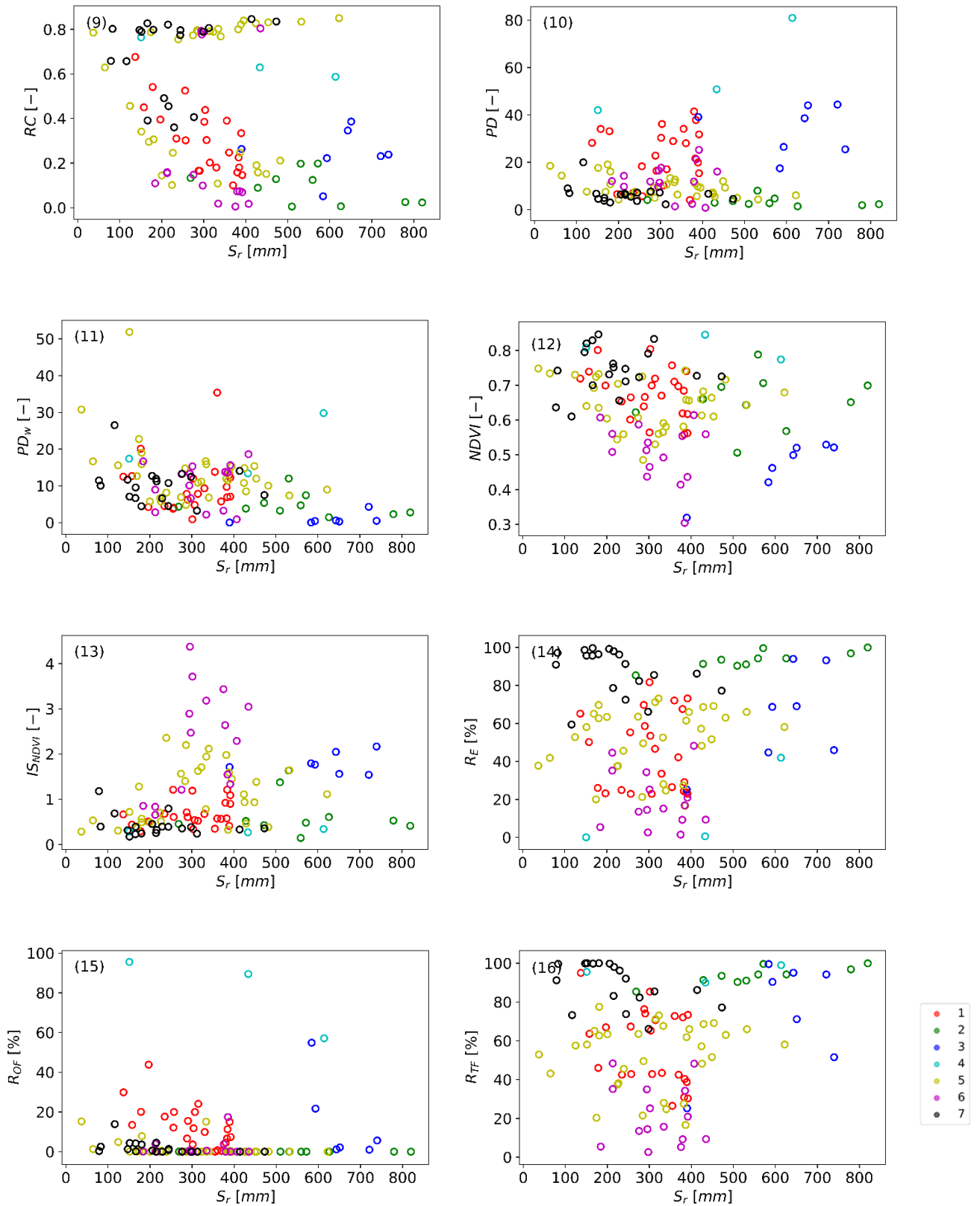


Figure 5.15.2 Root zone storage capacity S_r and (9) runoff coefficient RC , (10) peak distribution PD , (11) peak distribution in low flow period PD_{low} , (12) Normalized difference vegetation index $NDVI$, (13) NDVI seasonality index IS_{NDVI} , (14) Proportion of eucalypt forests R_E , (15) proportion of other forests (including rainforests and vine thickets, acacia, callitris, casuarina, melaleuca and others) R_{OF} , (16) proportion of total forests R_{TF} .

6

Discussion

The study demonstrates that the climate-derived root zone storage capacity is strongly related to climate signatures, hydrological signatures and vegetation signatures, and climate and vegetation play different roles depending on the catchment under various natural conditions. The study catchments are divided into seven clusters. For different clusters, the root zone storage capacity can be climate-dominated, vegetation-dominated, or climate and vegetation are as important as each other. The results can be thus be used to explore the physical meaning and broader application of S_r for land and water management purposes. Below, the possible reasons for differences in correlation and the implications of the findings are discussed.

6.1 General characteristics of all study catchments

Climate signatures The analysis confirms that the strongest correlations between S_r and the catchment characteristics can be found when all clusters are considered together; these clusters mainly differ in climate signatures. It can be seen that not all climate variables have the same influence (Fig 5.15.1) on S_r values. The long-term mean annual potential evaporation (water demand), the seasonality index of precipitation (change in the water supply), and the similarity index (timing of precipitation) turn out to be significant. The positive correlation between S_r values and the precipitation seasonality index indicates a certain buffering of seasonality effects on the discharge. It is interesting that S_r values are more sensitive to water demand E_p and the change of water supply. Based on the similarity index (Fig 5.15.1 (8)), the catchments can be roughly divided into two classes. With zero as the boundary, those with values close to 1 present the precipitation is in the phase of the potential evaporation, those with values close to -1 present the precipitation is out of phase with the potential evaporation. The former has warm to hot summer and mild to warm winter, mostly located in Queensland and Northern Territory; while the latter has a temperate climate, located in the coastal areas in the south of Australia (including both the east and the west). Further, the different analyses show that for the warmer regions, the influence of climate signatures is more significant (Fig 5.14. Cluster 1, 3, 4).

Vegetation signatures As NDVI reflects the effects of plant canopy and is related to vegetation coverage, this can be simply illustrated by the influences of eucalypt forests and other forests. In general, higher eucalypt forests coverage leads to higher S_r values, whereas higher other forests coverage results in lower S_r values. When the proportion of forests, including eucalypt forests and other forests, is larger than approximately 80%, the influence of vegetation signatures is more significant than that of climate signatures. However, the heterogeneity of the study catchments can cause different performances for eucalypt forests. Previous studies have found that many tree species can grow roots to depths of more than 10 m (Jackson et al., 1996; Davidson et al., 2011; Eamus et al., 2015) with maximum rooting depths reaching about 60 m for Eucalyptus trees (Stone and Kalisz 1991). A deep rooting profile increases the amount of water available for plant growth and provides a buffering role of deep soil layer through the storage of water during the wet season, further withdrawn during dry seasons (Oliveira et al. 2005; Nardini et al. 2015). Furthermore, Eucalyptus with fast root growth capacity, its roots can reach the groundwater table at a depth of

12 m after 2 years and the proportion of water taken up near the groundwater table was much higher during dry periods (Christina et al., 2017). In a word, deep rooting can increase the amount of water available for the trees and provide a significant role for large amounts of water stored in wet season which can be used in dry season, resulting in high transpiration and eventually a higher estimation of S_r . Thus, it is essential to separately consider the effects of eucalypt forests and other forests, and also the combined effect of eucalypt forests and other forests should not be neglected. Furthermore, although the climate-derived root zone storage capacity is out of the influence of soil, whereas the growth and development of vegetation are largely affected by soil characteristics, which again affects the evaporation rates. On the other hand, how does the development of vegetation and climate exactly coincide? For instance, if the precipitation decreases, the vegetation has to adjust root pattern to develop a large S_r to store water for overcoming the drought period, otherwise, the vegetation is not adaptable to the change, and then the vegetation type will change.

Hydrological signatures The hydrological signatures reflect the combined results of vegetation and climate as the precipitation (water supply), the evaporation (water demand), and surface and subsurface vegetation characteristics all influence the generation of runoff. When considering all study catchments, S_r values are more sensitive to the seasonality index of the discharge, the peak distribution, and runoff coefficient. The change of discharge is consistent with the change of precipitation since the water supply directly determines how much water the root zone system can release. The peak distribution in the low flow period and runoff coefficient RC are both negatively correlated with S_r values. While humid catchments are characterized by low S_r and high RC , vegetation in more arid catchments requires a higher S_r to store more water, resulting in lower RC and thus in higher plant transpiration. The peak distribution presents a similar pattern. This emphasizes the role of co-evolution of climate and vegetation.

6.2 Specific characteristics of different clusters

Cluster 1 (red dots) The presented results show that among the compared characteristics S_r values of this cluster are strongest related to various climate variables as well as other forests factor. The catchments here have warm humid summer and mild winter. On the whole, sufficient water is available on the surface, the vegetation is productive and evaporation rates present a similar level with precipitation. In this cluster, the proportion of eucalypt forests varies from medium to high, while it does not show a strong dominated effect; instead, other forests factor presents a noticeably negative correlation with S_r values. Compared with other catchments, the S_r values of this cluster are at a medium to a low level. This is because there is no drought period throughout the entire year, and precipitation is coincided with potential evaporation, leading to the impact on precipitation and transpiration is inconspicuous. However, in the warm and humid regions, it can significantly reduce the flood peak and runoff, resulting in higher calculated values of S_r . Besides, the increase in runoff coefficient in this cluster causes lower S_r values, which is consistent with the correlation between the two characteristics when considering all study catchments.

Cluster 2 (green dots) The results show that S_r values are sensitive to vegetation signatures. The catchments of this cluster have mild to cool temperate climate, located in the southwestern coastal area in Western Australia. Precipitation and potential evaporation in this cluster show opposite trends, with mild and dry summer and mild and rainy winter, which results in insufficient water supply in summer for vegetation transpiration. One of the most important characteristics of these catchments is the proportion of eucalypt forests are all larger than 95%. According to the eucalypts characteristics described in section 6.1, the eucalypts root system can derive deficient water from groundwater for vegetation transpiration, and transfer and store redundant water in winter to overcome drought period. These characteristics all cause a larger amount of transpiration, which subsequently is shown as a medium to a high level of S_r values, with a maximum of more than 800 mm. However, from Fig 5.15.2, it is clear there is no actual strong positive correlation between

eucalypt forests and S_r values. Similarly, S_r values are also insensitive to climate variables. It is difficult to assess how additional groundwater access affects the root zone system. However, it reveals that the eucalypt forest can adapt to the Mediterranean climate and is not restricted by insufficient precipitation.

Cluster 3 The analysis confirms that the S_r values are more sensitive to climate signatures, and differ from cluster 1, the influence of vegetation can be neglected. The catchments of this cluster have hot humid summer and warm dry winter, located in the north in North Territory and Queensland. Although in this cluster, the catchment eucalypt forests coverage is at a medium to a high level and there are certain other forests, the high temperature and humid climate conditions determine the importance of climate signatures. It can be regarded that although the precipitation is in phase of potential evaporation, the summer precipitation is much higher than the potential evaporation demand; while the winter precipitation is close to zero. Due to close to the equator, the winter evaporation is still at a high level, making these basins encounter more than a quarter of drought period. In fact, for most catchments, the long-term mean annual precipitation is less than the potential evaporation. These characteristics lead to the vegetation having to develop a large root zone to store enough water to overcome the drought. It can be seen that the S_r values of the catchments are generally greater than 500 mm. Interestingly, compared with other catchments, the relationship between climate signatures and S_r values reflects the opposite relationship, such as high evaporation, high precipitation, and seasonality of evaporation corresponding to low S_r values. Due to the large seasonal variation of precipitation, winter evaporation is largely limited by the lack of precipitation. Although similar to cluster 2, these catchments are covered by vast eucalyptus forests, whereas abundant rainwater in summer and the suitable temperature is consistent with the growing needs of vegetation. This is the reason why climate factors play a more crucial role. Another important factor is the small sample size, which means that it lacks sufficient mathematical-statistical significance.

Cluster 4 The results present that the S_r values are dominated by other forests, followed by various climate and hydrological signatures. First, as there are only three catchments in this cluster, the statistical characteristics are expected to an extent by adding more samples. However, due to the special climate and vegetation characteristics, it is reasonable to turn out the conclusion. The catchments in this cluster have a tropical rain forest climate. In summer, it is controlled by the equatorial low-pressure zone, leading to sufficient summer precipitation. In winter, as it is located on the east side of the Great Dividing Range, orographic rains often occur. Overall, the annual precipitation can generally meet the transpiration needs of vegetation. It can be seen that the coverage of other forests in two of the basins is more than 85% and they are both tropical rainforests; the coverage of the rainforests in the third catchment is similar to that of eucalypt forests, each accounting for approximately 50%. It can be clearly seen that the S_r values of the catchments covered by tropical rainforests are at low and medium levels, with higher rainforest coverage corresponds to lower S_r values, while catchments with higher eucalypt forest coverage result in larger S_r values. This is also consistent with the previous description. According to the results of the first four clusters, it is recognized that when the vegetation coverage area of the watershed exceeds 80%, the vegetation signatures can give full play to its influence, and the impact of climate on the S_r value will be weakened.

Cluster 5 From the geographical point of view, these two clusters are promiscuously distributed in the coastal regions from southeast Queensland to southern Victoria, which is why they are discussed together. It is difficult to define which of the climatic signatures and vegetation signatures presents a stronger correlation with S_r values. In general, these catchments reflect the co-evolutionary effect of climate and vegetation on the S_r value. These catchments are in a temperate monsoon climate zone, with little seasonal changes in precipitation. The precipitation in some catchments is consistent with evaporation, and precipitation of others is opposite to evaporation.

The most important difference between these two clusters is reflected in the eucalypt forests and NDVI seasonality index. Cluster 5 has medium to high eucalyptus coverage (greater than 30% and less than 80%), while cluster 6 generally has eucalyptus coverage of less than 40%; cluster 5, NDVI seasonality index does not show a strong correlation with S_r values, and the cluster 6 not only has the highest NDVI seasonality index, but high NDVI directly causes high S_r values. When it comes to climatic signatures and hydrological signatures, seasonal changes in evaporation and runoff coefficient also show a strong correlation with S_r values. This makes us have to think about the vegetation signatures that distinguish these two clusters. In fact, for most catchments, irrigated agriculture is negligible, whereas cluster 6 has a relatively high proportion of irrigation (although still less than 10%), which is also the reason why the seasonal index of NDVI changes enormously. The S_r values of cluster 6 are generally lower than cluster 5, which also reflects the impact of irrigated agriculture on S_r values. Since this study does not discuss in depth whether surface irrigation or groundwater irrigation is used in these catchments, it is difficult to define the impact of irrigation on the entire water balance system, which is expected further research in the future.

Cluster 7 The results reveal that the S_r values are more sensitive to vegetation signatures, mainly eucalypt forests, followed by the seasonality index of potential evaporation. The catchments are located in the Great Dividing Range of New South Wales, Victoria, and Tasmania. The temperature is relatively low throughout the year, while there is sufficient precipitation, especially in winter. Precipitation is out of phase with potential evaporation. The seasonality indexes in the climate signatures are positively correlated with the S_r value. Since there is sufficient precipitation and potential evaporation is at a reduced level, the calculated S_r value is at a medium to a low level. The forest coverage of Cluster 7 is generally more than 80%, thus, the vegetation factor plays a more decisive role. What is interesting is that unlike the catchments in other clusters, eucalypt forests here show a negative correlation with S_r values. This speculation is based on the fact that the runoff coefficient of some catchments is at a high level, floating around 0.8, which means that most water supplies leave the root system by runoff rather than transpiration. If the coverage of eucalypt forests is high and the amount of transpiration does not correspond a high level, one possible reason is that due to the particularity of mountain topography and climate, the root system of eucalyptus forests in this area may develop different patterns, making the effect of S_r value is closer to other forests.

7

Conclusion

This study aimed to explore the application of climate-derived root zone storage capacity in Australia and identify the influence of various climatic, hydrological and vegetation signatures on root zone storage capacity. This study starts from a direct application of climate-derived root zone storage capacity as previous studies have proved its usefulness, subsequently the comparison with the climatic, hydrological and vegetation signatures reversely demonstrate the broad application of climate-derived S_r .

When all selected catchments are taken into account, climatic signature present the most significant correlation with S_r , which is plausible as the S_r values are derived from climate data. Based on the first region-based classification, it is evident that the correlation with climatic signatures differs in different classes (see section 5.1). This preconceived classification, actually the catchments in the same region enjoy a similar climate, provides a simple pattern to classify catchments. The climatic signatures, especially the change of climate condition, definitely influence the S_r values of several catchments, such as in Northern Territory, but it obviously cannot play a role throughout the whole continent. The hydrological signatures which are related to the discharge that is the significant output of the climate-derived method, directly reflect the hydrological functioning. From the correlations with S_r , the rough region-based classification is also effective in the class which is highly correlated with climate. Additionally, the catchments in the Northeastern Queensland with tropical rainy climate present a high correlation with S_r values. It is reasonable as the discharge can be regarded as the result of the combined action of climate and vegetation. As for the vegetation signatures. When considering all catchments, the correlation with S_r values did not show patterns as strong as expected. Furthermore, the region-based classification is only effective in specific classes, and what is interesting is that the catchments in the north show a strong correlation between S_r values and most climatic, hydrological and vegetation signatures. One possible reason might be that fewer samples are less statistic meaning, another possible reason could be that S_r has a very strong physical meaning in tropical regions.

The results of Principal Component Analysis revealed that the vegetation signatures are less correlated with the majority of the climate signatures, although they are both present correlations with S_r , and the hydrological signatures present a stronger correlation with both the other two categories. As the S_r values present a higher loading value on the third principal component, the first three components of PCA were taken into account. On the one hand, it is essential for containing sufficient information and avoiding oversimplification. On the other hand, the three-dimensional diagram results in complicated results which might be difficult to explain. However, the results of K-Means clustering re-identify the catchment classes and provide them qualitative and quantitative description (see section 5.4.2), of them, three clusters present the consistent result in the two-dimension projection, which means these clusters reveal unambiguous characteristics and are generally concentrated in a certain climate zone, or can be clearly distinguished visually on the map (it could also be the reason for the small number of samples). Cluster 2 is dominated by vegetation signatures (NDVI and eucalypt forests), located in the southwest of Western Australia, predominantly covered by eucalypt forests, developing a positive correlation with S_r values.

Cluster 3 is dominated by climatic signatures (temperature or potential evaporation, and seasonality index of precipitation), located in the northern tropical area in Northern Territory and Queensland. Higher potential evaporation leads to higher S_r values, while the interesting is the seasonal precipitation could slightly reduce the S_r values which are different from other clusters. Cluster 4 is governed by both climatic and vegetation signatures (precipitation and rainforest), located in the northeast of Queensland, positively correlated with the former and negatively correlated with the latter.

For other four clusters, due to the different loading values of the same signature on the three principal components and the high loading value of S_r on the third component, the same cluster clusters around different signatures in different dimensions, which means, in fact, the effective signatures are more complicated. However, the same cluster can still be identified by several signatures, although basically, it is a combination of climatic and vegetation signature, and even additionally with hydrological signatures. Furthermore, these clusters are scattered on the map, there is no clear geographical boundary between different clusters, especially shown in Cluster 5, 6 and 7. The catchments are scattered in the southeastern coastal area of New South Wales to Victoria, South Australia, and Tasmania. They are affected by the combined influences of climatic, hydrological and vegetation signatures to varying degrees. This result could due to, from the results, the large range of S_r values in these clusters, the influence of climatic and vegetation signatures is not as strong as expected. In general, the clustering results obtained by the PCA and K-Means clustering methods have greatly distinguished the study catchments. However, the application of the first three components has taken into account as far as possible the impact of different catchment characteristics on classification. Obviously, there are certain similarities between different clusters, while they also present differences at the same time. For instance, Cluster 4 and Cluster 7 are both vegetation-dominated, but Cluster 4 is more affected by climatic and hydrological characteristics, and the topographic factor of Cluster 7, which is not involved in this study, they can still present different clustering results.

The most interesting in this study is the broad distribution of eucalypts. The results show that, unlike other types of forests, especially rainforests, eucalypts show a negative correlation with S_r when considering all catchments. However, when specific to an individual cluster, the role of eucalyptus has a certain difference (shown in Cluster 7). Since different eucalypt types, including low open forests, tall open forests, woodlands, etc., are together considered, one possible reason might be the different types could present various influence. Another reason could be the topography and climate, Cluster 7 is in alpine regions, which means other signatures are expected to involve.

In addition, this study is enormously based on the accuracy of the input data. Since the requirement for long-term time-series data and the relatively small catchment size, when estimating the catchment areal precipitation and temperature, it is necessary to make some tradeoffs in the selection of weather stations. Thus, the weather station with sufficient data series while the distance is relatively larger was determined, which could result in less accuracy. Therefore, it is expected to consider the choice of catchment more carefully. Furthermore, the temperature-based Hamon Evapotranspiration method was used in estimating the potential evaporation, while Australia is strongly affected by the monsoon climate in the east and south, this method might underestimate the potential evaporation, and a more precise method is needed if possible. Besides, the effect of eucalypts is expected to explore in further research, and the regions with few catchments in the north, the application is expected to be introduced to verify in more catchments.

Bibliography

- Adegoke, J. O., & Carleton, A. M. (2002). Relations between soil moisture and satellite vegetation indices in the US Corn Belt. *Journal of hydrometeorology*, 3(4), 395-405.
- Allen, R. G., Pereira, L. S., Raes, D., & Smith, M. (1998). Crop evapotranspiration-Guidelines for computing crop water requirements-FAO Irrigation and drainage paper 56. Fao, Rome, 300(9), D05109.
- Ankenbauer, K. J., & Loheide, S. P. (2017). The effects of soil organic matter on soil water retention and plant water use in a meadow of the Sierra Nevada, CA. *Hydrological Processes*, 31(4), 891-901.
- Australian Collaborative Land Use and Management Program (ACLUMP) © Department of Agriculture, Water and the Environment. <https://www.agriculture.gov.au/abares/aclump/about-aclump>
- Australian Government, Bureau of Meteorology (2015). La Niña – Detailed Australian Analysis. <http://www.bom.gov.au/climate/enso/lnlist/>
- Berghuijs, W. R., Sivapalan, M., Woods, R. A., & Savenije, H. H. (2014). Patterns of similarity of seasonal water balances: A window into streamflow variability over a range of time scales. *Water Resources Research*, 50(7), 5638-5661.
- Berghuijs, W. R., & Woods, R. A. (2016). A simple framework to quantitatively describe monthly precipitation and temperature climatology. *International Journal of Climatology*, 36(9), 3161-3174.
- Beven, K. (2006). A manifesto for the equifinality thesis. *Journal of hydrology*, 320(1-2), 18-36.
- Brocca, L., Ciabatta, L., Massari, C., Camici, S., & Tarpanelli, A. (2017). Soil moisture for hydrological applications: open questions and new opportunities. *Water*, 9(2), 140.
- Budyko, M. I., Miller, D. H., & Miller, D. H. (1974). *Climate and life* (Vol. 508). New York: Academic press.
- Campos, I., Gonzalez-Piqueras, J., Carrara, A., Villodre, J., & Calera, A. (2016). Estimation of total available water in the soil layer by integrating actual evapotranspiration data in a remote sensing-driven soil water balance. *Journal of Hydrology*, 534, 427-439.
- Catchment scale land use of Australia © Department of Agriculture, Water and the Environment. <https://www.agriculture.gov.au/abares/aclump/land-use/catchment-scale-land-use-of-australia-commodities-update-december-2018>
- Climate Data Online (CDO) © Copyright Commonwealth of Australia 2020, Bureau of Meteorology. <http://www.bom.gov.au/climate/data/>
- Climate zone map: Australia wide @ 2015 Australian Building Codes Board . <https://www.abcb.gov.au/Resources/Tools-Calculators/Climate-Zone-Map-Australia-Wide>
- Christina, M., Nouvellon, Y., Laclau, J. P., Stape, J. L., Bouillet, J. P., Lambais, G. R., & Le Maire, G. (2017). Importance of deep water uptake in tropical eucalypt forest. *Functional Ecology*, 31(2), 509-519.
- Collins, D. B. G., & Bras, R. L. (2007). Plant rooting strategies in water - limited ecosystems. *Water Resources Research*, 43(6).
- Crow, W. T., Berg, A. A., Cosh, M. H., Loew, A., Mohanty, B. P., Panciera, R., ... & Walker, J. P. (2012). Upscaling sparse ground-based soil moisture observations for the validation of coarse-resolution satellite soil moisture products. *Reviews of Geophysics*, 50(2).
- Davidson, E., Lefebvre, P. A., Brando, P. M., Ray, D. M., Trumbore, S. E., Solorzano, L. A., ... & Nepstad, D. C. (2011). Carbon inputs and water uptake in deep soils of an eastern Amazon forest. *Forest Science*, 57(1), 51-58.
- de Boer-Euser, T., McMillan, H. K., Hrachowitz, M., Winsemius, H. C., & Savenije, H. H. (2016). Influence of soil and climate on root zone storage capacity. *Water Resources Research*, 52(3), 2009-2024.

- de Boer-Euser, T., Palalane, J., Savenije, H., & Juárez, D. (2019). How climate variations are reflected in root zone storage capacities. *Physics and Chemistry of the Earth, Parts A/B/C*, 112, 83-90.
- Didan, K. (2015). MOD13C2 MODIS/Terra Vegetation Indices Monthly L3 Global 0.05Deg CMG V006 [Data set]. NASA EOSDIS Land Processes DAAC. Accessed 2020-03-27 from <https://doi.org/10.5067/MODIS/MOD13C2.006>
- Didan, K., Barreto, A. (2016). NASA MEaSUREs Vegetation Index and Phenology (VIP) Vegetation Indices Monthly Global 0.05Deg CMG [Data set]. NASA EOSDIS Land Processes DAAC. Accessed 2020-03-26 from <https://doi.org/10.5067/MEaSUREs/VIP/VIP30.004>
- Dorigo, W. A., Xaver, A., Vreugdenhil, M., Gruber, A., Hegyiova, A., Sanchis-Dufau, A. D., ... & Drusch, M. (2013). Global automated quality control of in situ soil moisture data from the International Soil Moisture Network. *Vadose Zone Journal*, 12(3).
- Eamus, D., Zolfaghar, S., Villalobos-Vega, R., Cleverly, J., & Huete, A. (2015). Groundwater-dependent ecosystems: recent insights from satellite and field-based studies. *Hydrology and Earth System Sciences*.
- Euser, T., Winsemius, H. C., Hrachowitz, M., Fenicia, F., Uhlenbrook, S., & Savenije, H. H. G. (2013). A framework to assess the realism of model structures using hydrological signatures. *Hydrology and Earth System Sciences*, 17 (5), 2013.
- Feddes, R. A., Hoff, H., Bruen, M., Dawson, T., De Rosnay, P., Dirmeyer, P., ... & Pitman, A. J. (2001). Modeling root water uptake in hydrological and climate models. *Bulletin of the American meteorological society*, 82(12), 2797-2810.
- Federer, C. A., Vörösmarty, C., & Fekete, B. (1996). Intercomparison of methods for calculating potential evaporation in regional and global water balance models. *Water Resources Research*, 32(7), 2315-2321.
- Field, C. B., Chapin III, F. S., Matson, P. A., & Mooney, H. A. (1992). Responses of terrestrial ecosystems to the changing atmosphere: a resource-based approach. *Annual Review of Ecology and Systematics*, 23(1), 201-235.
- Gao, H., Hrachowitz, M., Schymanski, S. J., Fenicia, F., Sriwongsitanon, N., & Savenije, H. H. G. (2014). Climate controls how ecosystems size the root zone storage capacity at catchment scale. *Geophysical Research Letters*, 41(22), 7916-7923.
- Gentine, P., D'Odorico, P., Lintner, B. R., Sivandran, G., & Salvucci, G. (2012). Interdependence of climate, soil, and vegetation as constrained by the Budyko curve. *Geophysical Research Letters*, 39(19).
- Gumbel, E. J. (1941). The return period of flood flows. *The annals of mathematical statistics*, 12(2), 163-190.
- Hamon, W. R. (1963). Computation of direct runoff amounts from storm rainfall. *International Association of Scientific Hydrology Publication*, 63, 52-62.
- Hotelling, H. (1933). Analysis of a complex of statistical variables into principal components. *Journal of educational psychology*, 24(6), 417.
- Huete, A., Didan, K., Miura, T., Rodriguez, E. P., Gao, X., & Ferreira, L. G. (2002). Overview of the radiometric and biophysical performance of the MODIS vegetation indices. *Remote sensing of environment*, 83(1-2), 195-213.
- Hydrological Reference Stations (HRS) © Copyright Commonwealth of Australia 2020, Bureau of Meteorology. <http://www.bom.gov.au/water/hrs/#id=102101A&panel=data-download&pill=daily>
- Isik, S., & Singh, V. P. (2008). Hydrologic regionalization of watersheds in Turkey. *Journal of Hydrologic Engineering*, 13(9), 824-834.
- Jackson, R. B., Canadell, J., Ehleringer, J. R., Mooney, H. A., Sala, O. E., & Schulze, E. D. (1996). A global analysis of root distributions for terrestrial biomes. *Oecologia*, 108(3), 389-411.
- Kleidon, A. (2004). Global datasets of rooting zone depth inferred from inverse methods. *Journal of Climate*, 17(13), 2714-2722.

- Leng, G., Leung, L. R., & Huang, M. (2017). Significant impacts of irrigation water sources and methods on modeling irrigation effects in the ACME Land Model. *Journal of Advances in Modeling Earth Systems*, 9(3), 1665-1683.
- MacQueen, J. (1967, June). Some methods for classification and analysis of multivariate observations. In *Proceedings of the fifth Berkeley symposium on mathematical statistics and probability* (Vol. 1, No. 14, pp. 281-297).
- Milly, P. C. D. (1994). Climate, soil water storage, and the average annual water balance. *Water Resources Research*, 30(7), 2143-2156.
- Miura, T., Huete, A. R., Yoshioka, H., & Holben, B. N. (2001). An error and sensitivity analysis of atmospheric resistant vegetation indices derived from dark target-based atmospheric correction. *Remote sensing of Environment*, 78(3), 284-298.
- Montgomery, K. (2006). Variation in temperature with altitude and latitude. *Journal of Geography*, 105(3), 133-135.
- Murray, F. W. (1966). On the computation of saturation vapor pressure (No. P-3423). Rand Corp Santa Monica Calif.
- Myneni, R., Knyazikhin, Y., Park, T. (2015). MOD15A2H MODIS/Terra Leaf Area Index/FPAR 8-Day L4 Global 500m SIN Grid V006. NASA EOSDIS Land Processes DAAC. <https://doi.org/10.5067/MODIS/MOD15A2H.006>
- National Vegetation Information System V5.1 © Australian Government Department of the Environment and Energy 2018. <http://environment.gov.au/fed/catalog/search/resource/details.page?uuid=%7B991C36C0-3FEA-4469-8C30-BB56CC2C7772%7D>
- Nardini, A., Casolo, V., Dal Borgo, A., Savi, T., Stenni, B., Bertoincin, P., ... & McDowell, N. G. (2016). Rooting depth, water relations and non-structural carbohydrate dynamics in three woody angiosperms differentially affected by an extreme summer drought. *Plant, cell & environment*, 39(3), 618-627.
- Nijzink, R., Hutton, C., Pechlivanidis, I., Capell, R., Arheimer, B., Freer, J., ... & Hrachowitz, M. (2016). The evolution of root-zone moisture capacities after deforestation: a step towards hydrological predictions under change?. *Hydrology and Earth System Sciences*, 20(12), 4775-4799.
- Oliveira, R. S., Bezerra, L., Davidson, E. A., Pinto, F., Klink, C. A., Nepstad, D. C., & Moreira, A. (2005). Deep root function in soil water dynamics in cerrado savannas of central Brazil. *Functional Ecology*, 19(4), 574-581.
- Perrin, C., Michel, C., & Andréassian, V. (2003). Improvement of a parsimonious model for streamflow simulation. *Journal of hydrology*, 279(1-4), 275-289.
- Rouse, J. W., Haas, R. H., Schell, J. A., & Deering, D. W. (1974). Monitoring vegetation systems in the Great Plains with ERTS. *NASA special publication*, 351, 309.
- Scheffer, M., Holmgren, M., Brovkin, V., & Claussen, M. (2005). Synergy between small - and large - scale feedbacks of vegetation on the water cycle. *Global change biology*, 11(7), 1003-1012.
- Schnur, M. T., Xie, H., & Wang, X. (2010). Estimating root zone soil moisture at distant sites using MODIS NDVI and EVI in a semi-arid region of southwestern USA. *Ecological Informatics*, 5(5), 400-409.
- Schymanski, S. J., Sivapalan, M., Roderick, M. L., Beringer, J., & Hutley, L. B. (2008). An optimality-based model of the coupled soil moisture and root dynamics. *Hydrology and earth system sciences*, 12(3), 913-932.
- Singh, P. K., Kumar, V., Purohit, R. C., Kothari, M., & Dashora, P. K. (2009). Application of principal component analysis in grouping geomorphic parameters for hydrologic modeling. *Water resources management*, 23(2), 325.
- Shahzad, Z., & Amtmann, A. (2017). Food for thought: how nutrients regulate root system architecture. *Current opinion in plant biology*, 39, 80-87.

- Shamir, E., Imam, B., Morin, E., Gupta, H. V., & Sorooshian, S. (2005). The role of hydrograph indices in parameter estimation of rainfall–runoff models. *Hydrological Processes: An International Journal*, 19(11), 2187-2207.
- Soylu, M. E., Kucharik, C. J., & Loheide II, S. P. (2014). Influence of groundwater on plant water use and productivity: development of an integrated ecosystem–variably saturated soil water flow model. *Agricultural and Forest Meteorology*, 189, 198-210.
- Tang, G., Carroll, R. W., Lutz, A., & Sun, L. (2016). Regulation of precipitation-associated vegetation dynamics on catchment water balance in a semiarid and arid mountainous watershed. *Ecohydrology*, 9(7), 1248-1262.
- Terrestrial Biophysics and Remote Sensing Lab (TBRs), Theoretical Basis for the Enhanced Vegetation Index. Accessed March 2008 from <http://tbrs.arizona.edu/cdrom/Index.html>.
- The Editors of Encyclopaedia Britannica (2016, October 12). Lapse rate. Retrieved from <https://www.britannica.com/science/lapse-rate>
- Troch, P. A., Martinez, G. F., Pauwels, V. R., Durcik, M., Sivapalan, M., Harman, C., ... & Huxman, T. (2009). Climate and vegetation water use efficiency at catchment scales. *Hydrological Processes: An International Journal*, 23(16), 2409-2414.
- Vörösmarty, C. J., Federer, C. A., & Schloss, A. L. (1998). Potential evaporation functions compared on US watersheds: Possible implications for global-scale water balance and terrestrial ecosystem modeling. *Journal of Hydrology*, 207(3-4), 147-169.
- Wang-Erlandsson, L., Van Der Ent, R. J., Gordon, L. J., & Savenije, H. H. G. (2014). Contrasting roles of interception and transpiration in the hydrological cycle–Part 1: Temporal characteristics over land. *Earth System Dynamics*, 5(2), 441-469.
- Wang-Erlandsson, L., Bastiaanssen, W. G., Gao, H., Jagermeyr, J., Senay, G. B., Van Dijk, A., ... & Savenije, H. H. (2016). Global root zone storage capacity from satellite-based evaporation. In *EGU General Assembly Conference Abstracts* (Vol. 18).
- Wang, X., Xie, H., Guan, H., & Zhou, X. (2007). Different responses of MODIS-derived NDVI to root-zone soil moisture in semi-arid and humid regions. *Journal of hydrology*, 340(1-2), 12-24.
- Water Data Online (WDO) © Copyright Commonwealth of Australia 2020, Bureau of Meteorology. <http://www.bom.gov.au/waterdata/>
- Werth, S., & Güntner, A. (2009). Calibration analysis for water storage variability of the global hydrological model WGHM. *Hydrol Earth Syst Sci Discuss*, 6, 4813-4861.
- Widén-Nilsson, E., Halldin, S., & Xu, C. Y. (2007). Global water-balance modelling with WASMOD-M: Parameter estimation and regionalisation. *Journal of Hydrology*, 340(1-2), 105-118.
- Wilson, N., Tickle, P.K., Gallant, J., Dowling, T., Read, A. 2011. 1 second SRTM Derived Hydrological Digital Elevation Model (DEM-H) version 1.0. Record 1.0.4. Geoscience Australia, Canberra. Retrieved from <http://pid.geoscience.gov.au/dataset/ga/71498>
- Winsemius, H. C., Schaefli, B., Montanari, A., & Savenije, H. H. G. (2009). On the calibration of hydrological models in ungauged basins: A framework for integrating hard and soft hydrological information. *Water Resources Research*, 45(12).
- Zhao, J., Xu, Z., & Singh, V. P. (2016). Estimation of root zone storage capacity at the catchment scale using improved Mass Curve Technique. *Journal of Hydrology*, 540, 959-972.
- Zhang, S. X., Bari, M., Amirthanathan, G., Kent, D., MacDonald, A., & Shin, D. (2014). Hydrologic reference stations to monitor climate-driven streamflow variability and trends. In *Hydrology and Water Resources Symposium 2014* (p. 1048). Engineers Australia.
- Zhang, L., Dawes, W. R., & Walker, G. R. (2001). Response of mean annual evapotranspiration to vegetation changes at catchment scale. *Water resources research*, 37(3), 701-708.
- Zeng, X. (2001). Global vegetation root distribution for land modeling. *Journal of Hydrometeorology*, 2(5), 525-530.

A

Station information

A.1 Discharge station summary

The following tables provide two parts information: the discharge station and selected catchment. For the discharge station, the location of the discharge station including basin, river, station name and station number (AWRC ID) are summarised; for the catchment, the size, the longest stream length and the maximum and minimum elevation in the catchment are summarised.

Queensland

<i>Basin</i>	<i>River</i>	<i>Station</i>	<i>AWRC ID</i>	<i>Area [km²]</i>	<i>Location</i>		<i>Longest Stream [km]</i>	<i>Elevation [m]</i>	
					<i>Longitude [E]</i>	<i>Latitude [S]</i>		<i>Max</i>	<i>Min</i>
Barwon-Condamine-Culgoa Rivers	Dalrymple Creek	Allora	422319B	227	152.0143	28.0352	55	1071	459
	Emu Creek	Emu Vale	422313B	138	152.2272	28.2289	35	1380	491
	Kings Creek	Aides Bridge	422334A	579	151.8604	27.9267	77	975	427
	Swan Creek	Swanfels	422306A	74	152.2835	28.1647	13	1249	528
Brisbane River	Bremer River	Adams Bridge	143110A	113	152.5117	27.8277	26	880	79
	Stanley Rriver	Peachester	143303A	87	152.8416	26.8385	29	542	95
Burnett River	Barambah Creek	Litzows	136202D	580	152.0433	26.3007	92	733	303
	Barker Creek	Brooklands	136203A	278	151.8188	26.7368	42	1109	384
Burrum River	Isis River	Bruce Highway	137201A	402	152.3684	25.2666	45	340	18
	Gregory River	Isis Highway	137101A	389	152.2405	25.0862	80	659	41
Daintree River	Bloomfield River	China Camp	108003A	215	145.2808	16.1807	37	1244	150
Don River	Don River	Ida Creek	121001A	516	148.1174	20.2888	48	798	78

Flinders-Norman Rivers	Elizabeth Creek	Mount Surprise	917107A	382	144.3065	18.1336	54	978	432
Herbert River	Blunder Creek	Wooroora	116015A	105	145.4363	17.7371	33	1059	662
	Millstream	Archer Creek	116013A	269	145.3409	17.6523	54	1380	637
	Wild River	Silver Valley	116014A	491	145.2959	17.6266	58	1234	638
Johnstone River	Liverpool Creek	Upper Japoonvale	112102A	66	145.9057	17.7147	16	338	66
Logan-Albert Rivers	Albert River	Lumeah Number 2	145101D	153	153.0446	28.0542	45	1136	83
	Burnett Creek	Upstream Maroon Dam	145018A	74	152.6085	28.2196	21	1243	233
	Canungra Creek	Main Road Bridge	145107A	89	153.1583	27.9976	45	1159	79
	Running Creek	Dieckmans Bridge	145010A	141	152.8907	28.2453	39	1002	101
	Teviot Brook	Croftby	145011A	75	152.5701	28.148	20	1327	170
Mary River	Kandanga Creek	Hygait	138113A	155	152.645	26.39	54	678	85
	Tinana Creek	Tagigan Road	138009A	100	152.7838	26.0773	29	381	71
Proserpine River	Gregory River	Lower Gregory	122004A	58	148.5484	20.3004	11	741	28
South Coast	Coomera River	Army Camp	146010A	88	153.1928	28.0258	43	1119	104
	Currumbin Creek	Nicolls Bridge	146012A	27	153.4237	28.1787	19	595	18
	Tallebudgera Creek	Tallebudgera Creek Road	146095A	51	153.4025	28.1497	19	924	12
Tully-Murray Rivers	Cochable Creek	Powerline	113004A	83	145.6301	17.7396	23	1167	134

New South Wales

<i>Basin</i>	<i>River</i>	<i>Station</i>	<i>AWRC ID</i>	<i>Area</i>	<i>Location</i>		<i>Longest Stream [km]</i>	<i>Elevation [m]</i>	
					<i>Longitude [E]</i>	<i>Latitude [S]</i>		<i>Max</i>	<i>Min</i>
Border Rivers	Tenterfield Creek	Clifton	416003	318	151.7246	29.0312	79	1325	650
Clyde River-Jervis Bay	Currambene Creek	Falls Creek	216004	92	150.6001	34.9684	26	306	16
Gwydir River	Copes Creek	Kimberley	418005	220	151.1148	29.9164	44	1185	747
Hawkesbury River	Nepean River	Maguires Crossing	212209	69	150.5337	34.4765	22	823	536
Hunter River	Williams River	Tillegra	210011	184	151.6873	32.3187	55	1507	92
Macleay River	Apsley River	Apsley Falls	206018	800	151.7691	31.0504	77	1130	899
	Wollomombi River	Coninside	206014	337	152.0273	30.476	65	1472	908
Manning River	Barnard River	barry	208009	141	151.3154	31.5795	25	1410	596
	Nowendoc River	Nowendoc	208007	207	151.7157	31.5164	33	1436	836

Murrumbidgee River	Adelong Creek	B low Road	410061	142	148.0685	35.3323	32	1000	350
	Goobarragandra River	Lacmalac	410057	648	148.3484	35.329	50	1716	299
	Gudgenby River	Tennent	410731	655	149.0683	35.5722	59	1739	614
	Cotter River	Gingera	410730	126	148.8219	35.5881	22	1912	982
	Molonglo River	Burbong	410705	474	149.3132	35.3356	58	1302	676
	Queanbeyan River	Tinderry	410734	509	149.35	35.6144	59	1539	786
Shoalhaven River	Corang River	Hockeys	215004	188	150.0331	35.1473	31	915	515
Tuross River	Tuross River	Tuross Vale	218001	91	149.5103	36.2646	23	1303	936
Upper Murray	Bowna Creek	Yambla	401015	282	146.9751	35.9175	19	662	199
	Maragle Creek	Maragle	401009	213	148.0999	35.9256	36	1324	376
	Big River	Jokers Creek	401216	358	147.4722	36.9327	45	1983	691
	Cudgewa Creek	Berringama	401208	352	147.6777	36.2119	28	1270	386
	Gibbo River	Gibbo Park	401217	385	147.7093	36.7566	48	1751	495
	Nariel Creek	Upper Nariel	401212	261	147.8295	36.445	46	1763	495
	Snowy Creek	Below Granite Fl	401210	408	147.4134	36.5685	40	1946	316

Victoria

<i>Basin</i>	<i>River</i>	<i>Station</i>	<i>AWRC ID</i>	<i>Area</i>	<i>Location</i>		<i>Longest Stream [km]</i>	<i>Elevation [m]</i>	
				[km ²]	<i>Longitude [E]</i>	<i>Latitude [S]</i>		<i>Max</i>	<i>Min</i>
Avoca River	Avoca River	Amphitheatre	408202	76	143.4056	37.182	16	784	274
Avon	Richardson River	Carrs Plains	415226	127	142.7869	36.7416	33	295	157
Broken River	Holland Creek	Kelfeera	404207	456	146.0592	36.6112	59	1132	174
Campaspe River	Axe Creek	Longlea	406214	234	144.4281	36.7735	31	705	166
	Campaspe River	Redesdale	406213	642	144.5403	37.0151	86	1000	223
	Mount pleasant Creek	Runnymede	406224	188	144.6377	36.5457	45	386	135
East Gippsland	Errinundra River	Errinundra	221207	158	148.9153	37.447	28	1201	143
Glenelg River	Jimmy Creek	Jimmy Creek	238208	23	142.5071	37.3744	9	1070	319
Goulburn	Acheron River	Taggerty	405209	631	145.7129	37.3177	53	1451	207
	Big River	Frenchman Creek Junction	405264	332	146.0761	37.5194	31	1435	450

	Brankeet Creek	Ancona	405251	119	145.7855	36.9688	18	957	318
	Ford Creek	Mansfield	405245	117	146.0536	37.0383	21	738	308
	Major Creek	Graytown	405248	301	144.9146	36.8544	32	570	143
	Mollison Creek	Pyalong	405238	164	144.8573	37.1203	32	773	246
	Murrindindi River	Murrindindi Above Colwells	405205	107	145.564	37.4137	29	1010	318
	Yea River	Devlins Bridge	405217	356	145.4731	37.3827	36	952	215
Kiewa River	Running Creek	Running Creek	402206	127	147.0442	36.5393	23	1189	251
	Yackandandah Creek	Osbornes Flat	402204	255	146.9068	36.3046	28	1162	218
Loddon River	Bet bet Creek	Norwood	407220	361	143.6288	36.9917	58	616	196
	Creswick Creek	Clunes	407214	305	143.7898	37.2966	40	731	298
	Piccaninny Creek	Minto	407253	597	144.4694	36.4519	100	439	119
Mitchell-Thomson Rivers	Latrobe River	Near Noojee	226222	66	145.893	37.8822	14	863	262
	Loch River	Noojee	226220	105	146.0068	37.8667	16	1090	249
	Morwell River	Boolarra	226407	120	146.3054	38.407	20	517	105
	Tambo River	U/S of Smith Creek	224213A	445	147.393	37.495	107	1859	178
Ovens River	Boggy Creek	Angleside	403226	109	146.3625	36.6063	31	850	187
	Happy valley Creek	Rosewhite	403214	144	146.8201	36.5775	21	1169	245
	Morses Creek	Wandiligong	403232	125	146.9794	36.7513	23	1253	325
	Reedy Creek	Woolshed	403221	206	146.6012	36.3109	27	900	229
South Gippsland	Tarwin River East Branch	Dumbalk North	227226	131	146.161	38.4996	30	420	57
	Wilkur Creek	Leongatha	227227	107	145.957	38.394	21	480	72
Wimmera	Wimmera River	Eversley	415207	305	143.1846	37.185	28	949	248

South Australia

<i>Basin</i>	<i>River</i>	<i>Station</i>	<i>AWRC ID</i>	<i>Area</i> [km ²]	<i>Location</i>		<i>Longest Stream</i> [km]	<i>Elevation [m]</i>	
					<i>Longitude</i> [E]	<i>Latitude</i> [S]		<i>Max</i>	<i>Min</i>
Gawler River	North Para River	Penrice	A5050517	112	139.0584	34.4632	26	578	298
Kangaroo Island	Rocky River upstream	Gorge Falls	A5130501	186	136.6979	35.9571	34	308	45
Millicent Coast	MORAMBRO CK	Bordertown-Naracoorte Road Bridge	A2390531	554	140.6597	36.6886	42	165	60
	STONY CREEK	Woakwine Range	A2390523	523	140.3622	37.7034	-	197	5
Onkaparinga River	Scott Creek	Scott Bottom	A5030502	27	138.673	35.1013	12	497	207
Torrens River	Sixth Creek	Castambul	A5040523	42	138.7529	34.873	16	600	194
Kanyaka Creek	Kanyaka Creek	Old Kanyaka Ruins	A5090503	161	138.29	32.09	-	548	287

Western Australia

<i>Basin</i>	<i>River</i>	<i>Station</i>	<i>AWRC ID</i>	<i>Area</i> [km ²]	<i>Location</i>		<i>Longest Stream</i> [km]	<i>Elevation [m]</i>	
					<i>Longitude</i> [E]	<i>Latitude</i> [S]		<i>Max</i>	<i>Min</i>
Busselton Coast	Margaret River North	Whicher Range	610008	15	115.4436	33.8066	10	190	143
Donnelly River	Carey Brook	Staircase Rd	608002	47	115.8435	34.3922	15	242	45
Frankland-Deep Rivers	Deep River	Teds Pool	606001	526	116.6158	34.7668	61	318	102
Murray River (WA)	Clarke Brook	Hillview Farm	613146	16	115.922	32.9977	11	320	94
	Harvey River	Dingo Rd	613002	140	116.0389	33.0871	26	473	188
	Yarragil Brook	Yarragil Formation	614044	69	116.1551	32.8114	19	369	173
Ord-Pentecost Rivers	Ord River	Bedford Downs	809310	458	127.6001	17.4259	49	924	434
Swan Coast-Avon River	Canning River	Glen Eagle	616065	490	116.172	32.228	51	570	217
	Darkin River	Pine Plantation	616002	628	116.293	32.069	37	545	158
	Helena River	Ngangaguringuring	616013	330	116.403	31.939	28	399	193
Hill River	Hill River	Hill River Springs	617002	841	115.37	30.28	-	157	345

Northern Territory

<i>Basin</i>	<i>River</i>	<i>Station</i>	<i>AWRC ID</i>	<i>Area</i>	<i>Location</i>		<i>Longest Stream [km]</i>	<i>Elevation [m]</i>	
				[km ²]	<i>Longitude [E]</i>	<i>Latitude [S]</i>		<i>Max</i>	<i>Min</i>
Adelaide River at Railway Bridge	Adelaide River	Railway Bridge	G8170002	523	131.1086	13.2415	46	259	48
	Green Ant Creek	Tipperary	G8140161	349	131.1023	13.7381	51	278	42
	Trephina Creek	Trephina Gorge	G1060005	377	134.3806	23.5368	49	1101	536
Finniss River	Elizabeth River	Stuart Hwy	G8150018	83	131.0738	12.6059	19	90	16
Roper River	Daly Waters Creek	Daly Waters	G9030124	329	133.3757	16.2598	44	278	206

Tasmania

<i>Basin</i>	<i>River</i>	<i>Station</i>	<i>AWRC ID</i>	<i>Area</i>	<i>Location</i>		<i>Longest Stream [km]</i>	<i>Elevation [m]</i>	
				[km ²]	<i>Longitude [E]</i>	<i>Latitude [S]</i>		<i>Max</i>	<i>Min</i>
Derwent River	Nive River	Gowan Brae	304497	179	146.4194	42.031	29	1307	803
East Coast	Ansons River	Ansons River DS Big Boggy CK	302214	177	148.2174	41.0464	30	462	16
Gordon River	Collingwood River	B/L Alma	308799	291	145.9288	42.1638	28	1391	339
	Leven River(14207)	Leven River at Bannons BR	314207	526	146.0906	41.251	55	1347	44
Tarma River	North Esk River	Ballroom	318067	402	147.384	41.494	44	1572	321

A.2 Precipitation and temperature station summary

The following tables provide meteorology station information, including precipitation and temperature. Based on the location of the runoff station, the runoff station of each represents a selected catchment. Precipitation stations and temperature stations located within the catchment or within 30 km and 50 km respectively from the boundary of the catchment are selected. For every catchment, at least two precipitation and one temperature station are concluded. The station number, the location (showing in latitude and longitude), the distance between the precipitation/temperature station and the runoff station are shown below.

Queensland

Runoff station	Precipitation Station					Temperature Station				
	Name	Number	Distance (km)	Latitude	Longitude	Name	Number	Distance (km)	Latitude	Longitude
422319B	Upper Forest Springs	41106	9.8	27.97	152.08	University Of Queensland Gatton	40082	62.9	27.54	152.34
	Clintonvale	41259	12.0	28.07	152.13	Amberley AMO	40004	72.4	27.63	152.71
	Glenrive	41276	18.5	27.93	152.16					
422313B	Helenvale	41167	8.0	28.17	152.28	Tabulam (Muirne)	57095	62.1	28.76	152.45
	Killarney Post Office	41056	15.5	28.33	152.30					
	Top Plains	41134	19.4	28.31	152.40					
422334A	Clifton Post Office	41018	4.5	27.93	151.91	University Of Queensland Gatton	40082	63.1	27.54	152.34
	Navilloween	41256	17.4	27.81	151.99					
	Upper Forest Springs	41106	21.4	27.97	152.08					
422306A	Helenvale	41167	1.0	28.17	152.28	Tabulam (Muirne)	57095	67.3	28.76	152.45
	Oakington	41464	4.8	28.15	152.33	University Of Queensland Gatton	40082	68.9	27.54	152.34
	Cunninghams Gap National Park	41456	18.2	28.06	152.37	Amberley AMO	40004	72.4	27.63	152.71
143110A	Rosevale	40183	4.1	27.85	152.48	Amberley AMO	40004	29.3	27.63	152.71
	Moorang	40400	9.5	27.91	152.47	University Of Queensland Gatton	40082	35.7	27.54	152.34
143303A	Maleny Denning Rd	40396	7.7	26.78	152.80	Cape Moreton Lighthouse	40043	65.2	27.03	153.47
	Beerburum Forest Station	40284	17.8	26.96	152.96					
	Palmwoods	40695	20.6	26.68	152.96					
136202D	Wooroolin Post Office	40255	25.6	26.41	151.82	Brian Pastures	40428	77.3	25.66	151.75
	Kilkivan Post Office	40111	30.6	26.09	152.24	Gayndah Airport	39066	86.8	25.62	151.62
	Nanango Wills St	40158	41.7	26.68	151.99	Maryborough	40126	109.8	25.51	152.72
136203A	Tarong	40199	2.6	26.74	151.84	University Of Queensland Gatton	40082	102.8	27.54	152.34

	<i>Kumbia Post Office</i>	40113	17.0	26.69	151.66					
	<i>Vincent Vale</i>	40307	27.6	26.97	151.71					
137201A	<i>Childers South</i>	39303	8.7	25.26	152.28	<i>Bundaberg Aero</i>	39128	40	24.91	152.32
	<i>Duckinwilla Creek</i>	40069	15.5	25.39	152.43	<i>Maryborough</i>	40126	44.1	25.51	152.72
	<i>Biggenden Post Office</i>	40021	42.0	25.51	152.05					
137101A	<i>Bingera Sugar Mill</i>	39186	17.8	24.93	152.20	<i>Bundaberg Aero</i>	39128	21.5	24.91	152.32
	<i>Childers South</i>	39303	38.9	25.26	152.28	<i>Maryborough</i>	40126	66.9	25.51	152.72
	<i>Biggenden Post Office</i>	40021	42.5	25.51	152.05					
108003A	<i>Cape Tribulation Store</i>	31012	20.9	16.10	145.46	<i>Low Isles Lighthouse</i>	31037	37.1	16.38	145.56
	<i>Shiptons Flat</i>	31112	42.8	15.80	145.24					
121001A	<i>Roma Peak</i>	33110	10.8	20.30	148.22	<i>Proserpine Airport</i>	33247	50.6	20.49	148.56
	<i>Hecate</i>	33158	33.4	20.50	148.34					
	<i>Collinsville Post Office</i>	33013	40.5	20.55	147.85					
917107A	<i>Rosella Plains Station</i>	30046	35.9	18.42	144.46	<i>Georgetown Post Office</i>	30018	81.6	18.29	143.55
	<i>Eveleigh Station</i>	30103	36.7	18.22	143.97	<i>Georgetown Airport</i>	30124	83.6	18.3	143.53
116015A	<i>Woodleigh</i>	31119	18.0	17.68	145.28	<i>South Johnstone Exp Stn</i>	32037	60.9	17.61	146
	<i>Innot Hot Springs Township</i>	31069	22.2	17.67	145.24	<i>Koombooloomba Dam</i>	31083	20.3	17.84	145.6
116013A	<i>Woodleigh</i>	31119	7.1	17.68	145.28	<i>South Johnstone Exp Stn</i>	32037	54.8	69.4	146
	<i>Evelyn State Forest</i>	31024	19.8	17.54	145.48	<i>Innisfail</i>	32025	74.5	17.52	146.03
	<i>Greenhaven</i>	31168	28.2	17.59	145.60					
116014A	<i>Woodleigh</i>	31119	5.7	17.68	145.28	<i>Koombooloomba Dam</i>	31083	39.4	33.9	145.6
	<i>Evelyn State Forest</i>	31024	21.4	17.54	145.48	<i>South Johnstone Exp Stn</i>	32037	74	69.4	146
						<i>Innisfail</i>	32025	78.7	17.52	146.03
112102A	<i>Menavale Alert</i>	32019	1.9	17.72	145.92	<i>Innisfail</i>	32025	25	17.52	146.03
	<i>Mena Creek Post Office</i>	32164	4.2	17.68	145.89	<i>South Johnstone Exp Stn</i>	32037	15.5	17.61	146
	<i>Japoonvale Warrakin Rd</i>	32119	8.4	17.66	145.96					
	<i>Bingil Bay</i>	32009	24.3	17.84	146.10					
	<i>Tully Sugar Mill</i>	32025	14.2	17.52	146.03					
145101D	<i>Lumeah</i>	40407	1.1	28.06	153.03	<i>Murwillumbah (Bray Park)</i>	58158	45.5	28.34	153.38
145018A	<i>Maroon Dam</i>	40677	6.7	28.18	152.66	<i>Tabulam (Muirne)</i>	57095	61.2	28.76	152.45
	<i>Wilsons Peak</i>	40485	8.9	28.25	152.52					

	<i>Woodenbong (Unumgar St)</i>	57024	18.6	28.39	152.61					
145107A	<i>Canungra Finch Road</i>	40042	2.0	28.01	153.17	<i>Murwillumbah (Bray Park)</i>	58158	43.6	28.34	153.38
	<i>Lumeah</i>	40407	13.8	28.06	153.03					
145010A	<i>Rathdowney Post Office</i>	40178	4.5	28.21	152.87	<i>Murwillumbah (Bray Park)</i>	58158	48.9	28.34	153.38
	<i>Mount Barney</i>	40394	10.6	28.23	152.78					
145011A	<i>Carneys Creek The Ranch</i>	40490	7.4	28.21	152.54	<i>Amberley AMO</i>	40004	58.9	27.63	152.71
	<i>Wilsons Peak</i>	40485	12.1	28.25	152.52					
138113A	<i>Traveston</i>	40206	15.8	26.33	152.79	<i>Double Island Point Lighthouse</i>	40068	74.2	25.93	153.19
	<i>Kenilworth Township</i>	40106	23.7	26.60	152.73	<i>Tewantin RSL Park</i>	40908	39.2	26.39	153.04
138009A	<i>Goomboorian</i>	40089	2.4	26.06	152.79	<i>Double Island Point Lighthouse</i>	40068	43.5	25.93	153.19
	<i>Traveston</i>	40206	27.4	26.33	152.79	<i>Tewantin RSL Park</i>	40908	43	26.39	153.04
122004A	<i>Kelsey Creek Dittmer Rd</i>	33127	17.5	20.43	148.45	<i>Mackay M.o</i>	33247	49.5	20.49	148.56
	<i>Proserpine Airport</i>	33247	21.3	20.49	148.56					
146010A	<i>Canungra Finch Road</i>	40042	2.9	28.01	153.17	<i>Murwillumbah (Bray Park)</i>	58158	39.2	28.34	153.38
	<i>Upper Mudgeeraba Water</i>	40606	15.9	28.11	153.33					
146012A	<i>Tallebudgera Guineas Creek Road</i>	40196	4.3	28.14	153.43	<i>Murwillumbah (Bray Park)</i>	58158	18.3	28.34	153.38
	<i>Murwillumbah (Bray Park)</i>	58158	18.3	28.34	153.38					
146095A	<i>Tallebudgera Guineas Creek Road</i>	40196	4.3	28.14	153.43	<i>Murwillumbah (Bray Park)</i>	58158	21.1	28.34	153.38
	<i>Elanora Water Treatment Plant</i>	40609	5.5	28.12	153.45					
	<i>Upper Mudgeeraba Water</i>	40606	8.7	28.11	153.33					
113004A	<i>Greenhaven</i>	31168	17.1	17.59	145.60	<i>Koombooloomba Dam</i>	31083	11.7	33.9	145.6
	<i>Evelyn State Forest</i>	31024	27.5	17.54	145.49	<i>South Johnstone Exp Stn</i>	32037	41.4	69.4	146

New South Wales

<i>Discharge station</i>	<i>Rainfall Station</i>					<i>Temperature Station</i>				
	<i>Name</i>	<i>Number</i>	<i>Distance (km)</i>	<i>Latitude</i>	<i>Longitude</i>	<i>Name</i>	<i>Number</i>	<i>Distance (km)</i>	<i>Latitude</i>	<i>Longitude</i>
416003	<i>Tenterfield (Aberfeldie)</i>	56050	2.4	29.02	151.75	<i>Tenterfield (Federation Park)</i>	56032	28.3	29.05	152.02
	<i>Tenterfield (Federation Park)</i>	56032	28.3	29.05	152.02					

204034	<i>Pinkett (Benbookra)</i>	56205	25.5	29.90	151.97	<i>Glen Innes Ag Research Stn</i>	56013	50.4	29.7	151.69
	<i>Kookabookra</i>	57103	33.5	30.01	152.01	<i>Guyra Hospital</i>	56229	50.7	30.21	151.68
	<i>Mount Mitchell (Tirranna)</i>	56163	43.4	30.00	151.85					
216004	<i>Culburra Treatment Works</i>	68083	14.1	34.93	150.75	<i>Ulladulla AWS</i>	69049	49.5	35.12	150.08
	<i>Bendalong STP</i>	68229	31.5	35.24	150.51	<i>Nerriga Composite</i>	69138	45	35.36	150.48
418005	<i>Tingha (Crystal Hill)</i>	56007	17.3	29.93	151.29	<i>Inverell (Raglan St)</i>	56242	15.1	29.78	151.11
	<i>Copeton Dam</i>	54128	21.3	29.89	150.90					
212209	<i>Mittagong (Alfred Street)</i>	68044	7.7	34.45	150.46	<i>Bankstown Airport AWS</i>	66137	74.3	33.92	150.99
	<i>Barrengarry (The Old School House)</i>	68217	23.4	34.69	150.53	<i>Nerriga Composite</i>	69138		35.36	150.48
210011	<i>Chichester Dam</i>	61151	8.4	32.24	151.68	<i>Lostock Dam</i>	61288	21.3	32.33	151.46
	<i>Clarence Town (Prince St)</i>	61010	30.7	32.59	151.77	<i>Paterson (Tocal AWS)</i>	61250	35.5	32.63	151.59
206018	<i>Walcha (Emu Creek)</i>	56010	13.5	30.94	151.71	<i>Woolbrook (Woolbrook Road)</i>	55136	40.8	30.97	151.35
	<i>Walcha (Thee St)</i>	56234	18.7	30.99	151.59					
206014	<i>Hillgrove (Hillview)</i>	57028	15.1	30.56	151.91	<i>Woolbrook (Woolbrook Road)</i>	55136	84.1	30.97	151.35
	<i>Guyra (Lyndhurst)</i>	57049	18.3	30.31	152.05	<i>Glen Innes Ag Research Stn</i>	56013	92.1	29.7	151.69
208009	<i>Nundle (Benoni)</i>	55078	28.0	31.41	151.09	<i>Murrurundi (Haydon Street)</i>	61051	49.2	31.77	150.84
	<i>Nundle (Chaffey Dam)</i>	55302	30.0	31.36	151.14	<i>Woolbrook (Woolbrook Road)</i>	55136	68	30.97	151.35
208007	<i>Nowendoc (Green Hills)</i>	60104	15.9	31.41	151.60	<i>Yarras (Mount Seaview)</i>	60085	52.2	31.39	152.25
	<i>Glen Morrison (Branga Plains)</i>	56083	32.1	31.26	151.55	<i>Woolbrook (Woolbrook Road)</i>	55136	70.1	30.97	151.35
410061	<i>Mount Horeb (Marathorn)</i>	72154	13.4	35.22	148.03	<i>Wagga Wagga AMO</i>	72150	58.4	35.16	147.46
	<i>Blowering Dam</i>	72056	17.5	35.39	148.25	<i>Burrinjuck Dam</i>	73007	60.4	35	148.6
410057	<i>Blowering Dam</i>	72056	11.7	35.39	148.25	<i>Burrinjuck Dam</i>	73007	60.4	35	148.6
	<i>Mount Horeb (Marathorn)</i>	72154	31.3	35.22	148.03	<i>Wagga Wagga AMO</i>	72150	82.6	35.16	147.46
410731	<i>Michelago (Soglio)</i>	70064	14.5	35.68	149.16	<i>Cooma Visitors Centre</i>	70278	49.1	36.23	149.12
	<i>Torrens (Darke St)</i>	70308	21.8	35.38	149.09	<i>Burrinjuck Dam</i>	73007	60.4	35	148.6
410730	<i>Adaminaby (Yaouk)</i>	71040	21.9	35.79	148.81	<i>Burrinjuck Dam</i>	73007	68.1	35	148.6
	<i>Michelago (Soglio)</i>	70064	32.0	35.68	149.16	<i>Cooma Visitors Centre</i>	70278	49.1	36.23	149.12
410705	<i>Sutton (Uba)</i>	70232	11.1	35.25	149.26	<i>Nerriga Composite</i>	69049	73.8	35.12	150.08
410734	<i>Michelago (Soglio)</i>	70064	18.5	35.68	149.16	<i>Cooma Visitors Centre</i>	70278	71.2	36.23	149.12
	<i>Jerrabattgulla (Gilston)</i>	70261	22.9	35.69	149.59					

	<i>Braidwood (Krawarree)</i>	70057	34.4	35.82	149.63					
215004	<i>Charleyong (Nerriga Road)</i>	69041	15.6	35.25	149.92	<i>Nerriga Composite</i>	69049	5.8	35.12	150.08
	<i>Lower Boro (Calderwood)</i>	70060	23.6	35.16	149.77	<i>Braidwood Racecourse AWS</i>	69132	38.1	35.43	149.78
218001	<i>Tuross</i>	69054	3.5	36.30	149.51	<i>Cooma Visitors Centre</i>	70278	71.2	36.23	149.12
	<i>Belowra Station</i>	69037	19.2	36.20	149.71	<i>Bega (Newtown Road)</i>	69002	55.2	36.69	149.84
	<i>Rock Flat (Old Post Office)</i>	70165	29.5	36.35	149.20	<i>Bega AWS</i>	69139	52.8	36.67	149.82
401015	<i>Albury Airport</i>	72146	16.9	36.07	146.95	<i>Rutherglen Research</i>	82039	46.5	36.1	146.51
	<i>Bungowannah (Roseleigh)</i>	74236	22.5	36.02	146.76	<i>Hume Reservoir</i>	72023	21.3	36.1	147.03
	<i>Culcairn Bowling Club</i>	74188	27.7	35.67	147.04					
401009	<i>Tumbarumba Post Office</i>	72043	18.1	35.78	148.01	<i>Dartmouth Reservoir</i>	82076	86.2	36.54	147.5
	<i>Tumbarumba (Landsdowne)</i>	72080	27.2	35.72	147.93	<i>Hume Reservoir</i>	72023	97.5	36.1	147.03
401216	<i>Omeo Shannon Vale</i>	83035	4.4	36.93	147.42	<i>Dartmouth Reservoir</i>	82076	44	36.54	147.5
	<i>Tawonga</i>	83038	43.1	36.66	147.13	<i>Hume Reservoir</i>	72023	99.6	36.1	147.03
401208	<i>Koetong</i>	82024	17.7	36.15	147.49	<i>Dartmouth Reservoir</i>	82076	39.2	36.54	147.5
	<i>Callaghan Creek Station</i>	82008	34.7	36.46	147.43					
401217	<i>Benambra (The Brothers)</i>	83064	21.3	36.94	147.78	<i>Dartmouth Reservoir</i>	82076	30.8	36.54	147.5
	<i>Dartmouth Reservoir</i>	82076	30.8	36.54	147.50					
401212	<i>Dartmouth Reservoir</i>	82076	30.8	36.54	147.50	<i>Dartmouth Reservoir</i>	82076	29.6	36.54	147.5
	<i>Towong Upper</i>	82060	32.3	36.20	148.02	<i>Hume Reservoir</i>	72023	80.4	36.1	147.03
401210	<i>Dartmouth Reservoir</i>	82076	30.8	36.54	147.50	<i>Dartmouth Reservoir</i>	82076	8.4	36.54	147.5
	<i>Tawonga</i>	83038	27.1	36.66	147.13					
	<i>Omeo Shannon Vale</i>	83035	39.5	36.93	147.42					

Victoria

<i>Discharge station</i>	Rainfall Station					Temperature Station				
	Name	Number	Distance (km)	Latitude	Longitude	Name	Number	Distance (km)	Latitude	Longitude
408202	<i>Moonambel</i>	79031	24.6	36.99	143.27	<i>Maryborough</i>	88043	32	37.06	143.73
	<i>Beaufort (Sheepwash)</i>	89082	37.3	37.50	143.28	<i>Ararat Prison</i>	89085	39	37.28	142.98
415226	<i>Warranook (Glenorchy)</i>	79016	5.2	36.73	142.73	<i>Longerenong</i>	79028	43.9	36.67	142.3
	<i>Tottington</i>	79079	30.1	36.79	143.12	<i>Ararat Prison</i>	89085	61.6	37.28	142.98

404207	<i>Molyullah (Killanoola)</i>	82109	4.8	36.61	146.11	<i>Strathbogie</i>	82042	39.1	36.85	145.73
	<i>Myrree (Joelyn)</i>	82033	22.2	36.70	146.29	<i>Lake Eildon</i>	88023	69.8	37.23	145.91
406214	<i>Knowsley</i>	81118	17.5	36.81	144.62	<i>Castlemaine Prison</i>	88110	37.9	37.08	144.24
	<i>Castlemaine Prison</i>	88110	37.9	37.08	144.24					
406213	<i>Malmsbury Reservoir</i>	88042	24.8	37.20	144.37	<i>Castlemaine Prison</i>	88110	27.6	37.08	144.24
	<i>Kyneton</i>	88123	27.5	37.25	144.44					
	<i>Lauriston Reservoir</i>	88037	29.8	37.25	144.38					
406224	<i>Colbinabbin</i>	81008	12.2	36.54	144.78	<i>Echuca Aerodrome</i>	80015	43.6	36.16	144.76
	<i>Knowsley</i>	81118	29.2	36.81	144.62	<i>Castlemaine Prison</i>	88110	68.9	37.08	144.24
221207	<i>Goongerah</i>	84134	21.4	37.34	148.71	<i>Point Hicks (Lighthouse)</i>	84070	50.3	37.8	149.27
	<i>Craigie (Bondi Forest Lodge)</i>	70326	39.0	37.15	149.15					
238208	<i>Mirranatwa (Bowacka)</i>	89019	11.3	37.40	142.38	<i>Ararat Prison</i>	89085	42.8	37.28	142.98
	<i>Moyston (Barton Estate)</i>	79050	17.9	37.32	142.70					
405209	<i>Buxton</i>	88130	11.7	37.42	145.71	<i>Lake Eildon</i>	88023	20	37.23	145.91
	<i>Lake Eildon</i>	88023	20.0	37.23	145.91					
405264	<i>Buxton</i>	88130	34.0	37.42	145.71	<i>Lake Eildon</i>	88023	35	37.23	145.91
	<i>Lake Eildon</i>	88023	35.0	37.23	145.91					
405251	<i>Strathbogie</i>	82042	14.3	36.85	145.73	<i>Strathbogie</i>	82042	14.3	36.85	145.73
	<i>Creightons Creek (Baronga (Creighton's C</i>	82096	24.4	36.90	145.52					
405245	<i>Lake Eildon</i>	88023	24.7	37.23	145.91	<i>Lake Eildon</i>	88023	24.7	37.23	145.91
	<i>Strathbogie North</i>	82043	34.5	36.79	145.82	<i>Strathbogie</i>	82042	35.5	36.85	145.73
405274	<i>Highlands (Glentannar)</i>	88031	17.8	37.07	145.41	<i>Lake Eildon</i>	88023	30.4	37.23	145.91
	<i>Creightons Creek (Baronga (Creighton's C</i>	82096	23.9	36.90	145.52					
	<i>Strathbogie</i>	82042	30.7	36.85	145.73					
405248	<i>Tabilk (Tabilk Winery)</i>	88124	15.6	36.83	145.09	<i>Mangalore Airport</i>	88109	24.3	36.89	145.19
	<i>Wanalta Daen Station</i>	81115	25.3	36.63	144.87					
	<i>Wanalta Daen Station</i>	81115	25.3	36.63	144.87					
	<i>Baynton</i>	88073	36.0	37.13	144.69					
405238	<i>High Camp (Lannermoor)</i>	88121	6.6	37.14	144.93	<i>Mangalore Airport</i>	88109	38.7	36.89	145.19
	<i>Baynton</i>	88073	14.6	37.13	144.69	<i>Castlemaine Prison</i>	88110	54.4	37.08	144.24

405205	<i>Glenburn</i>	88028	8.9	37.38	145.47	<i>Lake Eildon</i>	88023	36.7	37.23	145.91
	<i>Buxton</i>	88130	38.5	37.42	145.71					
405217	<i>Glenburn</i>	88028	0.2	37.38	145.47	<i>Lake Eildon</i>	88023	42.1	37.23	145.91
	<i>Buxton</i>	88130	21.2	37.42	145.71	<i>Mangalore Airport</i>	88109	60.2	36.89	145.19
402213	<i>Wooragee</i>	82057	14.7	36.30	146.73	<i>Hume Reservoir</i>	72023	26.5	36.1	147.03
	<i>Beechworth Composite</i>	82001	17.2	36.37	146.71	<i>Rutherglen Research</i>	82039	45.4	36.1	146.51
	<i>Dederang</i>	82090	21.7	36.48	147.03					
402206	<i>Dederang</i>	82090	6.8	36.48	147.03	<i>Rutherglen Research</i>	72023	48.2	36.1	147.03
	<i>Tawonga</i>	83038	15.0	36.66	147.13	<i>Dartmouth Reservoir</i>	82076	40.4	36.54	147.5
	<i>Eurobin</i>	83010	19.2	36.63	146.86					
402204	<i>Wooragee</i>	82057	15.8	36.30	146.73	<i>Hume Reservoir</i>	72023	24.9	36.1	147.03
	<i>Beechworth Composite</i>	82001	18.7	36.37	146.71	<i>Rutherglen Research</i>	82039	41.8	36.1	146.51
	<i>Dederang</i>	82090	22.2	36.48	147.03					
407220	<i>Maryborough</i>	88043	11.6	37.06	143.73	<i>Maryborough</i>	88043	11.6	37.06	143.73
	<i>Redbank</i>	79039	27.3	36.91	143.34					
407214	<i>Ballarat Aerodrome</i>	89002	23.9	37.51	143.79	<i>Ballarat Aerodrome</i>	89002	23.9	37.51	143.79
	<i>Glen Park (White Swan Reservoir)</i>	89048	27.2	37.52	143.93					
407253	<i>Kotta</i>	80095	26.0	36.22	144.54	<i>Castlemaine Prison</i>	88110	72.5	37.08	144.24
	<i>Colbinabbin</i>	81008	40.0	36.54	144.78					
	<i>Colbinabbin</i>	81008	40.0	36.54	144.78					
226222	<i>Noojee Forestry</i>	85292	9.0	37.89	146.00	<i>Morwell (Latrobe Valley Airport)</i>	85280	62.2	38.21	146.47
	<i>Jindivick</i>	85042	15.5	38.02	145.89					
226220	<i>Noojee Forestry</i>	85292	9.0	37.89	146.00	<i>Noojee (Slivar)</i>	85277	5.1	37.9	145.97
	<i>Jindivick</i>	85042	20.1	38.02	145.89					
226407	<i>East Tarwin (Mirboo Pastoral Company)</i>	85227	15.4	38.52	146.20	<i>East Tarwin (Mirboo Pastoral Company)</i>	85227	15.4	38.52	146.2
	<i>Madalya</i>	85053	21.5	38.51	146.52	<i>Morwell (Latrobe Valley Airport)</i>	85280	26.3	38.21	146.47
223214A	<i>Dargo</i>	84012	13.4	37.45	147.25	<i>Bairnsdale Airport</i>	85279	45.4	37.88	147.57
	<i>Tongio (Brooklands)</i>	84037	44.5	37.18	147.71					
403226	<i>Myrree (Joelyn)</i>	82033	12.2	36.70	146.29	<i>Rutherglen Research</i>	82039	57	36.1	146.51

403222	<i>Carboor</i>	82009	17.4	36.61	146.54	<i>Strathbogie</i>	82042	62	36.85	145.73
	<i>Eurobin</i>	83010	33.8	36.63	146.86	<i>Lake Eildon</i>	88023	78	37.23	145.91
	<i>Carboor</i>	82009	17.4	36.61	146.54	<i>Dartmouth Reservoir</i>	82076	82	36.54	147.5
403214	<i>Eurobin</i>	83010	7.3	36.63	146.86	<i>Hume Reservoir</i>	72023	55.7	36.1	147.03
	<i>Dederang</i>	82090	21.6	36.48	147.03					
403232	<i>Eurobin</i>	83010	16.6	36.63	146.86	<i>Dartmouth Reservoir</i>	82076	51.9	36.54	147.5
	<i>Tawonga</i>	83038	16.9	36.66	147.13					
403221	<i>Wooragee</i>	82057	11.5	36.30	146.73	<i>Rutherglen Research</i>	82039	24.2	36.1	146.51
	<i>Beechworth Composite</i>	82001	11.9	36.37	146.71					
227226	<i>East Tarwin (Mirboo Pastoral Company)</i>	85227	15.4	38.52	146.20	<i>Wilson's Promontory Lighthouse</i>	85096	73.3	39.13	146.42
	<i>Leongatha Sth Gippsland Water</i>	85049	19.8	38.48	145.93	<i>East Sale</i>	86127	50.3	38.61	145.6
227227	<i>Leongatha Sth Gippsland Water</i>	85049	10.2	38.48	145.93	<i>Wonthaggi</i>	86127	39.1	38.61	145.6
	<i>East Tarwin (Mirboo Pastoral Company)</i>	85227	25.6	38.52	146.20					
415207	<i>Ararat Prison</i>	89085	20.8	37.28	142.98		89085	20.8	37.28	142.98
	<i>Redbank</i>	79039	33.7	36.91	143.34					
	<i>Beaufort (Sheepwash)</i>	89082	37.3	37.50	143.28					

South Australia

<i>Discharge station</i>	Rainfall Station					Temperature Station				
	Name	Number	Distance (km)	Latitude	Longitude	Name	Number	Distance (km)	Latitude	Longitude
A5050517	<i>Truro</i>	24573	8.7	34.41	139.13	<i>Rosedale (Turretfield Research Centre)</i>	23343	22.7	34.55	138.83
	<i>Dutton - Section 228</i>	24509	13.9	34.35	139.13					
A5130501	<i>Flinders Chase (Rocky River)</i>	22817	3.7	35.95	136.74	<i>Neptune Island</i>	18115	86.2	35.34	136.12
	<i>Vivonne Bay (Highgate)</i>	22839	35.2	35.96	137.09	<i>Stenhouse Bay</i>	22049	78	35.28	136.94
A2390531	<i>Bordertown (Beeamma Section 95)</i>	26058	10.2	36.61	140.71	<i>Mount Gambier Aero</i>	26021	117.5	37.75	140.77
	<i>Frances</i>	26007	26.3	36.71	140.96	<i>Coonawarra</i>	26091	68.2	37.29	140.83
A2390523	<i>Pelican Point</i>	26111	24.8	37.92	140.42	<i>Mount Gambier Aero</i>	26021	36.3	37.75	140.77

	<i>Mount Gambier Aero</i>	26021	36.3	37.75	140.77					
	<i>Mount Schank (Jethia)</i>	26067	45.5	37.96	140.77					
A5030502	<i>Mount Bold Reservoir</i>	23734	2.2	35.12	138.68	<i>Mount Barker</i>	23733	16	35.07	138.85
	<i>Cherry Gardens</i>	23709	4.6	35.06	138.66	<i>Adelaide (Kent Town)</i>	23090	20.5	34.92	138.62
	<i>Aldgate</i>	23817	10.6	35.02	138.74					
A5040523	<i>Adelaide (Hope Valley Reservoir)</i>	23096	6.5	34.86	138.68	<i>Adelaide (Kent Town)</i>	23090	13	34.92	138.62
	<i>Uraidla</i>	23750	9.2	34.96	138.74	<i>Parafield Airport</i>	23013	14.1	34.8	138.63
A5090503	<i>Hawker (Wilson)</i>	19050	12.3	31.99	138.34	<i>Hawker</i>	19017	24.8	31.9	138.44
	<i>Hawker</i>	19017	24.8	31.90	138.44					

Western Australia

<i>Discharge station</i>	<i>Rainfall Station</i>					<i>Temperature Station</i>				
	<i>Name</i>	<i>Number</i>	<i>Distance (km)</i>	<i>Latitude</i>	<i>Longitude</i>	<i>Name</i>	<i>Number</i>	<i>Distance (km)</i>	<i>Latitude</i>	<i>Longitude</i>
610008	<i>Yoongarillup</i>	9771	7.6	33.74	115.47	<i>Jarrahwood</i>	9842	20.4	33.8	115.67
	<i>Jarrahwood</i>	9842	20.4	33.80	115.67					
608002	<i>Pemberton</i>	9592	19.2	34.45	116.04	<i>Pemberton</i>	9592	19.2	34.45	116.04
	<i>Manjimup</i>	9573	31.7	34.25	116.15					
606001	<i>Vermeulen</i>	9928	12.4	34.84	116.72	<i>Pemberton</i>	9592	62.9	34.45	116.04
	<i>Bangalup</i>	9506	42.9	34.47	116.92	<i>Manjimup</i>	9573	71.4	34.25	116.15
	<i>Deeside</i>	9530	47.1	34.38	116.41					
613146	<i>Brunswick Junction</i>	9513	24.8	33.21	115.85	<i>Dwellingup</i>	9538	34.2	32.71	116.06
	<i>Dwellingup</i>	9538	34.2	32.71	116.06					
613002	<i>Brunswick Junction</i>	9513	22.4	33.21	115.85	<i>Dwellingup</i>	9538	41.7	32.71	116.06
	<i>Dwellingup</i>	9538	41.7	32.71	116.06					
614044	<i>Dwellingup</i>	9538	14.3	32.71	116.06	<i>Dwellingup</i>	9538	14.3	32.71	116.06
	<i>Bannister</i>	9507	36.7	32.68	116.52	<i>Halls Creek Meteorological Office</i>	2012	89.1	18.23	127.66

809310	<i>Warmun</i>	2032	79.4	17.02	128.22		2032	77.9	17.02	128.22
	<i>Halls Creek Meteorological Office</i>	2012	89.1	18.23	127.66					
616065	<i>Karragullen</i>	9168	13.0	32.12	116.12	<i>Perth Airport</i>	9021	37.9	31.93	115.98
	<i>Karnet</i>	9111	24.9	32.44	116.08	<i>Karnet</i>	9111	24.9	32.44	116.08
616002	<i>Karragullen</i>	9168	17.1	32.12	116.12	<i>Perth Airport</i>	9021	33.6	31.93	115.98
	<i>Chidlow</i>	9007	23.0	31.86	116.27		9111	45.5	32.44	116.08
616013	<i>Chidlow</i>	9007	15.4	31.86	116.27	<i>Northam</i>	10111	39.9	31.65	116.66
	<i>Bickley</i>	9240	26.1	32.01	116.14					
617002	<i>Warradarge</i>	8278	23.6	30.07	115.31	<i>Geraldton Airport Comparison</i>	9131	32.5	30.31	115.03
	<i>Tambrey</i>	9054	44.2	30.60	115.64					

Northern Territory

Discharge station	Rainfall Station					Temperature Station				
	Name	Number	Distance (km)	Latitude	Longitude	Name	Number	Distance (km)	Latitude	Longitude
G8170002	<i>Darwin River Dam</i>	14183	47.6	12.83	130.97	<i>Darwin Airport</i>	14015	93.4	12.42	130.89
	<i>Humpty Doo Collard Road</i>	14226	49.7	12.58	131.08					
G8140161	<i>Mango Farm</i>	14938	45.0	13.74	130.68	<i>Darwin Airport</i>	14015	147.1	12.42	130.89
	<i>The Pines</i>	14204	50.7	13.76	131.57	<i>Douglas River Research Farm</i>	14901	14	13.83	131.19
G0060005	<i>The Garden</i>	15521	28.3	23.28	134.42	<i>Alice Springs Airport</i>	15590	57.4	23.8	133.89
	<i>Bond Springs Homestead</i>	15631	46.6	23.54	133.92					
G8150018	<i>McMinns Lagoon</i>	14219	6.3	12.55	131.08	<i>Darwin Airport</i>	14015	28.1	12.42	130.89
	<i>Howard Springs Nature Park</i>	14149	16.8	12.46	131.05					
G9030124	<i>Daly Waters Airstrip</i>	14626	0.5	16.26	133.38	<i>Daly Waters Airstrip</i>	14626	0.5	16.26	133.38
	<i>Daly Waters</i>	14618	1.0	16.25	133.37	<i>Larrimah</i>	14612	77.7	15.57	133.21
	<i>Hayfield</i>	14656	54.1	16.73	133.50					

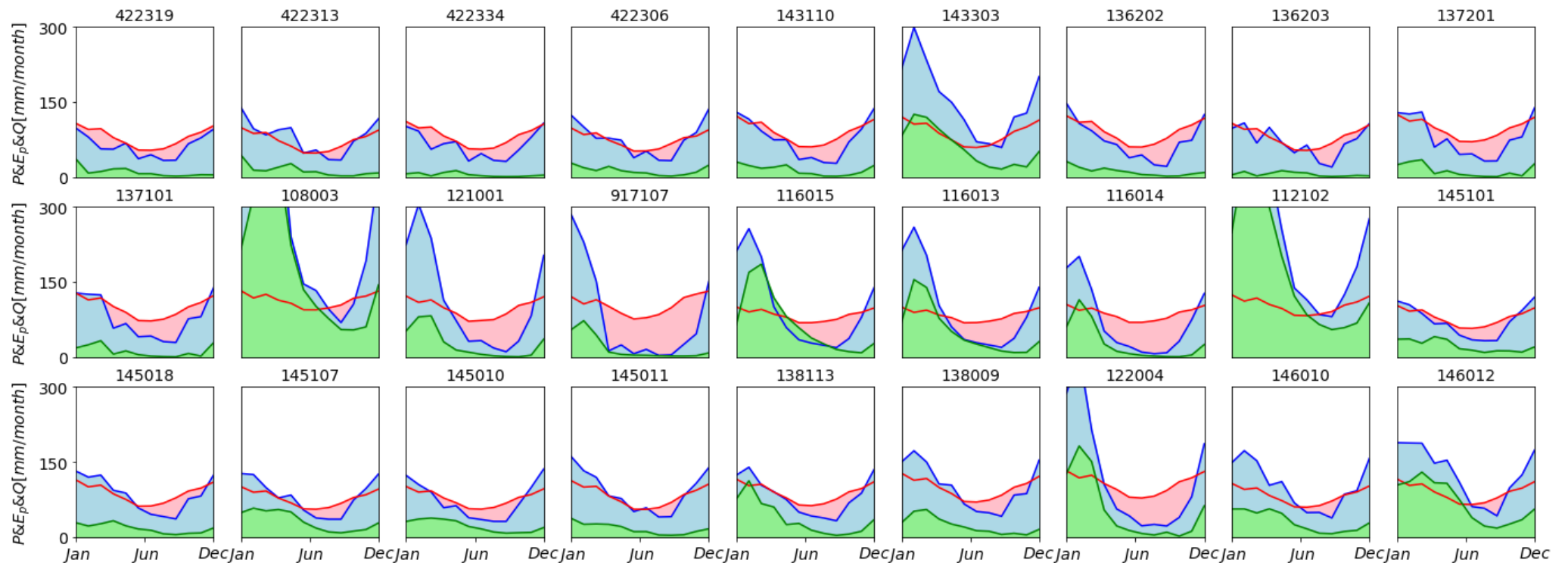
Tasmania

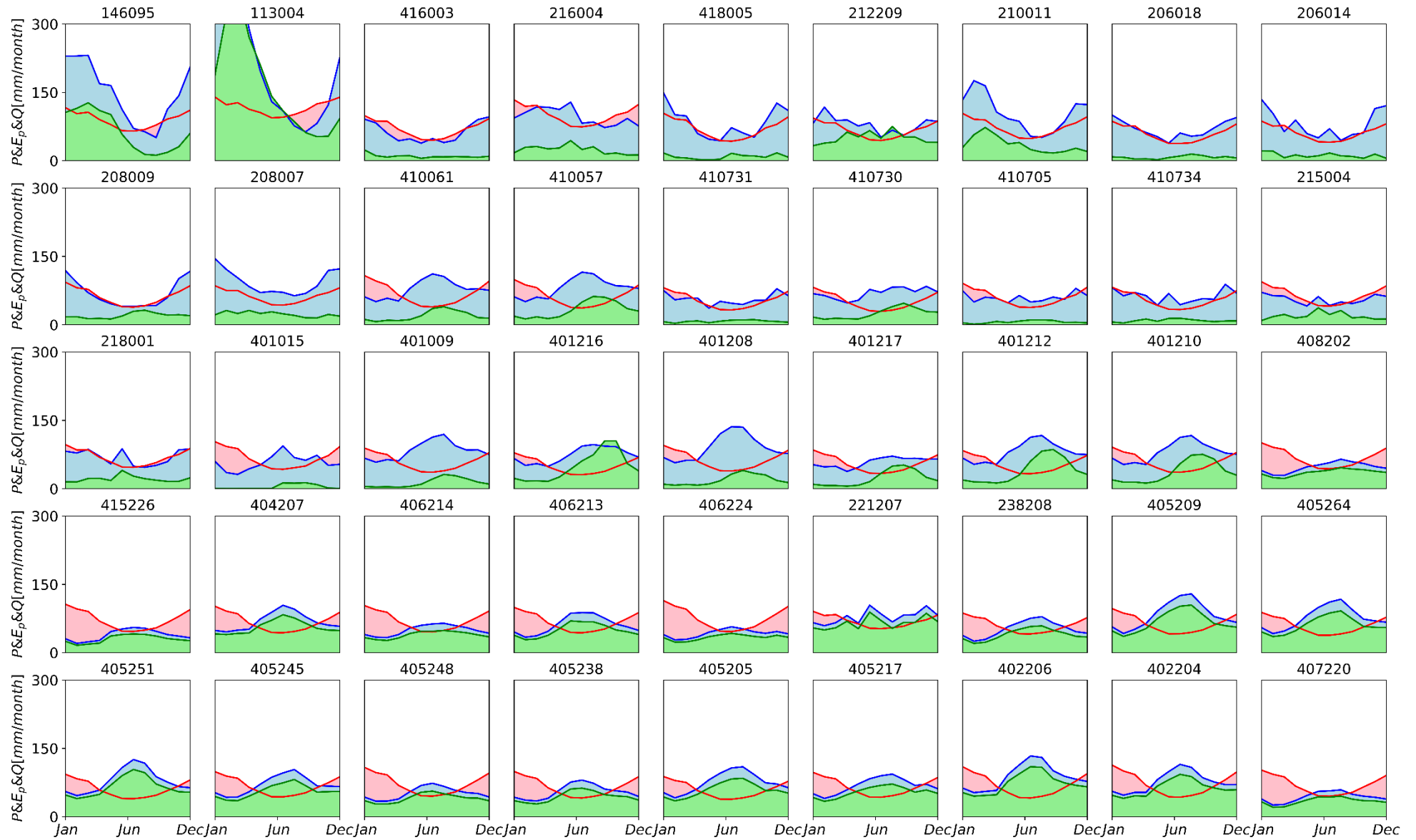
<i>Discharge station</i>	<i>Rainfall Station</i>					<i>Temperature Station</i>				
	<i>Name</i>	<i>Number</i>	<i>Distance (km)</i>	<i>Latitude</i>	<i>Longitude</i>	<i>Name</i>	<i>Number</i>	<i>Distance (km)</i>	<i>Latitude</i>	<i>Longitude</i>
304497	<i>Miena Dam</i>	96046	25.5	41.98	146.72	<i>Butlers Gorge</i>	96071	22.1	42.12	146.18
	<i>Lake St Clair National Park</i>	96071	22.1	42.12	146.18	<i>Maydena Post Office</i>	96003	29.5	42.28	146.28
302214	<i>Larapuna (Eddystone Point)</i>	92045	12.3	40.99	148.35	<i>Larapuna (Eddystone Point)</i>	92045	12.3	40.99	148.35
	<i>Pioneer (Main Road)</i>	92030	23.9	41.08	147.94	<i>Scottsdale (West Minstone Road)</i>	91219	62.3	41.17	147.49
	<i>Pyengana (Forest Lodge Road)</i>	92051	33.3	41.27	147.95					
308799	<i>Lake St Clair National Park</i>	96071	21.0	42.12	146.18	<i>Butlers Gorge</i>	96071	21	42.12	146.18
	<i>Queenstown (South Queenstown)</i>	97091	32.3	42.10	145.55	<i>Maydena Post Office</i>	96003	31	42.28	146.28
314207	<i>Ulverstone (Knights Road)</i>	91102	11.1	41.16	146.15	<i>Forthside Research Station</i>	91186	15.4	41.2	146.27
	<i>Wilmot (Back Road)</i>	91105	14.8	41.37	146.17					
	<i>Aberdeen (Melrose Road)</i>	91313	20.2	41.25	146.33					
	<i>Barrington Post Office</i>	91153	18.3	41.34	146.28					
318067	<i>Musselboro (Elverton)</i>	91197	4.6	41.49	147.44	<i>Scottsdale (West Minstone Road)</i>	91219	36.8	41.17	147.49
	<i>Deddington (Marathon)</i>	91077	10.5	41.58	147.45					

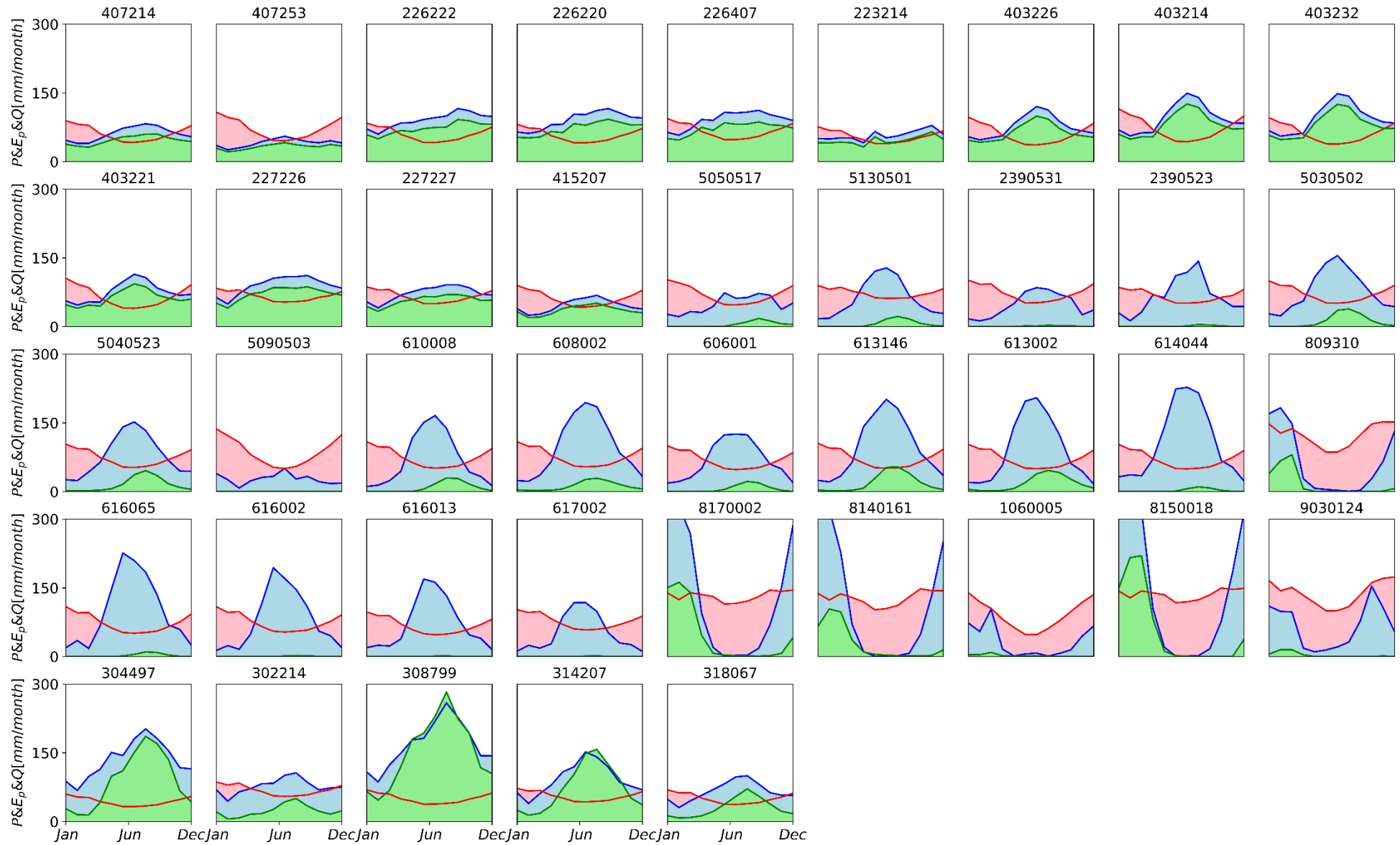
B

Climate condition (P, Ep, Q)

The 113 catchments long-term monthly mean precipitation, potential evaporation and discharge are presented below. The title is the discharge station number, precipitation, potential evaporation and discharge are represented by blue, red and green lines, respectively. The order of the subplots is from left to right and from top to bottom, consistent with the order in Appendix A.









Gumbel distribution results

The Gumbel distribution results of 113 catchments are presented below. The title is the discharge station number, the blue diamonds are the S_r values, the black dashed line and red dots are the Gumbel results with return period 5, 10, 20, 40, 60 and 100 years, S_{r20} is highlighted by the cross of the red line and black dashed line and text mark. The order of the subplots is from left to right and from top to bottom, consistent with the order in Appendix A.

